Negative regulation of oncogenic Ras signaling by mitogen-activated protein kinase phosphatase-3

A DISSERTATION
SUBMITTED TO THE FACULTY OF THE GRADUATE SCHOOL
OF THE UNIVERSITY OF MINNESOTA
BY

Nicholette A. Zeliadt

IN PARTIAL FULFILLMENT OF THE REQUIREMENTS
FOR THE DEGREE OF
DOCTOR OF PHILOSOPHY

Elizabeth V. Wattenberg

June 2010

Acknowledgements

None of this work would have been possible without the incredible help and talent of my advisor, Betsy Wattenberg. Words do not feel adequate enough to thank her for the time and energy she has invested in me as a scientist, and the encouragement and trust she demonstrated in allowing me to pursue my own ideas. Since I began working in her lab nine years ago, she has been an excellent and patient teacher, role model, and exemplar of scientific integrity.

Thanks also to my thesis committee members: Lisa Peterson, Bill Toscano, Laura Mauro, and Carol Lange. You provided me with very helpful suggestions and inspiration when I needed it most. Thank you for all your time, support, and invaluable personal and professional advice.

I am also very grateful to the University of Minnesota Graduate School, the Division of Environmental Health Sciences, Graduate Women in Science/Sigma Delta Epsilon, and the Minnesota Environmental Health Association for providing financial support during my training.

Thank you also to the administrative staff in the Division of Environmental Health Sciences. You have always been a pleasure to work with and have made my experience in the division very memorable.

I extend my gratitude to the wonderful people I have had the privilege of working with over the years. Diane Toscano has demonstrated incredible patience, kindness and generosity, and I thank her for her understanding, kind and gentle nature. Special thanks to Jerry Sedgwick for teaching me everything I know about microscopy and Photoshop, and for his creative inspiration. I have greatly appreciated our discussions over the years. Janel Warmka helped me to get started as an independent scientist in Betsy's lab, and has been a wellspring for helpful and thoughtful discussions ever since. Thanks also to Anita Wichmann, Aaron Charlson, and Eric Solberg for memorable times in Betsy's lab and for making the lab such a pleasurable place to work. Thank you to Mark Distefano and members of the Distefano lab: James Wollack, Dan Abate, Josh Ochocki, and Amanda DeGraw. You have all been wonderful to work with, and I have learned so much from

each of you. Special thanks to Richard Sessler, for his commitment to truth and integrity, for his meticulous approach to experimentation, for challenging me to become a better scientist, and pushing me to be a more critical thinker. Our discussions are forever a source of inspiration to me.

Thank you to all my wonderful friends—you've not only provided physical and emotional support, but also shared my joys and disappointments throughout this demanding experience. You listened patiently as I vented frustrations, helped me to brainstorm, gave me different perspectives, encouragement, and shared your opinions with honesty and objectivity. I especially thank Abinadi Meza for his witty humor, curious nature, inspiration, encouragement, and ability to explain complex ideas. I am forever indebted to Ruth Meza for her love, selflessness, and willingness to always help me. And many thanks to Will Ratcliff for sharing his love of science, expertise in statistics, incomparable sense of humor, and for his patience and kindness.

Finally, I express my utmost appreciation to my sister (and best friend), brother, mom and dad. I cannot thank you enough for your encouragement, selflessness, support, love, patience and understanding. I could not be who or where I am today without you.

Abstract

Activating mutations in the Ras oncogene are found in ~30% of all human cancers. Ras is a central regulator of intracellular signaling pathways, such as the Raf/MEK1/2/ERK1/2 protein kinase cascade, that modulate cell cycle progression, cell proliferation, and cell survival. Chronic activation of Ras-stimulated pathways is believed to play a key role in cellular transformation, although constitutive activation of Ras alone is not sufficient for tumor development. The goal of these studies is to further understand the biochemical events that occur during carcinogenesis in cells that express activated Ras that make cells susceptible to tumor promoting stimuli. This knowledge is important for the development of new strategies to diagnose, prevent and treat cancer. To date, attempts at developing small molecule inhibitors of oncogenic Ras have been unsuccessful. Therefore, efforts have instead focused on targeting downstream effectors of Ras, such as the Raf/MEK1/2/ERK/12 cascade, or preventing the posttranslational prenylation of Ras that is critical for its function. The aim of these studies is two-fold: 1) to elucidate the signaling events that occur in cells exposed to tumor-promoting stimuli; and 2) to develop tools for the study of prenylation in living cells.

Previous studies in our lab showed that the MAP kinase phosphatase MKP-3 is a vulnerable target of tumor promoting stimuli during carcinogenesis in cells that express activated Ras. Therefore, we sought to further understand the mechanisms that control the expression of MKP-3. We found that MKP-3 RNA and protein expression is intricately controlled by ERK1/2. We also found that MKP-3 is engaged in a negative feedback loop that is important in limiting oncogenic Ras signaling through the Raf/MEK1/2/ERK1/2 pathway. We also previously showed that one tumor promoter known as palytoxin stimulates ERK1/2-dependent changes in gene expression. These studies relied on the use of pharmacological inhibitors of MERK1/2, the ERK1/2 activating kinase. Recent reports have revealed that MEK1/2 inhibitors also inhibit MEK5, the kinase that activates the MAP kinase ERK5. Therefore, we re-evaluated the effect of palytoxin in cells with activated Ras, with a focus on ERK5. We found that palytoxin also triggers the activation

of ERK5. Palytoxin-stimulated ERK5 contributes to the upregulation of c-Fos, a signaling event that we previously attributed solely to ERK1/2.

Prenylation of Ras is a post-translational modification that is critical for Ras function. Drugs that disrupt prenylation are therefore promising cancer therapeutics, and several such inhibitors have been tested recently in clinical trials. More information regarding the mechanistic details of protein prenylation and functional consequences of disrupting prenylation in the cell is needed. In a collaborative study with the Distefano lab in the department of chemistry, I tested the uptake and localization of cell-penetrating peptides that will be useful for the study of prenylation in living cells. We found that prenylated peptides are rapidly taken up by cells and localize in a perinuclear fashion. In contrast to previous studies of cell-penetrating peptides, uptake is more dependent on the presence of the hydrophobic prenyl moiety than on the identity of amino acids that make up the peptides. These results, discussed in Chapters IV and V, may be valuable for the development of more specific inhibitors of Ras prenylation.

Altogether, the studies presented in this thesis provide new insights into the biochemical mechanisms involved in the negative regulation of oncogenic signaling pathways. This information may be useful for the development of new ways to treat and prevent cancer.

Table of Contents

List of Figures

Chapter II

Chapter III

Chapter IV

Chapter V

Chapter I

Introduction

Mutation of Ras is one of the most common molecular defects found in human cancers (Bos, 1989). Ras is a central regulator of intracellular signaling pathways, such as the Raf/MEK1/2/ERK1/2 protein kinase cascade, that modulate diverse biological process, including cell cycle progression, cell proliferation, and cell death (Campbell et al., 1998). Ras mutation frequently results in its constitutive activation (Barbacid, 1987). Chronic activation of Ras-stimulated pathways is believed to play a key role in cellular transformation. However, constitutive activation of Ras alone is not sufficient for tumor development (Vogelstein and Kinzler, 1993). The goal of these studies is to further our understanding of biochemical changes that occur during carcinogenesis in cells that express activated Ras that make cells susceptible to tumor promoting stimuli. This knowledge is important for the development of new strategies to diagnose, prevent and treat cancer.

To date, attempts at developing small molecule inhibitors of oncogenic Ras have been unsuccessful (Newell, 2005). Therefore, efforts have instead focused on other approaches, including 1) targeting downstream effectors of Ras, such as the Raf/MEK1/2/ERK/12 cascade, or 2) preventing the posttranslational prenylation of Ras that is critical for its transforming properties (Downward, 2003; Roberts and Der, 2007). The aim of these studies is two-fold: Chapters 2 and 3 of this thesis discuss studies focused on understanding signaling events that occur in initiated cells exposed to tumor-promoting stimuli; Chapters 4 and 5 discuss studies focused on the development and application of cell-penetrating peptides for the study of prenylation in living cells.

1.1 Background

Background briefly reviews: 1) the multi-stage mouse skin model of carcinogenesis, 2) the small GTPase Ras, 3) the role of MAP kinase signaling in cancer, and 4) the regulation of MAPK signaling by MAP kinase phosphatases.

1.1.1 The multi-stage mouse skin model of carcinogenesis

The multi-stage mouse skin model has yielded fundamental information for the study of carcinogenesis (Yuspa and Poirier, 1988). In this model, tumors result from

the stepwise accumulation of genetic changes over the course of several well-defined stages (DiGiovanni, 1992). The first stage, known as initiation, is a rapid, irreversible phase involving carcinogen-induced DNA damage (Yuspa and Morgan, 1981; Zarbl et al., 1985). The next stage, known as promotion, is a longer stage and is potentially reversible if exposure to tumor promoting-stimuli is ceased early enough (Slaga, 1983). In this stage, repeated application of a tumor promoter causes abnormal activation of signal transduction pathways, thereby enabling the clonal expansion of initiated cells to form papillomas (Slaga et al., 1980; Yuspa, 1986). The most widely studied class of tumor promoter is the phorbol esters, represented by 12-*O*-tetradecanoylphorbol-13-acetate (TPA) (Baird and Boutwell, 1971). The stochastic accumulation of additional genetic changes during tumor progression, the final stage, ultimately leads to the outgrowth of malignant tumors (DiGiovanni, 1992; Yuspa, 1986).

One important feature of this model is the observation that neither initiation nor tumor promotion alone is sufficient for tumorigenesis (Slaga, 1983). Furthermore, tumor promotion must follow initiation (Slaga, 1983). Given the long latency of most human cancers, and the potentially reversible nature of tumor promotion, research has focused on understanding the biochemical events that occur during tumor promotion with the anticipation that such biochemical changes may be prevented or targeted therapeutically to treat cancer (Yuspa, 1986).

1.1.2 The small GTPase Ras

One frequent, early mutation that occurs during the initiation stage of the multi-stage mouse skin model results in the constitutive activation of the oncogene, Ras (Balmain et al., 1984). Constitutive activation of Ras by mutation is also a frequent early event in many human cancers (Bos, 1989). For example, activated forms of Ras have been found in approximately 30% of lung, 36% of colon, and 90% of pancreatic cancers (Almoguera et al., 1988; Fang and Richardson, 2005; Sebolt-Leopold and Herrera, 2004).

Ras is the founding member of the family of small GTPases and is normally activated in response to a wide variety of extracellular stimuli that modulate many

cellular activities, including cell proliferation, cell motility, differentiation, survival, and apoptosis (Rajalingam et al., 2007). Ras proteins (H-, K-, and N-Ras) normally cycle between the active, GTP-bound state and the inactive, GDP-bound state (Campbell et al., 1998). Ras mutations, which frequently occur in codons 12, 13, or 61, result in reduced efficiency of GTP hydrolysis and maintain Ras in the active conformation (Barbacid, 1987).

Post-translational modification of Ras with a small lipid moiety, known as prenylation, is critical for Ras function. Prenyltransferases catalyze the addition of a 15-carbon farnesyl or 20-carbon geranylgeranyl group to a cysteine residue in the 'CAAX' box (where C stands for cysteine, A for an aliphatic amino acid, and X for any amino acid), a highly conserved motif found in the *C*-terminus of prenylated proteins (Wright and Philips, 2006; Zhang and Casey, 1996). Prenylation causes Ras to be localized to the plasma membrane and situates Ras near its signaling partners (Hancock et al., 1991a; Hancock et al., 1991b). Disruption of prenylation prevents Ras signaling to downstream targets, and has been the focus of drug design (Kloog and Cox, 2000). However, recent evidence suggests that prenyltransferase inhibitors exhibit anti-tumor activity even in the absence of an oncogenic Ras mutation (Hill et al., 2000; Lerner et al., 1997). Therefore, further study of the molecular mechanisms of protein prenylation and the biochemical consequences of inhibiting prenylation is needed.

Ras signals are transmitted through at least two major pathways in the cell—the phosphatidylinositol 3-kinase (PI3-K) pathway and the Raf/MEK1/2/ERK1/2 cascade (Campbell et al., 1998). Upon activation, PI3-K stimulates the serine/threonine kinase Akt, which transmits signals that promote cell survival, cell cycle progression, and cell proliferation (Chang et al., 2003; Franke et al., 1995; Fresno Vara et al., 2004). Perhaps the best-characterized effectors of Ras signaling, however, are the Raf serine/threonine kinases (A-Raf, B-Raf, and C-Raf) (Schreck and Rapp, 2006). Activated Ras recruits Raf to the plasma membrane, where Raf becomes activated (Wellbrock et al., 2004). Raf then phosphorylates and activates the kinases MEK1/2, which in turn phosphorylate and activate ERK1/2 (Howe et al., 1992). Once

activated, ERK1/2 can phosphorylate cytoplasmic substrates and translocate to the nucleus to phosphorylate and modulate the activity of transcription factors such as Elk-1, STAT, and AP-1, ultimately leading to changes in gene expression (Chen et al., 1992; Vial and Marshall, 2003).

Classically, this evolutionally conserved Ras/Raf/MEK1/2/ERK1/2 signaling pathway has been viewed as a relatively simple, linear route from receptor to nucleus. However, recent studies demonstrate that members of this cascade participate in complex feedback loops and engage in crosstalk with other pathways (Bhalla et al., 2002; Eblaghie et al., 2003; Shen et al., 2003; Smith et al., 2005; Xiao et al., 2002; Zimmermann et al., 1997). Understanding the molecular mechanisms of such crosstalk and feedback will have important implications for the efficacy of drugs, which are typically designed to target single molecules but are likely to have broader effects (Jeffrey et al., 2007).

While oncogenic Ras plays a pivotal role in carcinogenesis, aberrant Ras/Raf/MEK1/2/ERK1/2 signaling is also implicated in cancers in which Ras is not mutated, such as breast cancer (Hori et al., 2000), thyroid cancer (Ouyang et al., 2006), and melanoma (Bloethner et al., 2005). These tumors exhibit deregulated Ras/Raf/MEK1/2/ERK1/2 signaling as a result of alternate changes, including Ras overexpression, changes in transmembrane receptors that result in constitutive stimulation of Ras, or oncogenic mutation of Raf (Dunn et al., 2005; Giehl 2005). Given the widespread involvement of aberrant Ras/Raf/MEK1/2/ERK1/2 signaling in a wide variety of human cancers, it is imperative that we understand how this pathway is regulated during carcinogenesis.

1.1.3 The role of MAPK signaling in cancer

ERK1/2 belongs to the family of mitogen-activated protein kinases (MAPKs), which also includes c-Jun N-terminal kinase (JNK), p38, and ERK5 (Dhillon et al., 2007). Activation of MAPKs requires dual-phosphorylation of threonine and tyrosine residues located in the conserved T-X-Y motif (where X is glutamate, proline, or glycine in ERK1/2 and ERK5, JNK, or p38, respectively) of the kinase activation loop (Chen et al., 2001; Kato et al., 1997). Mitogenic stimuli typically activate

ERK1/2, whereas stress-inducing agents activate JNK and p38. Both mitogenic and stress-inducing stimuli can activate ERK5 (Abe et al., 1996; Kato et al., 1998).

Upon activation, MAPKs bind to and phosphorylate various substrates in the cytoplasm and nucleus. While the precise function of each MAPK appears to be stimulus and cell-type specific, activation of JNK and p38 generally stimulates cell cycle arrest and apoptosis, and ERK1/2 activation contributes to cellular proliferation, survival and differentiation (Dhillon et al., 2007). ERK5 is unique in that it contains a large *C*-terminal transcriptional activation domain, and can directly interact with and enhance the activity of transcription factors such as c-Fos and MEF-2 (Kato et al., 1997; Nishimoto and Nishida, 2006; Terasawa et al., 2003). The role of ERK5 in modulating downstream events is not entirely clear, due in part to the apparent high degree of overlap between ERK1/2 and ERK5 substrates (Nishimoto and Nishida, 2006). Nevertheless, ERK5 has been shown to be involved in cell cycle progression and differentiation (Kato et al., 1998; Liu et al., 2006).

Abnormalities in MAPK signaling feature prominently in all of the processes considered to be hallmarks of cancer, including: 1) self-sufficiency in growth signals, 2) insensitivity to anti-growth signals, 3) evasion of apoptosis, 4) limitless replicative potential, 5) the ability to invade tissue and metastasize, and 6) the ability to sustain angiogenesis for nutrient supply (Hanahan and Weinberg, 2000). MAPK signaling thus plays a critical role in tumorigenesis, and an understanding of the molecular mechanisms of MAPK function is important for the treatment of cancer (Dhillon et al., 2007).

The MAPKs are activated by an astounding array of stimuli yet are capable of coordinating highly specific biological outcomes. The precise biochemical response depends on several factors, including the dynamic regulation of the magnitude and duration of MAPK activity, as well as subcellular localization (Raman et al., 2007). These factors are determined in part by a delicate balance between the activity of kinases that activate MAPKs and the phosphatases that inactivate MAPKs. Traditionally, studies have focused on understanding the upstream kinases that catalyze dual phosphorylation of MAPKs. Much less is known about the equally

important role of phosphatases that inactivate MAPKs.

1.1.4 The regulation of MAPK signaling by MAP kinase phosphatases

MAPKs can be inactivated by serine/threonine phosphatases such as PP2A, tyrosine-specific phosphatases, such as PTP1B, or dual-specificity phosphatases (DUSPs) that remove phosphate groups from both threonine and tyrosine residues (Keyse, 1998). While many of these phosphatases can dephosphorylate numerous phosphoproteins throughout the cell, a subgroup of the DUSP phosphatase family, known as the MAP kinase phosphatases (MKPs), has gained considerable attention because these phosphatases appear to be specific for MAPKs (Keyse, 2000).

There are at least 10 MKPs, all of which share conserved structural features including a *C*-terminal catalytic domain and *N*-terminal substrate interaction motifs (Owens and Keyse, 2007). The MKPs differ in their tissue expression, subcellular localization, and substrate specificity (Farooq and Zhou, 2004). Recent studies suggest that MKPs are important in finely tuning the magnitude and duration of MAPK signaling (Caunt et al., 2008a; Caunt et al., 2008b; Volmat et al., 2001).

The MKPs are regulated dynamically, both in their expression and activity (Jeffrey et al., 2007). Several MKPs are rapidly induced by stimuli that activate their substrate MAPKs (Brondello et al., 1997; Volmat et al., 2001). The activity of many of the dual-specificity phosphatases can be regulated through multiple post-translational mechanisms. For example, MKP-1, -2, and -3 are all phosphorylated by ERK1/2, which results in the stabilization of MKP-1 by slowing its proteasomal degradation (Brondello et al., 1999). Conversely, MKP-3 phosphorylation results in its destabilization (Marchetti et al., 2005). Reversible oxidation of the catalytic cysteine residue in the active site of MKPs can also regulate phosphatase activity (Kamata et al., 2005; Levinthal and Defranco, 2005; Seth and Rudolph, 2006). Additionally, MKP activity may be modulated through conformational changes. For example, MKP-1, -2, -3, undergo catalytic activation upon substrate binding (Camps et al., 1998b; Chen et al., 2001; Hutter et al., 2000; Nichols et al., 2000; Slack et al., 2001).

We became interested in MKP-3 once we identified it as the target of the tumor

promoter, palytoxin (Warmka et al., 2004). These studies revealed that palytoxin could stimulate the activation of ERK1/2 in cells that express oncogenic Ras by triggering the downregulation of MKP-3. Other studies associated progression of pancreatic cancer to a more invasive phenotype with loss of MKP-3, and identified MKP-3 as a potential tumor suppressor (Furukawa et al., 2003; Furukawa et al., 2005). Together, these studies suggest that MKP-3 may play an important role in tumor promotion. Little was known about how the expression of MKP-3 is controlled, however.

Early studies suggested that, unlike MKP-1 and -2, MKP-3 is not an inducible gene (Groom et al., 1996). However, more recent studies have provided evidence that MKP-3 RNA is upregulated by many different stimuli, including serum (Iyer et al., 1999; Reffas and Schlegel, 2000), TNFα (Breitschopf et al., 2000), NGF (Camps et al., 1998a; Mourey et al., 1996; Muda et al., 1996; Vician et al., 1997), and retinoic acid (Liu et al., 2005; Moreno and Kintner, 2004; Reffas and Schlegel, 2000). Furthermore, MKP-3 RNA is upregulated in cells that express mutant, constitutively active forms of the EGF receptor, Ras, or Raf (Bloethner et al., 2005; Croonquist et al., 2003; Ouyang et al., 2006; Ramnarain et al., 2006; Sato et al., 2006; Sweet-Cordero et al., 2005). This suggests that signaling through the Raf/MEK1/2/ERK1/2 pathway is involved in regulating MKP-3 expression. However, the mechanisms underlying the regulation of MKP-3 expression have not been fully elucidated. The studies presented in Chapter II address the specific modulation of MKP-3 expression by the Ras/Raf/MEK1/2/ERK1/2 pathway, and the physiological role of MKP-3 in cells that express activated Ras.

Modulation of ERK1/2 signal strength, duration and/or localization is important for determining cellular responses to various stimuli (Ebisuya et al., 2005; Halfar et al., 2001; Hu et al., 2000; Murphy and Blenis, 2006; Pouyssegur et al., 2002; Ramos, 2008; Santos et al., 2007; Torii et al., 2004; von Kriegsheim et al., 2009; Whitehurst et al.; 2004). For example, EGF treatment of rat PC12 neuroblastoma cells stimulates transient ERK activation and results in proliferation (Marshall, 1995). In contrast, NGF treatment of PC12 cells, which induces prolonged ERK activation, leads to

differentiation and neurite outgrowth (Traverse et al., 1992).

Recent evidence suggests that MKP-3, a cytoplasmic ERK1/2-specific phosphatase, is uniquely positioned to precisely regulate spatio-temporal activity of ERK1/2 (Groom et al., 1996; Karlsson et al., 2004; Muda et al., 1996). MKP-3 contains a functional nuclear export signal (NES) that may be involved in mediating the cytoplasmic localization of ERK, which lacks an identifiable NES (Karlsson et al., 2004). Additionally, overexpression of a catalytically inactive form of MKP-3 causes ERK1/2 to be retained in the cytoplasm and results in cell cycle arrest through a mechanism that requires the NES of MKP-3 (Brunet et al., 1999; Karlsson et al., 2004). These studies suggest that loss of MKP-3 during carcinogenesis may deregulate ERK1/2 activity in part by altering ERK1/2 localization. Altogether, these data highlight the importance of understanding how MKP-3 is regulated because changes in MKP-3 expression or activity could alter ERK1/2 activity, resulting in profound changes to cell fate and function.

1.2 Summary

In the following chapters I present 4 published papers. In chapter two, we demonstrate that ERK1/2 and MKP-3 are engaged in a dynamic negative feedback loop in which ERK1/2 controls the expression and stability of MKP-3, which in turn regulates the magnitude and duration of ERK1/2 activity. Chapter three demonstrates that the tumor promoter palytoxin stimulates the activation of ERK5 through a mechanism that is distinct from the way in which palytoxin activates ERK1/2. Furthermore, we present evidence that ERK5 is involved in regulating the palytoxin-stimulated expression of c-Fos. In chapter four, I discuss the development and characterization of cell-penetrating peptides that will be useful for understanding the process of protein prenylation in living cells. Finally, in chapter five, we further examine the mechanism of cell-penetrating peptide uptake by living cells by probing the relationship between peptide sequence and level of internalization. Altogether, this research shows that understanding the negative regulation of oncogenic signaling pathways may hold promising information for the development of new ways to treat and prevent cancer.

Chapter II

Reciprocal regulation of extracellular signal regulated kinase 1/2 and mitogen activated protein kinase phosphatase-3

Rationale. Previous studies by our lab demonstrated that the tumor promoting agent, palytoxin, disrupts MKP-3 function in cells that express activated Ras, thereby unleashing Ras-stimulated signaling through the Raf/MEK1/2/ERK1/2 pathway (Warmka et al., 2004). Studies by others have demonstrated that MKP-3 expression is frequently lost during the late stages of human pancreatic cancer, which exhibits a high frequency of Ras mutation, suggesting that MKP-3 may play an important role as a tumor suppressor (Furukawa et al., 2003; Furukawa et al., 2005). Together, these data suggest that MKP-3 may be a vulnerable target of tumor promoting stimuli during carcinogenesis in cells that express activated Ras. Relatively little is known about how the expression of MKP-3 is regulated, however. Furthermore, it is unknown how the upregulation of MKP-3 affects cell fate and function in cells that express activated Ras. Understanding how the expression of MKP-3 is regulated in human cells that express activated Ras and how this phosphatase modulates Ras-stimulated signaling pathways is potentially important for the development of new strategies to prevent, treat, and diagnose cancer. The purpose of this study was to investigate the hypothesis that Ras-stimulated ERK activation leads to the upregulation of MKP-3, which then participates in a negative feedback loop to counteract hyper-stimulated Raf/MEK1/2/ERK1/2 signaling.

Results. We found that targeted knockdown of MKP-3 unleashed Ras signaling through the Raf/MEK1/2/ERK1/2 cascade. This supports our earlier finding that the tumor promoter palytoxin can elicit activation of ERK1/2 by triggering the loss of MKP-3 in cells with activated Ras. We also found that ERK1/2 has multiple effects on both MKP-3 RNA and protein: mitogen-stimulated ERK1/2 activation resulted the destabilization of existing MKP-3 protein; concurrently, active ERK1/2 stimulated *de novo* synthesis of MKP-3 RNA, which ultimately led to the recovery of MKP-3 protein. Finally, we demonstrated that MKP-3 participates in a negative feedback look to control the

magnitude and duration of ERK1/2 phosphorylation.

Conclusions and Significance. The finding that targeted loss of MKP-3 results in increased ERK1/2 phosphorylation is significant because it confirmed our earlier finding that palytoxin-stimulated downregulation of MKP-3 unleashes Ras-stimulated signaling of the Raf/MEK1/2/ERK1/2 cascade. It was also one of the first reports to investigate the physiological role of endogenous MKP-3. Several simultaneous or subsequent reports from other laboratories have confirmed our findings, highlighting the importance negative feedback role of MKP-3 in regulating ERK1/2 in cell culture models and in mice (Britson et al., 2009; Chan et al., 2008; Ekerot et al., 2008; Furukawa et al., 2008; Jurek et al., 2009; Maillet et al., 2008; Zhang et al., 2010). The finding that MKP-3 undergoes biphasic modulation upon activation of ERK1/2 revealed important information about how MKP-3 expression is controlled in living cells, and confirmed earlier *in vitro* studies (Marchetti et al., 2005). Finally, the observation that MKP-3 modulates the magnitude and duration of ERK1/2 phosphorylation is significant because other work suggests that the magnitude and duration of ERK1/2 signaling can have a profound effect on cell fate and function (Ebisuya et al., 2005; Halfar et al., 2001; Hu et al., 2000; Murphy and Blenis, 2006; Pouyssegur et al., 2002; Ramos, 2008; Santos et al., 2007; Torii et al., 2004; von Kriegsheim et al., 2009; Whitehurst et al., 2004).

Contributions. I contributed directly to the work published in this paper by conducting all the experiments. These experiments were planned and results interpreted in discussions with Dr. Laura Mauro and Dr. Elizabeth Wattenberg. I also contributed to preliminary and non-published work by generating cells that stably express MKP-3 shRNA, and by determining whether ERK5 is a substrate for MKP-3. The remainder of this chapter is the published paper reprinted from *Toxicology and Applied Pharmacology*, Vol 232, Nicholette A. Zeliadt, Laura J. Mauro, and Elizabeth V. Wattenberg, "Reciprocal regulation of extracellular signal regulated kinase 1/2 and mitogen activated protein kinase phosphatase-3," pp 408-417, Copyright (2008), with permission from Elsevier.

2.1 Abstract

Mitogen activated protein kinase phosphatase-3 (MKP-3) is a putative tumor suppressor. When transiently overexpressed, MKP-3 dephosphorylates and inactivates extracellular signal regulated kinase (ERK) 1/2. Little is known about the roles of endogenous MKP-3, however. We previously showed that MKP-3 is upregulated in cell lines that express oncogenic Ras. Here we tested the roles of endogenous MKP-3 in modulating ERK1/2 under conditions of chronic stimulation of the Ras/Raf/MEK1/2/ERK1/2 pathway by expression of oncogenic Ras. We used two cell lines: H-ras MCF10A, breast epithelial cells engineered to express H-Ras, and DLD-1, colon cancer cells that express endogenous Ki-Ras. First, we found that MKP-3 acts in a negative feedback loop to suppress basal ERK1/2 when oncogenic Ras stimulates the Ras/Raf/MEK1/2/ERK1/2 cascade. ERK1/2 was required to maintain elevated MKP-3, indicative of a negative feedback loop. Accordingly, knockdown of MKP-3, via siRNA, increased ERK1/2 phosphorylation. Second, by using siRNA, we found that MKP-3 helps establish the sensitivity of ERK1/2 to extracellular activators by limiting the duration of ERK1/2 phosphorylation. Third, we found that the regulation of ERK1/2 by MKP-3 is countered by the complex regulation of MKP-3 by ERK1/2. Potent ERK1/2 activators stimulated the loss of MKP-3 within 30 min due to an ERK1/2-dependent decrease in MKP-3 protein stability. MKP-3 levels recovered within 120 min due to ERK1/2-dependent resynthesis. Preventing MKP-3 resynthesis, via siRNA, prolonged ERK1/2 phosphorylation. Altogether, these results suggest that under the pressure of oncogenic Ras expression, MKP-3 reins in ERK1/2 by serving in ERK1/2-dependent negative feedback pathways.

2.2 Introduction

Extracellular signal regulated kinase (ERK) 1/2 is a major molecular switch in signal transduction (Chen et al., 2001). This serine/threonine kinase and mitogen activated protein kinase (MAPK) family member is activated by various mitogens, regulates several enzymes and transcription factors, and is centrally involved in regulating cell

proliferation, differentiation, and gene expression in many systems. Accordingly, aberrant ERK1/2 regulation has been implicated in carcinogenesis (Dhillon et al., 2007). Typically, ERK1/2 is phosphorylated and activated upon stimulation of the Ras/Raf/MEK1/2/ERK1/2 protein kinase cascade. The magnitude and duration of ERK1/2 activity is determined by the balance between the activity of MEK1/2, the kinases that phosphorylate and activate ERK1/2, and the activity of phosphatases that can dephosphorylate and inactivate ERK1/2. Maintaining the tight regulation of ERK1/2 is critical because the duration and magnitude of its activity can profoundly affect cell fate and function (Marshall, 1995; McCawley et al., 1999; Murphy et al., 2002). The regulation of ERK1/2 activation by phosphorylation has been studied extensively. Far less is known about the role of specific phosphatases in the negative regulation of ERK1/2.

MAPK phosphatases (MKPs) have emerged as an important class of modulators of protein kinase signaling pathways (Camps et al., 2000; Farooq and Zhou, 2004; Owens and Keyse, 2007). MKPs, which are members of the protein tyrosine phosphatase superfamily and are also known as dual specificity phosphatases, specifically dephosphorylate the threonine and tyrosine residues located within the activation loop of MAPKs. MKP family members can differ with respect to several characteristics, including the following: subcellular location, tissue-specific expression, inducibility by various types of signals, and selectivity for dephosphorylating specific MAPKs, including ERK1/2, c-Jun N-terminal kinase (JNK), and p38.

Among the MKPs that are likely negative regulators of ERK1/2, MKP-3 is a particularly interesting candidate because of its specificity for dephosphorylating ERK1/2 and because of evidence that suggests it may be a tumor suppressor (Groom et al., 1996; Muda et al., 1996; Furukawa et al., 2003). For example, MKP-1 and MKP-2 are nuclear phosphatases that can dephosphorylate ERK, JNK and p38 in a manner that appears to be cell-type specific (Guan and Butch, 1995; Chu et al., 1996; Franklin and Kraft, 1997; Reffas and Schlegel, 2000). In contrast, MKP-3 has been identified as an ERK1/2-specific phosphatase that is localized within the cytoplasm (Muda et al., 1996). MKP-3 has been investigated mainly with the use of exogenous overexpression systems

(Kamakura et al., 1999; Castelli et al., 2004; Marchetti et al., 2005). The diverse roles of endogenous MKP-3 in regulating endogenous MAPKs have not been established in most systems. Furthermore, little is known about the regulation of endogenous MKP- 3. Interestingly, elevation of MKP-3 mRNA does not always correlate with increases in MKP-3 protein (Reffas and Schlegel, 2000). This suggests that the MKP-3 protein undergoes complex regulation.

Our previous work revealed that MKP-3 protein levels are upregulated in cell lines that express oncogenic Ras (Warmka et al., 2004). Moreover, we showed that the potent skin tumor promoter palytoxin stimulates the downregulation of MKP-3 in keratinocytes derived from initiated mouse skin, which express oncogenic Ras (Warmka et al., 2002). This further suggests that MKP-3 is an important negative regulator in carcinogenesis. Importantly, the Ras/ Raf/MEK1/2/ERK1/2 pathway is frequently deregulated in human carcinogenesis (Downward, 2003). Altogether, these observations led us to investigate the regulation and function of endogenous MKP-3 under conditions where the Ras/Raf/MEK1/2/ERK1/2 pathway is chronically stimulated by expression of oncogenic Ras. Investigating the role of MKP-3 in the regulation of ERK1/2 within the context of oncogenic Ras expression is a crucial part of the quest for a better understanding of the various mechanisms by which ERK1/2 activity is modulated during carcinogenesis.

The studies presented here suggest that ERK1/2 and MKP-3 engage in a dynamic interaction that helps rein in the ERK1/2 response under the pressure of oncogenic Ras expression. We used the following cell lines for these studies: H-ras MCF10A, a human breast epithelial cell line engineered to express oncogenic H-Ras, and DLD-1, a colon cancer cell line that expresses endogenous oncogenic Ki-Ras. First, we found that MKP-3 is involved in a negative feedback loop that suppresses basal ERK1/2 activity when expression of oncogenic Ras is the primary stimulus for the Ras/ Raf/MEK1/2/ERK1/2 cascade. Second, our studies using siRNA revealed that MKP-3 helps establish the sensitivity of ERK1/2 to extracellular activators by limiting the duration of ERK1/2 phosphorylation. Third, we found that the regulation of ERK1/2 by MKP- 3 is countered by the regulation of MKP-3 by ERK1/2, a process that involves modulating the balance between ERK1/2-dependent degradation and resynthesis of MKP-3. Altogether, the

studies presented here suggest that in cells that express oncogenic Ras, ERK1/2 activity is governed, at least in part, by its repartee with MKP-3.

2.3 Materials and Methods

2.3.1 Materials. Dulbecco's Modified Eagle Medium/F12 (DMEM/F12), heat-inactivated horse serum, and L-glutamine were purchased from Invitrogen Corporation (Carlsbad, CA). 12-*O*-tetradecanoylphorbol-13-acetate (TPA), cholera toxin, hydrocortisone, insulin, cycloheximide, actinomycin D, and epidermal growth factor (EGF) were purchased from Sigma (St. Louis, MO). Recombinant human tumor necrosis factor alpha (TNF-α) was purchased from R&D Systems, Inc. (Minneapolis, MN).

2.3.2 Cell culture. H-ras MCF10A cells were the generous gift of Dr. Aree Moon (College of Pharmacy, Duksung Women's University, Seoul, Korea) and were grown in DMEM/F12 supplemented with 5% horse serum, 0.5 μg/ml hydrocortisone, 10 μg/ml insulin, 20 ng/ml EGF, 0.1 μg/ml cholera toxin, and 2 mM L-glutamine. DLD-1 cells were purchased from ATCC (Manassas, VA) and were grown in DMEM supplemented with 10% fetal bovine serum (Intergen Company, Purchase, NY). All cells were grown in a humidified incubator at 37 °C with 5% CO_2. For all experiments, cells were plated in complete medium at a density of approximately 3.5×10^5 cells/cm^2. H-ras MCF10A cells were incubated for 24–40 h after plating, and then were incubated in serum-free media without the supplements listed above for an additional 1–24 h. DLD-1 cells were incubated for 24 h after plating, and then were incubated in serum-free media for an additional 24 h. All experiments were conducted in serum-free media unless otherwise indicated. Incubation of the cells with DMSO (used as a vehicle in some experiments) did not affect protein or RNA levels. The data shown in the figures are representative of at least three independent experiments.

2.3.3 Antibodies and immunoblotting. Cell lysates were prepared using the following buffer: 50 mM Tris–HCl, 1% NP-40, 0.25% Na-deoxycholate, 150 mM NaCl, 1 mM EDTA, 1 mM PMSF, 1 μg/ml aprotinin, 1 μg/ml leupeptin, 1 mM Na_3VO_4, 1 mM NaF. Lysates were cleared by centrifugation (16,000 ×g, 10 min, 4°C). 10–40 μg of protein was resolved using 10% SDS-polyacrylamide minigels, and then transferred to

Immobilon-P PVDF membrane (Millipore, Bedford, MA). After blocking in a TBST/5% milk solution, immunoblots were incubated overnight at 4°C using the following primary antibodies and dilutions: phospho-p44/42 MAPK (Thr-202/Tyr-204) (E10) (mouse monoclonal) (1:2000), and phospho-MEK1/2 (Ser-217/221) (rabbit polyclonal) (1:2000) from Cell Signaling (Beverly, MA), and ERK2 (C-14) (rabbit polyclonal) (1:2000), MEK1 (12-B) (rabbit polyclonal) (1:500), MKP-3 (C-20) (goat polyclonal) (1:1000) and β-tubulin (H- 235) (rabbit polyclonal) (1:2000) from Santa Cruz Biotechnology (Santa Cruz, CA). The following secondary antibodies were used: anti-mouse IgG horseradish peroxidase-linked antibody and anti-rabbit IgG horseradish peroxidase-linked antibody from Cell Signaling, and bovine anti-goat IgG horseradish peroxidase-linked antibody from Santa Cruz Biotechnology. The use of the anti-β-tubulin antibody in immunoblots has been published in Legendre et al. (2003). The use of the other antibodies in immunoblots is described in Warmka et al. (2004). The signal for MKP-3 immunoblots was detected using the SuperSignal West Femto chemiluminescent substrate from Pierce Biotechnology (Pierce Biotechnology, Rockford, IL). All other immunoblots were visualized using the Pierce SuperSignal West Pico substrate. Blots were stripped by incubation in 0.2 M NaOH.

2.3.4 Semi-quantitative RT-PCR. Total RNA was isolated from cells using the RNeasy Plus Mini Kit from QIAGEN (Valencia, CA). 1 μg of RNA was reverse-transcribed using random hexamers and the RNA PCR Core Kit from Applied Biosystems (Foster City, CA) following the manufacturer's protocol. Negative controls that lacked RNA or reverse transcriptase were included for each experiment. Relative transcript levels of MKP-3 and the endogenous control gene glyceraldehyde-3-phosphate dehydrogenase (GAPDH) were then determined by PCR from cDNA using the following primer pairs: human MKP-3 (accession no. X93920) forward 5′-GCCGCAGGAGCTATACGAGT-3′, reverse 5′- CCGTATTCTCGTTCCAGTCG-3′; human GAPDH (accession no. J04038) forward 5′-GTGAAGGTCGGAGTCAACGG-3′, reverse 5′-CTCCTGGAAGATGGTGATGG-3′. The following thermal cycling parameters were used: 95 °C for 2 min, 25 cycles of 95 °C for 30 s, 58.5 °C for 30 s, and 72 °C for 30 s. PCR reactions were stopped within the linear range of amplification for

each primer pair. PCR products were resolved on 2% NuSieve agarose gels containing ethidium bromide. The expected sizes of PCR products were 208 bp and 224 bp for MKP-3 and GAPDH, respectively. No PCR products were observed in negative controls. MKP-3 levels were normalized to GAPDH levels amplified from the same cDNA sample.

2.3.5 Small interfering RNA (siRNA). A duplex siRNA sequence targeting human MKP-3 was designed using the principles described in Reynolds et al. (2004) and purchased from Sigma-Proligo (Boulder, CO). A second duplex siRNA sequence, described in Liu et al. (2005) was also purchased from Sigma-Proligo. The 23-nucleotide duplexes used were (sense strands): duplex 1, AAGUGCGGAAUUGGUUAAUACdTT; and duplex 2, GUGCAACAGACUCGGAUGGUAdTT. Scrambled duplex siRNAs with the same GCAT content as the target siRNAs were used as a negative control: scrambled duplex 1, CAUUACGAAGUGGAUUGAGUAdTT; and scrambled duplex 2, CAUUACGGGAAAGUGCCGAGUdTT. For experiments, H-ras MCF10A cells were plated in complete medium approximately 20 h prior to transfection with a 200 nM mixture of MKP-3 or scrambled duplex siRNAs (with each duplex siRNA represented in equimolar amounts) using HiPerFect Transfection Reagent (QIAGEN Inc., Valencia, CA) according to the manufacturer's standard protocol. 24 h after transfection, cells were incubated in serum-free media for 1 h. DLD-1 cells were plated in complete medium and transfected with a 25 nM mixture of MKP-3 or scrambled duplex siRNAs (with each duplex siRNA represented in equimolar amounts) using HiPerFect Transfection Reagent according to the manufacturer's Fast Forward protocol. 24 h after transfection, cells were incubated in serum-free media for an additional 24 h. Alexa Fluor 488-labeled negative control siRNA, purchased from QIAGEN, was used to verify transfection efficiency.

2.3.6 Densitometry. Protein levels and PCR products were quantified using a Bio-Rad (Hercules, CA) Fluor-S MultiImager and Bio-Rad Quantity One software, or a Bio-Rad GS-700 Imaging Densitometer and Molecular Analyst software.

2.3.7 Statistical analyses. Statistical analyses were performed using JMP 7.0. To compare treatment means, we used a standard 1-way analysis of variance (ANOVA) model that contained a random factor designating the experiment number to account for

between-experiment variation. When 2-way ANOVA was used, this random factor was nested within time. This is important because film from replicate experiments was differentially exposed, resulting in between-experiment variability. Where ANOVA main effects were significant ($p<0.05$), all pairwise differences between means were assessed using Tukey's Honestly Significant Differences (HSD) test with $\alpha = 0.05$.

2.4 Results

2.4.1 Loss of MKP-3 results in increased ERK1/2 phosphorylation. Expression of oncogenic Ras, a frequent occurrence in human carcinogenesis, results in chronic stimulation of the Ras/Raf/MEK1/2/ ERK1/2 protein kinase cascade. We previously observed that MKP-3, a negative regulator of ERK1/2, is upregulated in cell lines that express oncogenic Ras (Warmka et al., 2004). This is illustrated in Fig. 1A, which shows that MKP-3 protein levels are higher in H-ras MCF10A cells, an immortalized human breast epithelial cell line engineered to stably express oncogenic H-Ras, than in parental MCF10A cells cultured under the same serum-starved conditions (Fig. 1A). To test the hypothesis that MKP-3 plays a role in a negative feedback pathway that inhibits ERK1/2 in cells that express oncogenic Ras, we knocked down MKP-3 with siRNA and monitored the phosphorylated, active forms of ERK1/2 by immunoblot in H-ras MCF10A cells and DLD-1 cells, a human colon cancer cell line that expresses an endogenous Ki-Ras oncogene (Shirasawa et al., 1993). Phospho-ERK1/2 was higher in H-ras MCF10A cells (Fig. 1B) and DLD-1 cells (Fig. 1C) in which MKP-3 was knocked down by siRNA than in nontransfected cells or cells transfected with scrambled siRNA (Figs. 1B and C, compare pERK1/2 in lane 2 to lanes 1 and 3, and compare open bars to filled and hatched bars). The siRNA reduced MKP-3 protein by over 90% (Figs. 1B and C, compare MKP-3 in lane 2 to lanes 1 and 3). The siRNA did not cause an increase in the phosphorylated, active forms of MEK1/2, the kinases that phosphorylate and activate ERK1/2 (Figs. 1B and C, top panel). We used lysates from TPA- or EGF-stimulated cells as positive controls for the detection of phospho-MEK1/2 (Figs. 1B and C, lane 4). These data indicate that in cells transfected with siRNA, the increase in phospho-ERK1/2 is due to the loss of its negative regulator MKP-3, and not due to an increase in the activity of

upstream kinases.

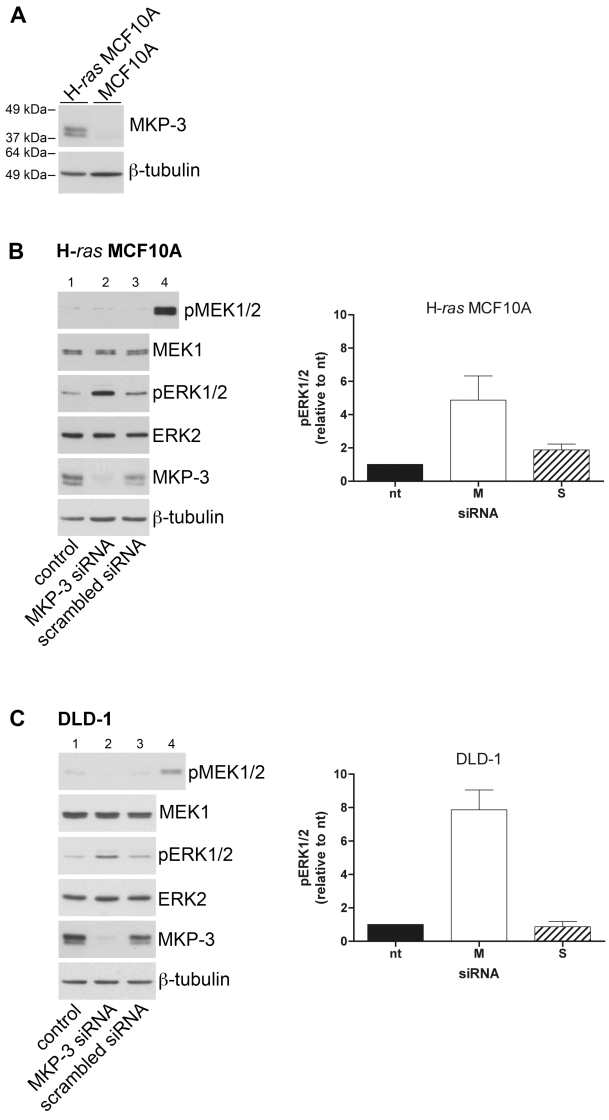

Figure 1

Fig. 1. MKP-3 knockdown via siRNA increases ERK1/2 phosphorylation in H-ras MCF10A and DLD-1 cells. (A) Whole cell lysates were prepared from serum starved MCF10A and H-ras MCF10A cells. MKP-3 (top panel) was detected by immunoblot analysis. The blot was stripped and reprobed for ß-tubulin (bottom panel) as a loading control. Whole cell lysates were prepared from (B) H-ras MCF10A cells or (C) DLD-1 cells that were either not transfected (lane 1), were transfected with duplex siRNA targeted against MKP-3 (lane 2), or were transfected with duplex scrambled siRNA (lane 3). The following proteins were detected by immunoblot analysis: dually phosphorylated, active MEK1/2 (pMEK1/2); total MEK1; dually

phosphorylated, active ERK1/2 (pERK1/2); total ERK2; or MKP-3. The MKP-3 blot was stripped and reprobed for ß-tubulin as a loading control. As a positive control for phospho-MEK1/2, nontransfected cells were incubated for 120 minutes with (B) 1.6 nM TPA (lane 4), or incubated for 30 minutes with (C) 3 nM EGF (lane 4). We and others have observed that MKP-3 typically runs as a doublet (Warmka et al., 2004; Camps et al., 1998a; Muda et al., 1996; Reffas and Schlegel, 2000). The graphs represent average pERK1/2 densitometry relative to non-transfected controls for (B) 10 independent experiments and (C) 6 independent experiments; error bars represent SEM. Filled bars (nt), not transfected. Open bars (M), transfected with duplex siRNA targeted against MKP-3. Hatched bars (S), transfected with duplex scrambled siRNA. Treatment of H-ras MCF10A and DLD-1 cells with MKP3 siRNA resulted in an increase in pERK1/2 levels relative to nontransfected control or treatment with scrambled siRNA (H-ras MCF10A: p= 0.006, n=30, 1-way ANOVA and Tukey's HSD, α=0.05; DLD-1: p=0.0008, n=18, 1-way ANOVA and Tukey's HSD, α=0.05). We did not detect a difference between nontransfected cells or cells transfected with scrambled siRNA.

Next, we tested the role of ERK1/2 in driving the upregulation of MKP-3. We blocked ERK1/2 activity by incubating H-ras MCF10A cells with the MEK1/2 inhibitor U0126 (Fig. 2A, top panel), and then monitored MKP-3 RNA by RT-PCR and MKP-3 protein by immunoblot (Figs. 2B and C). U0126 decreased MKP-3 RNA (Fig. 2B, top panel) and protein (Fig. 2C, top panel) by nearly 90% within 60 min and 8 h, respectively. Similar results were obtained using DLD-1 cells (data not shown). Altogether, these results indicate that ERK1/2 plays a major role in maintaining the elevation of MKP-3, and support the hypothesis that MKP-3 is involved in an ERK1/2-dependent negative feedback loop that suppresses ERK1/2 under conditions where expression of oncogenic Ras is the primary stimulus of the Ras/Raf/ MEK1/2/ERK1/2 pathway.

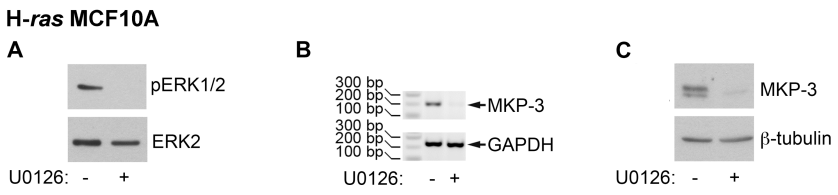

Figure 2

Fig. 2. ERK1/2 is required to maintain elevated levels of MKP-3 RNA and protein. (A) Whole cell lysates

were prepared from H-ras MCF10A cells that were incubated for 60 minutes in the absence (-) or the presence (+) of 3 μM U0126. Dually phosphorylated, active ERK1/2 (pERK1/2, top panel) or total ERK2 (bottom panel) were detected by immunoblot analysis. (B) Total RNA was extracted from H-ras MCF10A cells that were incubated for 60 minutes in the absence (-) or the presence (+) of 3 μM U0126. MKP-3 (top panel) and GAPDH (bottom panel) RNA levels were monitored by RT-PCR. (C) H-ras MCF10A cells were incubated for 8 hours in the absence (-) or presence (+) of 3 μM U0126. MKP-3 protein levels (top panel) were monitored in whole cell lysates by immunoblot analysis, followed by reprobing for β-tubulin (bottom panel) as a loading control. The data shown are representative of at least three independent experiments.

2.4.2 ERK1/2 is involved in the biphasic modulation of MKP-3. We next investigated the relationship between the modulation of ERK1/2 and MKP-3 under conditions where ERK1/2 is further activated by extracellular stimuli. When we incubated H-ras MCF10A cells with TPA, a potent activator of ERK1/2, we observed a striking biphasic modulation of MKP-3 (Fig. 3A, see panel labeled MKP-3 and hatched bars). MKP-3 protein levels decreased dramatically by 30 min. MKP-3 levels recovered by 120 min, however, at which point they were even higher than the initial levels (Fig. 3A). EGF, another potent activator of ERK1/2, stimulated a similar biphasic regulation of MKP-3 in H-ras MCF10A cells and DLD-1 cells (Figs. 3B and C). These intriguing results indicate that initially MKP-3 levels decrease while phospho-ERK1/2 is highly elevated, and that later MKP-3 levels increase while phospho-ERK1/2 decreases. These results suggest that MKP-3 acts in a negative feedback pathway that modulates the time course of ERK1/2 phosphorylation.

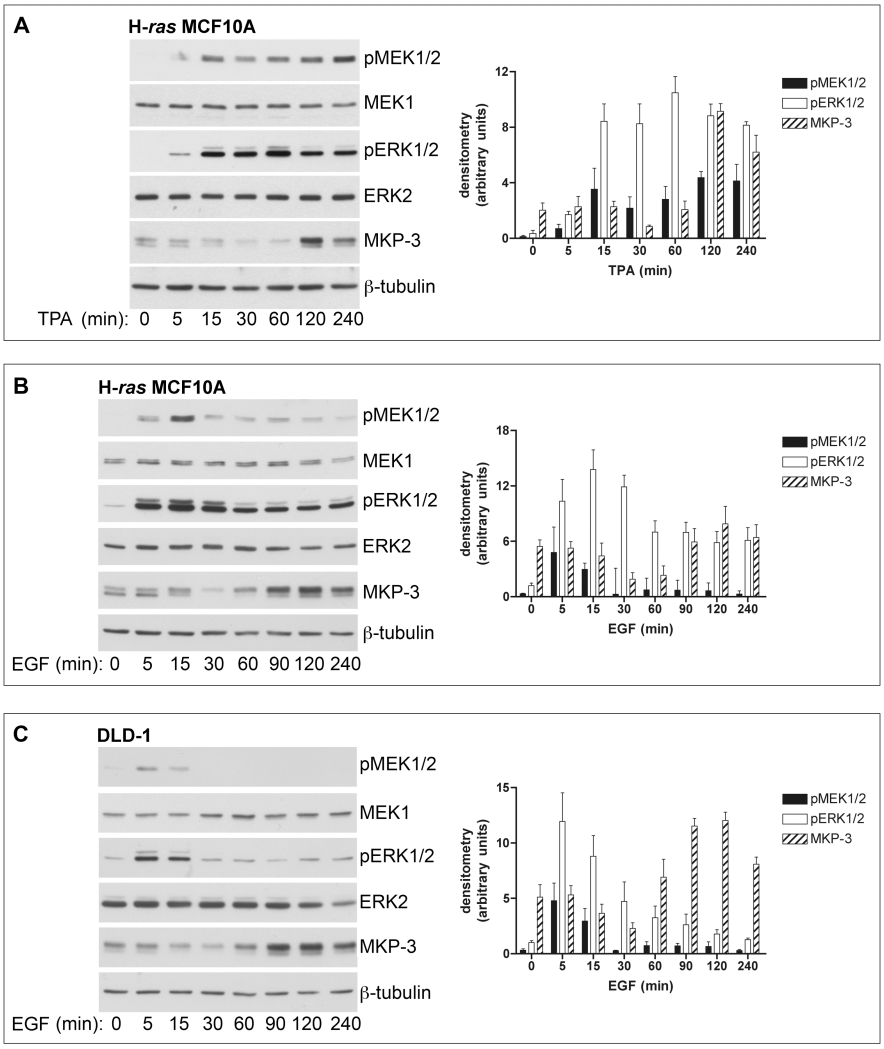

Figure 3

Fig. 3. TPA and EGF stimulate the loss and recovery of MKP-3 protein. Whole cell lysates were prepared from (A) H-ras MCF10A cells that were incubated for the indicated times with 1.6 nM TPA; (B) H-ras MCF10A cells; or (C) DLD-1 cells that were incubated for the indicated times with 3 nM EGF. The following proteins were detected by immunoblot analysis: dually phosphorylated, active MEK1/2 (pMEK1/2); total MEK1; dually phosphorylated, active ERK1/2 (pERK1/2); total ERK2; or MKP-3. The MKP-3 blot was stripped and reprobed for ß-tubulin as a loading control. The graphs represent average densitometry of pMEK1/2, pERK1/2, and MKP-3 for 3 independent experiments; error bars represent SEM. Filled bars, pMEK1/2. Open bars, pERK1/2. Hatched bars, MKP-3.

To understand the biphasic regulation of MKP-3, we began by investigating the initial loss of MKP-3 protein. The modulation of MKP-3 could be due to effects on both MKP-3

RNA and MKP-3 protein. We monitored the effects of TPA on MKP-3 RNA levels by RT-PCR. We found that TPA stimulates an increase in MKP-3 RNA, suggesting that the early loss of MKP-3 is not due to inhibition of MKP-3 gene expression (Figs. 4A, top panel, and B). To determine whether the initial decrease in MKP-3 could be due to a change in protein stability, we incubated cells with cycloheximide, an inhibitor of protein synthesis, in the presence or absence of TPA, and monitored the loss of MKP-3 protein over time by immunoblot. Incubation of the cells with TPA resulted in a more rapid decrease in MKP-3 protein than that observed in control cells (Fig. 4C, compare MKP-3 in lanes 2–5 to lanes 6–9, and Fig. 4E, compare open squares to filled squares). To determine whether the effect of TPA on MKP-3 stability was mediated by ERK1/2, we treated cells with a combination of TPA, the protein synthesis inhibitor cycloheximide, and U0126, which inhibits the activation of ERK1/ 2 by TPA (Fig. 4D, top panel). The TPA-stimulated decrease in MKP- 3 stability was abolished under these conditions (compare MKP-3 in lanes 1 and 6–9 in Figs. 4D to C, and E, filled circles). Similar results were obtained with EGF in H-ras MCF10A cells and DLD-1 cells (data not shown). These results indicate that the initial loss of MKP-3 is due to an ERK1/2-dependent decrease in MKP-3 protein stability.

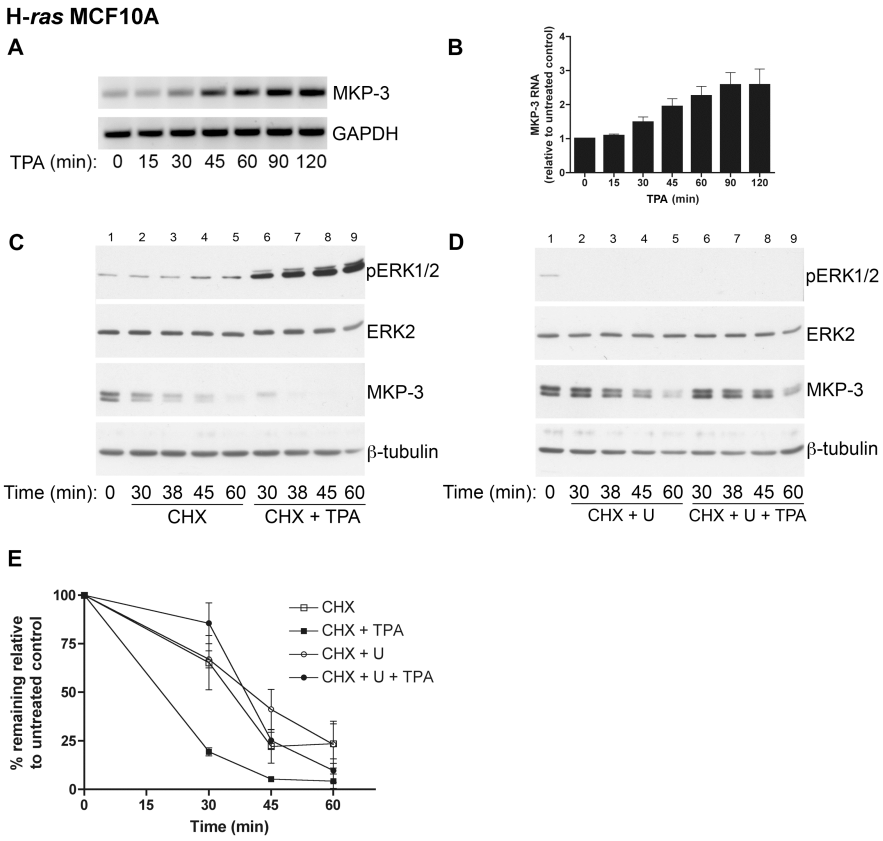

Figure 4

Fig. 4. TPA stimulates a decrease in MKP-3 protein stability through an ERK1/2-dependent pathway in H-ras MCF10A cells. (A) H-ras MCF10A cells were incubated with 1.6 nM TPA for the indicated times. Total RNA was extracted and the levels of MKP-3 RNA (top panel) and GAPDH RNA (bottom panel) were monitored by RT-PCR. (B) The graph represents average densitometry of MKP-3 RNA relative to untreated control from three independent experiments; error bars represent SEM. (C) H-ras MCF10A cells were incubated for the indicated times with 36 μM cycloheximide (CHX) alone or in the presence of 1.6 nM TPA (CHX + TPA). (D) H-ras MCF10A cells were incubated for the indicated times with cycloheximide in the presence of 3 μM U0126 (CHX + U), or U0126 and TPA together (CHX + U + TPA). (C) and (D) The following proteins were detected by immunoblot analysis: dually phosphorylated, active ERK1/2 (pERK1/2); total ERK2; MKP-3. The MKP-3 blot was stripped and reprobed for ß-tubulin as a loading control. (E) The graph represents average MKP-3 densitometry from three independent experiments; error bars represent SEM. Cycloheximide alone (open squares). Cycloheximide plus TPA (filled squares). Cycloheximide plus U0126 (open circles). Cycloheximide plus U0126 and TPA (filled circles). Incubation of the cells with TPA resulted in a more rapid decrease in MKP3 protein than that observed in control cells. We did not detect a difference among all other treatment groups (2-way ANOVA,

n=48, main effect of both time and treatment significant ($p<0.0014$). Differences among treatment means were assessed using Tukey's HSD, $\alpha=0.05$).

Next, we investigated the second phase, in which MKP-3 levels rebound. The observation that TPA stimulates an increase in MKP-3 RNA suggested that the ability of MKP-3 levels to rebound involves transcription (Fig. 4A, top panel). Accordingly, actinomycin D, an inhibitor of transcription, prevented the recovery of MKP-3 protein (Fig. 5A, top panel, compare lane 6 to lane 7, and lane 9 to lane 10, and B, compare open bars to hatched bars). U0126 blocked the ability of TPA to activate ERK1/2 (Fig. 5C, top panel) and blocked the TPA- stimulated increase in both MKP-3 protein (Fig. 5C) and MKP-3 RNA (Fig. 5D, top panel). Similar results were obtained using EGF in H-ras MCF10A cells and DLD-1 cells (data not shown). These data, altogether, support a role for ERK1/2-dependent transcription in the recovery of MKP-3 protein.

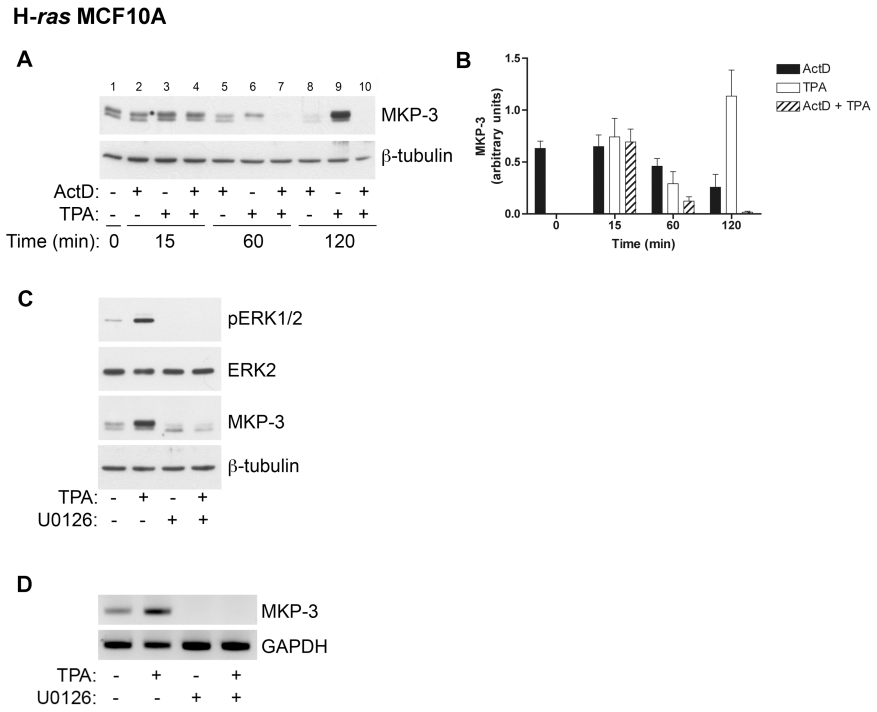

Figure 5

Fig. 5. TPA stimulates an ERK1/2-dependent increase in MKP-3 RNA in H-ras MCF10A cells. (A) H-ras MCF10A cells were incubated for the indicated times without (-) or with (+) 1.6 nM TPA and 6 μM

actinomycin D. MKP-3 protein levels were monitored in whole cell lysates by immunoblot (top panel). The blot was stripped and reprobed for β-tubulin (bottom panel) as a loading control. (B) The graph represents average MKP-3 densitometry from three independent experiments; error bars represent SEM. Filled bars, actinomycin D alone. Open bars, TPA alone. Hatched bars, actinomycin D plus TPA. (C) H-ras MCF10A cells were incubated without (-) or with (+) 1.6 nM TPA and 3 μM U0126 for 120 minutes. The following proteins were detected by immunoblot analysis: dually phosphorylated, active ERK1/2 (pERK1/2); total ERK2; and MKP-3. The MKP-3 blot was stripped and reprobed for ß-tubulin as a loading control. (D) H-ras MCF10A cells were incubated without (-) or with (+) 1.6 nM TPA and 3 μM U0126 for 90 minutes. Total RNA was extracted and the levels of MKP-3 RNA (top panel) and GAPDH RNA (bottom panel) were monitored by RT-PCR. The data shown are representative of at least three independent experiments.

2.4.3 MKP-3 modulates the magnitude and duration of ERK1/2 phosphorylation. The data shown in Fig. 3 indicate that phospho-ERK1/2 decreased and remained suppressed as MKP-3 increased, suggesting the MKP-3 may play a role in the temporal regulation of this kinase. In EGF-stimulated DLD-1 cells, the time course of ERK1/2 phosphorylation was close to the time course of MEK1/2 phosphorylation (Fig. 3C). This suggests that once MEK1/2 is inactivated, phosphatases are involved in rapidly reducing the pool of phospho-ERK1/2, and then maintaining ERK1/2 in its dephosphorylated state.

A role for MKP-3 in regulating the duration of ERK1/2 phosphorylation was revealed when we examined the effects of MKP-3 knockdown on EGF-stimulated ERK1/2 in DLD-1 cells (Figs. 6A and B). Blocking the resynthesis of MKP-3 with siRNA prolonged the EGF-stimulated elevation of ERK1/2 phosphorylation (Figs. 6A, top panel, and B, compare open bars to filled and hatched bars). Under conditions where the elevation of phospho-MEK1/2 and phospho-ERK1/2 was sustained for prolonged periods (greater than 8 h in TPA- and EGF-treated H-ras MCF10A cells), we could not detect an effect of MKP-3 knockdown on ERK1/2 phosphorylation (data not shown). Altogether, these results indicate that MKP-3 plays a role in a negative feedback pathway that curtails EGF-stimulated ERK1/2 activity in DLD-1 cells.

Finally, the observation that MKP-3 is involved in regulating basal and EGF-stimulated ERK1/2 phosphorylation in DLD-1 cells led us to determine if MKP-3 plays a

role in regulating the sensitivity of these cells to other ERK1/2 activators. Fig. 6C illustrates that the loss of MKP-3 sensitizes DLD-1 cells to TNF-α. We observed transient phosphorylation of ERK1/2 by TNF-α in DLD-1 cells (Fig. 6C, top panel). Knockdown of MKP-3 by siRNA increased the duration of TNF-α-stimulated ERK1/2 phosphorylation (Fig. 6C, top panel, and D, compare open bars to filled and hatched bars). These results suggest that the persistent elevation of MKP-3 helps establish the sensitivity of DLD-1 cells to ERK1/2 activators.

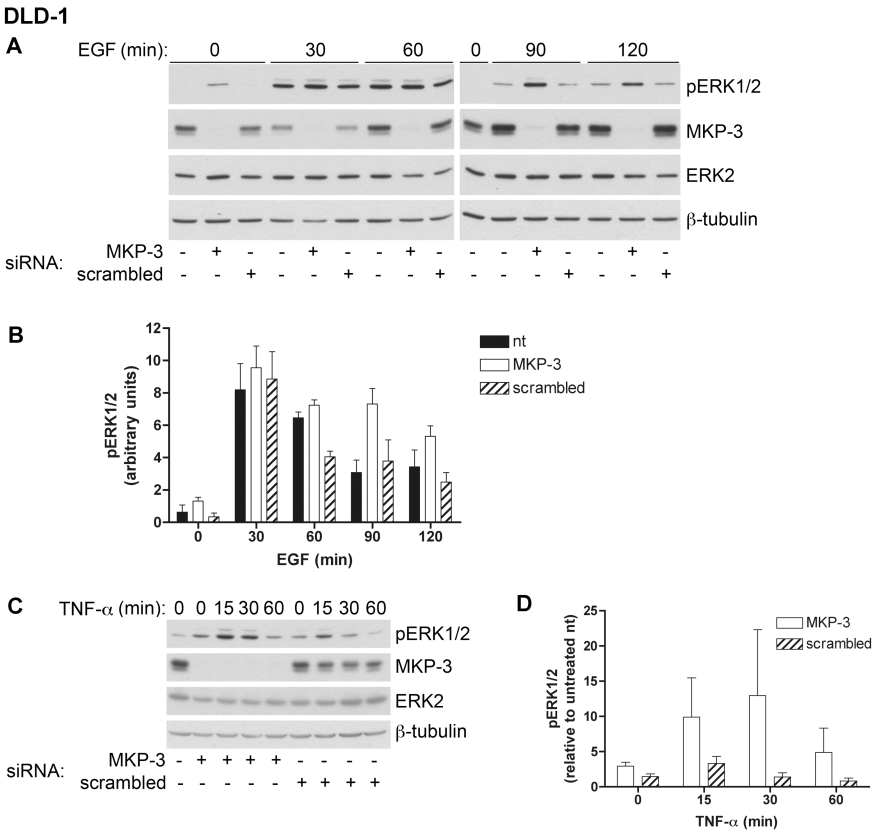

Figure 6

Fig. 6. Knockdown of MKP-3 via siRNA prolongs EGF- and TNF-α-stimulated ERK1/2 phosphorylation in DLD-1 cells. DLD-1 cells were either not transfected (-), or were transfected (+) with either duplex siRNA targeted against MKP-3 (MKP-3) or duplex scrambled siRNA (scrambled). The cells were then incubated for the indicated times with (A) 3 nM EGF or (C) 57 nM TNF-α. Protein from whole cell lysates was analyzed by immunoblot for the following proteins: dually phosphorylated, active ERK1/2 (pERK1/2); MKP-3; total ERK2; or ß-tubulin. Please note that the panels shown in (A) represent two different blots, but that the same lysate was used for the zero time point in both blots. (B) The graph represents average

pERK1/2 densitometry from three independent experiments; error bars represent SEM. Knockdown of MKP3 with siRNA prolonged the EGF-stimulated elevation of ERK1/2 phosphorylation. We did not detect a difference in the level of pERK1/2 in nontransfected and scrambled samples (2-way ANOVA, n=45, main effect of both treatment and time significant at $p<0.001$. Differences among treatment means were assessed using Tukey's HSD, $\alpha=0.05$). Filled bars, nontransfected. Open bars, transfected with duplex siRNA targeted against MKP-3. Hatched bars, transfected with duplex scrambled siRNA. (D) The graph represents average pERK1/2 densitometry relative to nontransfected controls from four independent experiments; error bars represent SEM. Knockdown of MKP3 with siRNA prolonged the TNFα-stimulated elevation of ERK1/2 phosphorylation. We did not detect a difference in the level of pERK1/2 in nontransfected and scrambled samples (2-way ANOVA, n=46 main effect of treatment significant at $p<0.017$. Differences among treatment means were assessed using Tukey's HSD, $\alpha=0.05$). Filled bars, nontransfected. Filled bars, nontransfected. Open bars, transfected with duplex siRNA targeted against MKP-3. Hatched bars, transfected with duplex scrambled siRNA.

2.5 Discussion

Aberrant regulation of the Ras/Raf/MEK1/2/ERK1/2 pathway frequently occurs in human carcinogenesis (Downward, 2003). Our work and the work of others have shown that MKP-3, a putative tumor suppressor and regulator of ERK1/2, is often upregulated in cells and tissues that exhibit abnormal activation of the Ras/Raf/MEK1/2/ERK1/2 pathway (Croonquist et al., 2003; Furukawa et al., 2003; Warmka et al., 2004; Sweet-Cordero et al., 2005). This observation led us to investigate the action of this phosphatase within the context of oncogenic Ras expression. MKP-3 has been mainly studied in *in vitro* and exogenous overexpression systems. Most studies that report on endogenous MKP-3 have focused on understanding the regulation of FGF-stimulated signaling during development *in vivo* (Kawakami et al., 2003; Tsang et al., 2004; Gomez et al., 2005; Li et al., 2007). To our knowledge, the roles and regulation of endogenous MKP-3 in cells that express oncogenic Ras have not been previously explored. This is an important area of investigation because expression of oncogenic Ras results in chronic stimulation of the Ras/Raf/MEK1/2/ERK1/2 pathway; under such conditions, which frequently occur in human carcinogenesis, MKP-3 may be a key modulator.

The results presented here revealed two types of roles for endogenous MKP-3 in suppressing ERK1/2 in cells that express oncogenic Ras. First, MKP-3 is involved in a

negative feedback pathway that suppresses ERK1/2 when expression of oncogenic Ras is the primary stimulus of the Ras/Raf/MEK1/2/ERK1/2 pathway (Fig. 7). We used two tools, the pharmacological inhibitor U0126 and siRNA targeted against MKP-3, to demonstrate that in serum-starved H-ras MCF10A and DLD-1 cells, ERK1/2 drives the upregulation of MKP-3, which in turn dephosphorylates and thus inactivates ERK1/2. This suggests that MKP-3 keeps the basal level of ERK1/2 activity in check even under the pressure of stimulation by oncogenic Ras. Knockdown of MKP-3 by siRNA also results in an increase in ERK1/2 phosphorylation when the cells are maintained in complete media (data not shown), indicating that MKP-3 inhibits ERK1/2 even in the presence of serum. Second, our studies indicate that MKP-3 can act in a negative feedback pathway that modulates the duration of ERK1/2 activity when cells that express oncogenic Ras undergo further stimulation by extracellular agents. This was revealed when we found that knockdown of MKP-3 by siRNA prolonged the EGF- and TNF-α-stimulated elevation of phospho-ERK1/2 in DLD-1 cells. In EGF-stimulated DLD-1 cells, the decrease in phospho-ERK1/2 preceded the recovery of MKP- 3, which suggests that other phosphatases may also be involved in the initial dephosphorylation of ERK1/2 (see Fig. 3C). We were not able to detect an effect of MKP-3 knockdown on TPA- or EGF-stimulated ERK1/2 phosphorylation in H-ras MCF10A cells under the conditions of our studies. TPA stimulated prolonged, highly elevated MEK1/2 activity in H-ras MCF10A cells (see Fig. 3A), which could counteract and mask the action of MKP-3 and thus explain the prolonged, elevated activation of ERK1/2. Further research is required to determine why the regulation of EGF-stimulated ERK1/2 differs so dramatically between H-ras MCF10A cells and DLD-1 cells, however. The two cell lines could certainly differ with respect to the balance between and access to ERK1/2 regulators because of differences in the following: 1) mechanism of oncogenic Ras expression (engineered overexpression in H-ras MCF10A cells versus endogenous expression in DLD-1); 2) expression of the oncogenic Ras family member (H-Ras versus Ki-Ras); and 3) the cell type (breast versus colon). Altogether, our studies indicate that the persistent elevation of MKP-3 can help restrict the ERK1/2 response of cells that express oncogenic Ras. The differences we observed between H-ras MCF10A and DLD-1 indicate, however, that the

effectiveness of MKP-3 in suppressing ERK1/2 is likely to vary depending on many conditions.

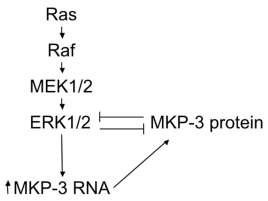

Figure 7

Fig. 7. Reciprocal regulation of ERK1/2 and MKP-3. Phosphorylation and activation of ERK1/2 typically occurs through stimulation of the Ras/Raf/MEK1/2 protein kinase cascade. The GTPase Ras activates the protein kinase Raf, which phosphorylates and activates the protein kinases MEK1/2. MEK1/2 is highly specific for phosphorylating and activating ERK1/2. The magnitude and duration of ERK1/2 activity is determined by the balance between the activity of MEK1/2, the kinases that phosphorylate and activate ERK1/2, and the activity of phosphatases, such as MKP-3, which dephosphorylate and inactivate ERK1/2. The levels of MKP-3 protein available to inhibit ERK1/2 are regulated, at least in part, by ERK1/2. ERK1/2 can stimulate an increase in the expression of MKP-3 RNA. This results in an increase in MKP-3 protein, which can then feedback and inhibit ERK1/2 activity. ERK1/2 can also stimulate a decrease in MKP-3 protein stability, however, which can cause a loss of MKP-3 protein. Thus, the levels of MKP-3 protein are determined, at least in part, by the balance between the stimulation of new MKP-3 gene expression and the stability of the MKP-3 protein.

The various roles of MKP-3 in regulating ERK1/2 are countered by the multiple mechanisms by which ERK1/2, in turn, regulates MKP-3 (Fig. 7). Stimulation of both cell lines revealed a striking ERK1/2-dependent biphasic modulation of MKP-3. The initial downregulation of MKP-3 appears to involve ERK1/2-dependent protein destabilization. Our results are consistent with those of Marchetti et al., who used hamster fibroblast cells that overexpress exogenous MKP-3 to show that ERK1/2 phosphorylates MKP-3 and targets it for proteasomal degradation (Marchetti et al., 2005). The function of the initial ERK1/2-dependent downmodulation of MKP-3 is not yet clear. It has been suggested that MKP-3, which is localized to the cytoplasm, may regulate the subcellular localization of ERK1/2 (Karlsson et al., 2004). Further studies are required to determine if the initial loss of MKP-3 in stimulated H-ras MCF10A and DLD-1 cells liberates ERK1/2 from its cytoplasmic anchor so that this kinase can translocate to other

subcellular compartments. Our studies indicate that transcription is required for MKP-3 protein levels to rebound following its initial downmodulation, and furthermore that ERK1/2 plays a major role in the regulation of both basal and stimulated MKP-3 gene expression. The rapid rebound in MKP-3 levels following its initial downmodulation suggests that cells that express oncogenic Ras are poised to maintain elevated MKP-3 levels, and thus limit ERK1/2 activity.

The regulation of MKP-3 gene expression varies widely depending on the system. In H-ras MCF10A cells the induction of MKP-3 is detected relatively rapidly (within 60 min). TPA and EGF induce MKP- 3 gene expression in a similar manner in the parental MCF10A cells, indicating that the ability to stimulate MKP-3 gene expression in this cell line does not depend on the expression of oncogenic Ras (data not shown). In other systems, the induction of MKP-3 is only detected after prolonged (greater than 12 h) exposure to stimuli (Woods and Johnson, 2006). Finally, MKP-3 has been reported to be mainly constitutively expressed and not strongly inducible in other systems, such as human skin fibroblasts (Groom et al., 1996; Dowd et al., 1998). Such differences may be due to cell-type dependent differences in the expression of transcriptional machinery and the operation of signaling networks.

The data presented here generally show greater levels of phospho-ERK2 (pp42 ERK) than phospho-ERK1 (pp44) in both resting and simulated H-ras MCF10A and DLD-1 cells. This apparent preferential phosphorylation of ERK2 over ERK1 has been observed in several cell lines (Pelech, 2006; Vantaggiato et al., 2006). Interestingly, stimulation of the cells with EGF or TPA resulted in increases in both ERK1 and ERK2 phosphorylation, whereas knockdown of MKP-3 in serum-starved cells, in which oncogenic Ras is the primary stimulus, mainly resulted in an increase in ERK2 phosphorylation. The mechanism underlying such apparent preferential phosphorylation has not been established, but it is likely to be due, at least in part, to the interactions between subcellular localization and levels of several proteins, including ERK1, ERK2, MEK1, MEK2, protein scaffolds, and protein phosphatases (Pelech, 2006; Lefloch et al., 2008).

The observation that knockout of ERK2 *in vivo* is lethal, whereas knockout of ERK1

is not indicates that ERK1 and ERK2 have different functions (Pages et al., 1999; Yao et al., 2003). This suggests that differential dephosphorylation and inactivation of ERK1 and ERK2 could affect the cellular response to stimuli that activate the Ras/Raf/MEK/1/2/ERK1/2 pathway. Further research is required to determine whether the specificity of MKP-3 differs for ERK1 versus ERK2. Although knockdown of MKP-3 in serum-starved H-ras MCF10A and DLD-1 cells appears to primarily result in an increase in phospho-ERK2 levels, we have found that knockdown of MKP-3 in other cell lines results in a clear increase in both phospho-ERK1 and phospho-ERK2 (data not shown). Muda et al., reported that MKP-3 binds equally well to both ERK1 and ERK2, as indicated by the ability of a GST-MKP-3 fusion protein to precipitate ERK1 and ERK2 from cell lysates prepared from cells in which the different ERK isoforms were overexpressed (Muda et al., 1998). To our knowledge a direct comparison of the specificity of MKP-3 for dephosphorylating ERK1 versus ERK2 has not been published, however. The balance between the phosphorylated and dephosphorylated states of ERK1 and ERK2 is likely to depend on a complex set of interactions and conditions, as discussed above.

It might be expected that expression of oncogenic Ras would result in superactivation of ERK1/2. Instead, our studies suggest that cells may adapt to the expression of oncogenic Ras, and the chronic stimulation of the Ras/Raf/MEK1/2/ERK1/2 pathway, by upregulating MKP-3, which then suppresses ERK1/2. This hypothesis is consistent with the concept of MKP-3 as a tumor suppressor, and might help explain, at least in part, why activation of Ras alone is not sufficient to induce tumors. That is, cells respond to the expression of oncogenic Ras by upregulating MKP-3, which serves to rein in ERK1/2 activity; disruption of MKP-3, in turn, unleashes ERK1/2 activity and thus contributes another step along the pathway of carcinogenesis. Previous results from our laboratory on the novel skin tumor promoter palytoxin support this hypothesis (Warmka et al., 2002; Zeliadt et al., 2003; Warmka et al., 2004). In the classic multi-stage mouse skin model of carcinogenesis, the first stage, known as initiation, typically involves activation of the oncogene Ras; subsequent repeated stimulation by tumor promoters results in tumor development (Balmain and Pragnell, 1983; Yuspa, 1998). We previously demonstrated

that palytoxin, a nonphorbol ester tumor promoter in the multi-stage mouse skin model of carcinogenesis, stimulates ERK1/2 activation by triggering the downmodulation of MKP-3 in mouse keratinocytes derived from initiated mouse skin that express oncogenic Ras (Warmka et al., 2004). Accordingly, we also showed that palytoxin modulates several targets that have been implicated in carcinogenesis, including c-Fos, AP-1, and matrix metalloprotease-13, through ERK1/2-dependent pathways in these cells (Warmka et al., 2002). Further research is required to determine whether knockdown of MKP-3 mimics palytoxin action and whether MKP-3 is a target for other carcinogenic agents.

Interestingly, studies that implicate MKP-3 as a tumor suppressor in pancreatic cancer, which is characterized by a high frequency of activating Ras mutations, reported an association between elevated expression of MKP-3 at early stages of pancreatic cancer, but a loss of MKP-3 at advanced stages (Furukawa et al., 2003). It has been estimated that oncogenic Ras is expressed in over 40% of colon tumors (Bos et al., 1987; Downward, 2003). In breast cancer the regulation of the Ras/Raf/MEK/1/2/ERK1/2 pathway is frequently undermined by the aberrant regulation of growth factor receptors (Santen et al., 2002). Limited information has been published concerning the expression of MKP-3 in these cancers (Cui et al., 2006). Further research is therefore required to determine how the expression of MKP-3 changes during colon and breast carcinogenesis and whether MKP-3 functions as a tumor suppressor in these types of cancers.

Given that activation of Ras frequently occurs in human cancers (Downward, 2003), there is an urgent need to understand the biochemical characteristics of cells that express activated Ras that make them particularly susceptible to agents and events that advance the process of carcinogenesis. The unstable nature of MKP-3 makes it a potentially vulnerable target in such cells. Altogether, the evidence that aberrant ERK1/2 activity plays a role in carcinogenesis together with the identification of MKP-3 as a potential tumor suppressor, underscores the importance of understanding the nature of the repartee between this centrally important protein kinase and its modulator.

Acknowledgments

We thank Dr. Aree Moon for her generous contribution of the H-ras MCF10A and

parental MCF10A cell lines, Margaret Byrne, Ngozika Okoye, and Aaron Charlson for their technical assistance with preliminary studies, and William C. Ratcliff for his assistance with statistical analysis. This work was supported by National Institutes of Health grant RO1-CA104609 (to E.V. W.). The National Institutes of Health was not involved in study design, collection, analysis, or interpretation of data, writing the manuscript, or the decision to submit the manuscript for publication.

Chapter III

Extracellular signal regulated kinase 5 mediates signals triggered by the novel tumor promoter palytoxin

Rationale. While the studies presented in Chapter II were in progress, we discovered several reports suggesting that ERK5 may be a substrate for MKP-3 (Kamakura et al., 1999; Rita Sarközi et al., 2007; Zou et al., 2006). These studies relied on overexpression of MKP-3 in cells and interactions between ERK5 and MKP-3 *in vitro*. There were no published studies examining the role of endogenous MKP-3 in regulating ERK5, however.

Our initial investigation into whether ERK5 was a substrate for MKP-3 relied on the use of U0126, a pharmacological inhibitor of MEK1/2, to prevent EGF-stimulated MKP-3 induction (see Fig. 5C in Chapter 2). An examination of the literature, however, revealed several reports demonstrating that several MEK1/2 inhibitors can also inhibit MEK5, the MAPK kinase that phosphorylates and activates ERK5 (Bain et al., 2007; Mody et al., 2001). These studies led to an MKP-3 siRNA-based approach to investigate the possibility that MKP-3 may play a role in the temporal regulation of EGF-stimulated ERK5 activation in DLD-1 cells (Fig. S1).

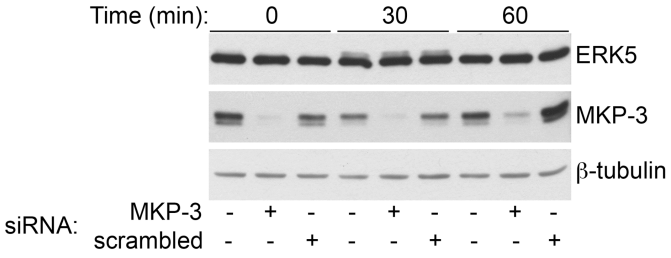

Fig. S1. Knockdown of MKP-3 via siRNA does not affect EGF-stimulated ERK5 activation. DLD-1 cells were either not transfected (-), or were transfected (+) with either duplex siRNA targeted against MKP-3 (MKP-3) or duplex scrambled siRNA (scrambled). The cells were then incubated for the indicated times with 3 nM EGF. Protein from whole cell lysates was analyzed by immunoblot for the following proteins: ERK5; MKP-3; or ß-tubulin.

I used an ERK5-specific antibody in an immunoblot of whole cell lysates to analyze the effect of MKP-3 knockdown on EGF-stimulated ERK5 activation. Others have demonstrated that ERK5 phosphorylation, which corresponds to ERK5 activity, is indicated by the appearance of a slower migrating form of ERK5 as detected by immunoblot (Kato et al., 1998; Esparis-Ogando et al., 2002; Mody et al., 2003; Scapoli et al., 2004; Woo et al., 2008; Montero et al., 2009).

The data shown in Fig. S1 do not support a role for MKP-3 in regulating ERK5 activation. Knockdown of MKP-3 with MKP-3 siRNA does not have an effect on the magnitude or duration of EGF-stimulated ERK5 activation. In support of this, another group recently published data demonstrating that overexpressed MKP-3 does not bind to or dephosphorylate ERK5 in cells, and MKP-3 overexpression does not block ERK5-dependent downstream signaling (Arkell et al., 2008). Altogether, these data suggest that MKP-3 does not play a major role in a negative feedback pathway that reduces EGF-stimulated ERK5 activity in DLD-1 cells.

The observation that MEK1/2 inhibitors can also inhibit MEK5 suggests that functions believed to be ERK1/2-dependent need to be reevaluated for the possible involvement of ERK5. Because we had previously shown that palytoxin stimulates c-Fos expression in an ERK1/2 dependent pathway using these inhibitors (Warmka et al., 2002), we decided to investigate whether ERK5 could be activated by palytoxin, and whether there was a role for ERK5 in modulating palytoxin-stimulated c-Fos expression. Furthermore, because palytoxin interacts with the Na+,K+-ATPase and stimulates ion influx, it induces a type of osmotic stress and activates the stress-activated MAPKs JNK and p38 (Kuroki et al., 1996; Kuroki et al., 1997; Li and Wattenberg, 1998; Li and Wattenberg, 1999; Wattenberg, 2007). Because ERK5 can also be activated by stress, such as osmotic shock and oxidative stress, we wanted to investigate the possibility that ERK5 may transduce palytoxin-induced signals (Abe et al., 1996).

Results. We found that palytoxin, but not TPA, activates ERK5 in two cell lines, 308 and HeLa cells. 308 cells are immortalized mouse keratinocytes derived from mouse skin that was initiated *in vivo* and express activated Ras. We used 308 cells extensively in our

original investigations of the biological effects of tumor promoters on MAPKs (Warmka et al., 2002; Warmka et al., 2004; Zeliadt et al., 2003; Zeliadt et al., 2004). We used HeLa cells because they have been used by others to characterize the function of ERK5 and other signaling pathways, and because are easier to transfect than 308 cells. Furthermore, because HeLa is a human cell line, these cells were amenable to the generation of stable cells that express an ERK5 shRNA that targets the human ERK5 gene.

We also found that palytoxin activates ERK5 through a Na+,K+-ATPase-dependent mechanism that is not mimicked by protein synthesis inhibitors or inhibition of phosphatases. This is distinct from the mechanism in which palytoxin activates ERK1/2, which we previously found was mimicked by inhibition of protein synthesis and involved down-regulation of the ERK1/2 phosphatase, MKP-3 (Warmka et al., 2004). Finally, we found that ERK5 contributes to the palytoxin-stimulated increase in c-Fos gene expression.

Conclusions and Significance. The finding that palytoxin can stimulate ERK5 activity is significant because it suggests that some of the roles previously attributed to ERK1/2 (through the use of MEK1/2 inhibitors) may need to be reevaluated. Furthermore, these studies revealed that tumor promoters such as palytoxin can activate several MAPK pathways through diverse mechanisms.

Contributions. I contributed directly to the work published in this paper by showing that ERK5 is involved in palytoxin-stimulated but not TPA-stimulated c-Fos RNA induction (see Fig. 10 and Fig. 11). For these experiments, Aaron Charlson plated, treated and harvested cells, and purified the RNA, and I carried out the cDNA synthesis, qPCR, and data analysis. I also conducted all statistical analyses of the data. I contributed to preliminary and non-published work by 1) demonstrating that differential doses of MEK1/2 inhibitors can be used to inhibit either ERK1/2 activation alone, or both ERK1/2 and ERK5 activation in HeLa cells treated with EGF; and 2) establishing conditions for immunoprecipitation and *in vitro* analysis of ERK5 activation. The remainder of this chapter is the published paper, reprinted from *Toxicology and Applied Pharmacology,*

Vol 241, Aaron T. Charlson, Nicholette A. Zeliadt, and Elizabeth V. Wattenberg, "Extracellular signal regulated kinase 5 mediates signals triggered by the novel tumor promoter palytoxin," pp 143-153, Copyright (2009), with permission from Elsevier.

3.1 Abstract

Palytoxin is classified as a non-12-*O*-tetradecanoylphorbol-13-acetate (TPA)-type skin tumor because it does not bind to or activate protein kinase C. Palytoxin is thus a novel tool for investigating alternative signaling pathways that may affect carcinogenesis. We previously showed that palytoxin activates three major members of the mitogen activated protein kinase (MAPK) family, extracellular signal regulated kinase 1 and 2 (ERK1/2), c-Jun N-terminal kinase (JNK), and p38. Here we report that palytoxin also activates another MAPK family member, called ERK5, in HeLa cells and in keratinocytes derived from initiated mouse skin (308 cells). By contrast, TPA does not activate ERK5 in these cell lines. The major cell surface receptor for palytoxin is the Na+,K+-ATPase. Accordingly, ouabain blocked the ability of palytoxin to activate ERK5. Ouabain alone did not activate ERK5. ERK5 thus represents a divergence in the signaling pathways activated by these two agents that bind to the Na+,K+-ATPase. Cycloheximide, okadaic acid, and sodium orthovanadate did not mimic the effect of palytoxin on ERK5. These results indicate that the stimulation of ERK5 by palytoxin is not simply due to inhibition of protein synthesis or inhibition of serine/threonine or tyrosine phosphatases. Therefore, the mechanism by which palytoxin activates ERK5 differs from that by which it activates ERK1/2, JNK, and p38. Finally, studies that used pharmacological inhibitors and shRNA to block ERK5 action indicate that ERK5 contributes to palytoxin-stimulated c-Fos gene expression. These results suggest that ERK5 can act as an alternative mediator for transmitting diverse tumor promoter-stimulated signals.

3.2 Introduction

Agents identified as tumor promoters in the classic multi-stage mouse skin model of carcinogenesis have helped reveal how the perturbation of signaling pathways contributes

to the development of cancer (Yuspa, 1998). Initiation, the first stage of carcinogenesis in this model, typically involves one treatment with a genotoxic agent and is characterized by activation of the oncogene Ras (Balmain and Pragnell, 1983). Tumor promotion, the second stage, involves repeated stimulation over a prolonged period by agents that are typically non-genotoxic, and results in the development of tumors. Interestingly, whereas initiation is irreversible, tumor promotion is reversible if treatment is ceased. This suggests that investigating the action of tumor promoters may aid the development of strategies to block carcinogenesis. The identification of protein kinase C as the receptor for the prototypical skin tumor promoter 12-*O*-tetradecanoylphorbol-13-acetate (TPA, also called PMA) helped establish that tumor promotion involves the subversion of signal transduction pathways (Nishizuka, 1984). The subsequent identification of non-TPA-type tumor promoters, which do not activate protein kinase C *in vitro* or require protein kinase C for signal transduction, indicated that protein kinase C-independent signaling pathways also play a role in carcinogenesis (Fujiki et al., 1986; Wattenberg et al., 1987). Accordingly, our laboratory has used the non-TPA-type tumor promoter palytoxin to investigate alternative signaling pathways that may play a role in carcinogenesis, but may have been missed by the historical focus on TPA-stimulated signaling.

The major cell surface receptor for palytoxin is the Na+,K+-ATPase (Habermann, 1989). Palytoxin, a large (Mr 2,681) water-soluble polyalcohol, which is isolated from zoanthids (genus Palythoa) (Moore, 1985), binds to the Na+,K+-ATPase and transforms the sodium pump into an ion channel. Palytoxin binding thus typically triggers sodium influx and potassium efflux. Our previous studies indicated that mitogen activated protein kinases (MAPKs) can mediate palytoxin-stimulated signaling (Kuroki et al., 1997; Li and Wattenberg, 1999; Warmka et al., 2002; Warmka et al., 2004).

MAPKs are a family of serine/threonine kinases that transmit a wide variety of signals to the cellular machinery that regulates gene expression, cell fate, and cell function (reviewed by Turjanski et al. (2007)). Several studies also indicate that aberrant regulation of MAPKs plays a role in carcinogenesis (Dhillon et al., 2007). The three groups of MAPKs that have been studied most extensively are the extracellular signal regulated kinases 1 and 2 (ERK1/2), the c-Jun N-terminal kinases (JNKs), and the p38s.

In general ERK1/2 tends to be activated by mitogenic agents, whereas JNK and p38 are typically activated by stress (Turjanski et al., 2007). Our work indicates that MAPKs can mediate the convergence of the different signaling pathways stimulated by palytoxin and TPA, thus providing a mechanism by which these different types of tumor promoters can regulate common biochemical targets that play an important role in carcinogenesis (Warmka et al., 2002; Warmka et al., 2004). For example, we found that palytoxin and TPA both increase ERK1/2 activity, although by different mechanisms, in mouse keratinocytes that are derived from initiated mouse skin and express oncogenic Ras (308 cells); this results in the ability of palytoxin and TPA to regulate common downstream nuclear targets, including the transcription factor AP-1 (Warmka et al., 2002; Warmka et al., 2004; Zeliadt et al., 2004).

ERK5 (also called Big MAP kinase 1 or BMK1) is a MAPK family member that is likely to play a role in carcinogenesis, but has not been studied as extensively as ERK1/2, JNK, and p38 (reviewed by Wang and Tournier (2006)). Like other MAPKs, activation of ERK5 requires dual phosphorylation on specific threonine and tyrosine residues (Mody et al., 2003). MAPKs are typically activated by a protein kinase cascade, such that a MAPK kinase kinase (MAPKKK or MEKK) phosphorylates and activates a MAPK kinase (MAPKK or MEK), which phosphorylates and activates a MAPK (Wang and Tournier, 2006). For example, Raf is a MAPKKK that phosphorylates and activates MEK1/2, which phosphorylates and activates ERK1/2 (reviewed by Dhillon et al. (2007)). MEKK2 and MEKK3 have been identified as MAPKKKs, which phosphorylate and activate MEK5, the MAPKK that phosphorylates and activates ERK5 (Chao et al., 1999; Sun et al., 2001). A unique, large *C*-terminal non-kinase domain makes ERK5 approximately twice the size of ERK1/2 (Lee et al., 1995; Zhou et al., 1995). This *C*-terminal domain contains a nuclear localization signal (Hayashi and Lee, 2004). ERK5, like other MAPK family members, can translocate from the cytoplasm to the nucleus, where it can regulate transcription factors, including MEF2C (myocyte enhancer factor), Sap1a, and c-Fos (Kato et al., 1997; Kamakura et al., 1999; Terasawa et al., 2003). ERK5 is activated by mitogens, such as epidermal growth factor (EGF), and also by stress, such as osmotic shock and oxidative stress (Abe et al., 1996; Kato et al., 1998). Because

palytoxin causes a type of osmotic stress by stimulating ion influx, we wanted to determine whether ERK5 mediates palytoxin-induced signals.

We used two cell culture models to determine whether ERK5 is involved in palytoxin signaling. We used 308 mouse keratinocytes, which were derived from mouse skin initiated in vivo with 7,12-dimethylbenz(a)anthracene and express endogenous oncogenic Ras (Strickland et al., 1988). This is thus an excellent model for studying tumor promoter action. We also used HeLa cells, a human cervical cancer cell line that has been used extensively to study MAPK signaling. HeLa cells, in contrast to keratinocytes, are relatively easy to transfect. This makes HeLa cells very useful for the study of signaling by methods that require the introduction of expression vectors. Our results indicate that ERK5 can mediate the transmission of palytoxin-stimulated signals from the Na+,K+-ATPase to the nucleus. In contrast to palytoxin, we did not detect activation of ERK5 by the prototypical phorbol ester tumor promoter TPA. Altogether, these studies indicate that ERK5 represents an alternative pathway through which diverse tumor promoters can transmit signals.

3.3 Materials and Methods

3.3.1 Materials. Palytoxin was purchased from the Hawaii Biotechnology Group, Inc. (Aiea, HI). U0126 was purchased from Calbiochem (La Jolla, CA). High glucose Dulbecco's modified Eagle medium, minimum essential medium, and fetal bovine serum were purchased from Invitrogen Corporation (Carlsbad, CA). TPA, cycloheximide, EGF, protein G agarose beads, ouabain, sodium orthovanadate, okadaic acid, phenylmethylsulfonyl fluoride (PMSF), NaF, β-glycerophosphate, aprotinin, leupeptin, and sorbitol were purchased from Sigma (St. Louis, MO). Calf intestinal alkaline phosphatase was purchased from New England Biolabs (Ipswich, MA).

3.3.2 Cell culture. HeLa cells were the generous gift of Dr. Audrey Minden (Susan Lehman Cullman Laboratory for Cancer Research, Department of Chemical Biology, Ernest Mario School of Pharmacy, Rutgers, The State University of New Jersey), and were grown as previously described (Li and Wattenberg, 1998). 308 cells were the generous gift of Dr. Stuart H. Yuspa (Laboratory of Cellular Carcinogenesis and Tumor

Promotion, National Cancer Institute), and were grown as previously described (Warmka et al., 2004). For experiments, HeLa and 308 cells were plated at a density of approximately $2.4 \times 10^4/cm^2$ and $5.6 \times 10^4/cm^2$, respectively. The following day, the cells were switched to serum free media. The cells were incubated in serum free media for approximately 24 h before treatment, unless otherwise indicated.

3.3.3 Antibodies and immunoblotting. Cell lysates were prepared using the following buffer unless otherwise noted: 50 mM Tris–HCl, 1% NP-40, 0.25% Na-deoxycholate, 150 mM NaCl, 1 mM EDTA, 1 mM PMSF, 1 μg/ml aprotinin, 1 μg/ml leupeptin, 20 mM β-glycerophosphate, 1 mM Na_3VO_4, and 1 mM NaF. Lysates were cleared by centrifugation (16,000 × g, 10 min, 4 °C). Protein (20–40 μg) was resolved using either 7.5% or 10% SDS–polyacrylamide minigels, and then transferred to Immobilon-P PVDF membrane (Millipore, Bedford, MA). After blocking in either a TBST/5% milk solution or TBST/3% BSA solution, immunoblots were incubated overnight at 4 °C using the following primary antibodies and dilutions: phospho-p44/42 MAPK (Thr-202/Tyr-204) (E10) (mouse monoclonal) (1:2000), phospho-ERK5 (Thr-218/Tyr-220) (rabbit polyclonal) (1:1000), ERK5 (rabbit polyclonal) (1:1000), phospho-p38 MAPK (Thr-180/Tyr-182) (rabbit polyclonal) (1:2000), and phospho-SAPK/JNK (Thr-183/Tyr-185) (G9) (mouse monoclonal) (1:2000) from Cell Signaling (Beverly, MA), and ERK2 (C-14) (rabbit polyclonal) (1:2000), JNK1 (FL) (rabbit polyclonal) (1:2000), and p38 (C-20) (rabbit polyclonal) (1:2000) from Santa Cruz Biotechnology (Santa Cruz, CA). The following secondary antibodies were used: anti-mouse IgG horseradish peroxidase-linked antibody and anti-rabbit IgG horseradish peroxidase-linked antibody from Cell Signaling. Immunoblots were visualized using the Pierce SuperSignal West Pico substrate.

3.3.4 Densitometry. Protein bands from immunoblots were quantified using a Bio-Rad (Hercules, CA) Fluor-S MultiImager and Bio-Rad Quantity One software.

3.3.5 Quantitative real-time PCR analysis. Total RNA was harvested from cells using the RNeasy Plus Mini Kit from Qiagen (Valencia, CA). RNA quality was verified spectrophotometrically using the A_{260}/A_{280} ratio. One microgram of RNA was reverse-transcribed using the SuperScript III from Invitrogen (Carlsbad, CA). Negative controls

that lacked RNA or reverse transcriptase were included for each primer pair. cDNA was diluted 1:10, and 2 µl of diluted cDNA were used in 25 µl PCR reactions with 200 nM of each primer and SYBR GreenER qPCR SuperMix for iCycler (Invitrogen). PCR was performed on a Bio-Rad iCycler iQ5 using the following primers: human c-Fos (accession no. NM_005252), 5′-CGGGCTTCAACGCAGACTA-3′ (forward) and 5′-CTGGTCGAGATGGCAGTGA-3′ (reverse); human GAPDH (accession no. NM_002046), 5′-GGGAAGGTGAAGGTCGGAGT-3′ (forward) and 5′-GAGTTAAAAGCAGCCCTGGTGA-3′ (reverse); mouse c-Fos (accession no. NM_010234), 5′-GGGGCAAAGTAGAGCAGCTA-3′ (forward) and 5′-GGCTGCCAAAATAAACTCCA-3′ (reverse); and mouse GAPDH (accession no. NM_008084), 5′-ATTGTCAGCAATGCATCCTG-3′ (forward) and 5′-ATGGACTGTGGTCATGAGCC-3′ (reverse). The amplification program was 50 °C for 2 min, 95 °C for 8 min 30 s, and 40 cycles of 95 °C for 15 s, 60 °C for 60 s. A melt curve analysis was performed on all amplification products, revealing a single peak and thus ensuring that products were specific. The software default values for baseline and threshold C_t values were used. The amplification efficiency of each primer pair was tested as described in (Schmittgen and Livak, 2008), and all efficiencies were approximately equal. Amplifications of unknowns were carried out within the dynamic range of each assay. The C_t range of target detection was 17–33. No PCR products were observed in negative controls. Data were analyzed using the comparative C_t method (Schmittgen and Livak, 2008) with GAPDH serving as the internal reference gene.

3.3.6 ERK5 knockdown. An ERK5 shRNA clone (V2LHS 202701) and a non-silencing control (RHS4346) were purchased from the Open Biosystems GIPZ Lentiviral shRNAmir library (Huntsville, AL). The lentiviruses were packaged in the 293-FT cell line (Invitrogen, Carlsbad, CA). Supernatants were collected 48 h after transfection, spun at 100 × g for 5 min, filtered through a 0.4 µm membrane, and stored at −80 °C. This preparation was used to infect HeLa cells. Selection in 0.2 µg/ml puromycin produced polyclonal stable cell lines. Knockdown of ERK5 was monitored by immunoblot analysis.

3.3.7 Immunoprecipitation. The vector that expresses epitope-tagged ERK5,

pcDNA3-FLAG-BMK1, was the generous gift of Dr. Jiing-Dwan Lee (Department of Immunology, The Scripps Research Institute, La Jolla, CA). Cells were transfected with 5 μg of pcDNA3-FLAG-BMK1. The next day, cells were washed twice with cold PBS, solubilized with lysis buffer (20 mM HEPES (pH 7.6), 1% Triton X-100, 137 mM NaCl, 0.1 mM Na_3VO_4, 25 mM β-glycerophosphate, 3 mM EDTA, and 1 mM phenylmethylsulfonyl fluoride), incubated for 10 min on ice, and centrifuged at 14,000 × g for 15 min at 4 °C. FLAG-BMK1 was immunoprecipitated from precleared lysate (500 μg total protein) by incubation for 2 h at 4 °C with anti-FLAG antibody (Sigma, St. Louis, MO) bound to protein G agarose beads. Phospho-FLAG-BMK1 was detected by immunoblot and an anti-phospho-ERK5 rabbit polyclonal antibody purchased from Cell Signaling (Beverly, MA).

3.3.8 Statistical analyses. Statistical analyses were performed using GraphPad Prism version 4.0 for Macintosh. To compare treatment means, we used a standard one-way analysis of variance (ANOVA). Where ANOVA main effects were significant ($p < 0.05$), all pairwise differences between means were assessed using Tukey's honestly significant differences (HSD) test. Statistical significance of quantitative real-time PCR data was assessed using a two-way ANOVA and the Bonferroni post-test. Post-hoc tests were conducted with $\alpha = 0.05$.

3.4 Results

3.4.1 Palytoxin, but not TPA, stimulates ERK5 in HeLa and 308 cells. We incubated HeLa cells (Fig. 1) and 308 mouse keratinocytes (Fig. 2) with palytoxin over a 240-min time course, and monitored ERK5 activation by immunoblot analysis. For these studies, we used the lowest concentrations of palytoxin that stimulated a detectable effect on ERK5 in HeLa and 308 cells, 30 and 100 pM, respectively. Several groups have established that ERK5 phosphorylation, which corresponds to ERK5 activity, is indicated by the appearance of a slower migrating form of ERK5 (Kato et al., 1998; Esparis-Ogando et al., 2002; Mody et al., 2003; Scapoli et al., 2004; Woo et al., 2008; Montero et al., 2009). Likewise, we found that palytoxin stimulated the phosphorylation of transiently expressed ERK5 in HeLa cells (Fig. 1, top panel) in a manner that corresponds

to the appearance of a slower migrating form of endogenous ERK5 (Fig. 1, second panel). Phosphorylation of transiently expressed ERK5 was detected using antibodies that bind to the dually phosphorylated, active form of ERK5; immunoblot analysis was not sensitive enough to detect endogenous phospho-ERK5 with these antibodies. Altogether, these results indicate that palytoxin triggers the activation of ERK5 in HeLa and 308 cells.

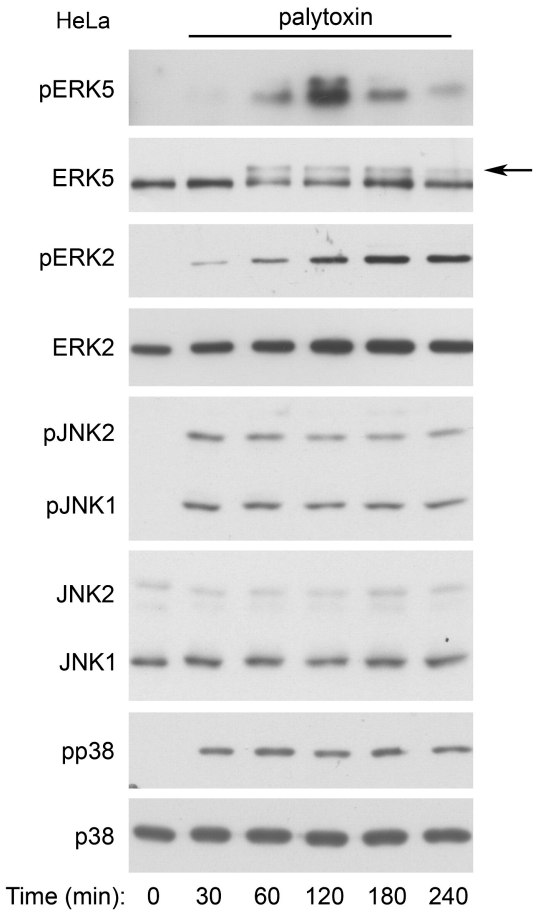

Fig. 1. Palytoxin stimulates ERK5 in HeLa cells. Top panel: HeLa cells transfected with pcDNA-FLAG-BMK1 (ERK5) were incubated with 30 pM palytoxin for the indicated times. FLAG-ERK5 was immunoprecipitated from whole cell lysates followed by immunoblotting with an antibody that detects the phosphorylated, active form of ERK5 (pERK5). Other panels: HeLa cells were incubated with 30 pM palytoxin for the indicated times. Whole cell lysates (20 µg protein) were analyzed by immunoblot for the following: ERK5; phosphorylated, active ERK1/2 (pERK2); total ERK2; phosphorylated, active JNK1 and JNK2 (pJNK1 and pJNK2); total JNK1 (JNK1 and JNK2); phosphorylated, active p38 (pp38); and total p38. Note: In HeLa cells, the total JNK1 antibody detects both JNK1 and JNK2. The arrow marks the

slower migrating form of ERK5. The data shown are representative of at least three independent experiments.

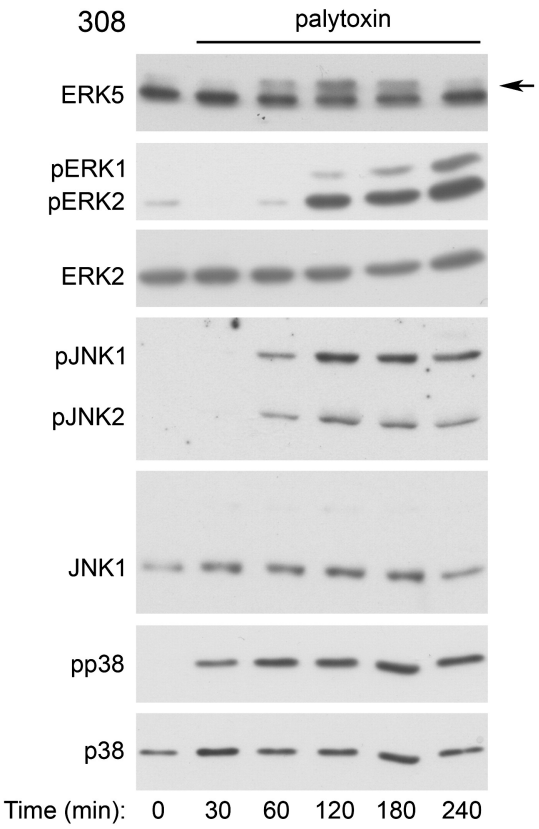

Fig. 2. Palytoxin stimulates ERK5 in 308 cells. 308 cells were incubated with 100 pM palytoxin for the indicated times. Whole cell lysates (20 µg of protein) were analyzed by immunoblot analysis for the following: ERK5; phosphorylated, active ERK1/2 (pERK1 and pERK2); total ERK2; phosphorylated, active JNK1 and JNK2 (pJNK1 and pJNK2); total JNK1; phosphorylated, active p38 (pp38); and total p38. The arrow marks the slower migrating form of ERK5. The data shown are representative of at least three independent experiments.

The time course of palytoxin-stimulated ERK5 phosphorylation differs significantly from the time courses of palytoxin-stimulated phosphorylation of the three major MAPK family members: ERK1/2, JNK, and p38 (Fig. 3 and Fig. 4). In HeLa cells, palytoxin-induced phosphorylation of ERK5 was detected by 60 min, remained highly elevated through 120 min, and decreased substantially by 240 min (Fig. 3, top panel). By contrast, palytoxin-induced ERK1/2 phosphorylation continued to increase gradually over the 240-

min time course (Fig. 3, second panel). Palytoxin induced a substantial increase in JNK and p38 phosphorylation by 30 min, prior to detection of ERK5 activation, and JNK and p38 phosphorylation remained elevated for at least 180 min (Fig. 3, third and fourth panels). Palytoxin also stimulated transient ERK5 phosphorylation, the slow accumulation of ERK1/2 phosphorylation, and sustained JNK and p38 phosphorylation in 308 cells (Fig. 4). In 308 cells, palytoxin-induced phosphorylation of ERK5, ERK1/2, JNK, and p38 was first detected at later time points than in HeLa cells (compare Fig. 3 and Fig. 4). The more sensitive cells are to palytoxin, the more rapid the response (Kuroki et al., 1996). Therefore the delay in detection of palytoxin-stimulated MAPK activation in 308 cells suggests that these cells may be less sensitive to palytoxin than HeLa cells. Altogether, the observation that palytoxin stimulates ERK5 activation with a time course that differs from that of ERK1/2, JNK, and p38 activation suggests that the mechanism by which palytoxin modulates ERK5 differs from the mechanisms by which palytoxin modulates the three major MAPK family members.

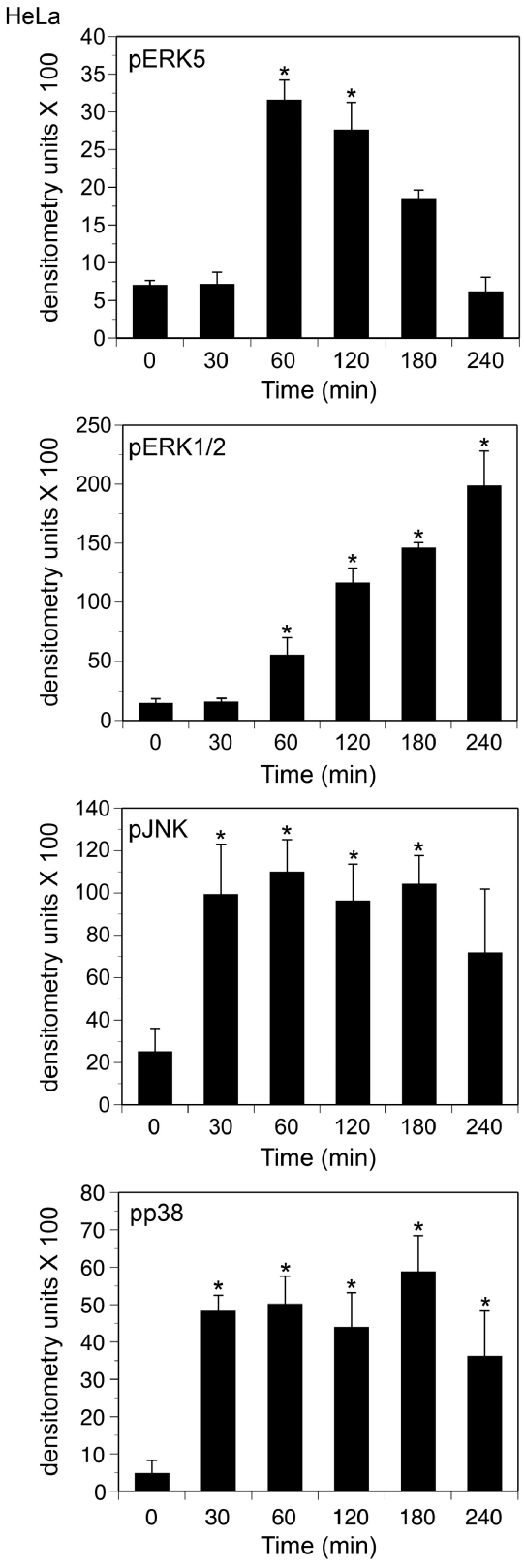
HeLa
pERK5
densitometry units X 100
Time (min)
pERK1/2
densitometry units X 100
Time (min)
pJNK
densitometry units X 100
Time (min)
pp38
densitometry units X 100
Time (min)

Fig. 3. Palytoxin stimulates ERK5 with a different time course than ERK1/2, JNK, and p38 in HeLa cells. HeLa cells were incubated with 30 pM palytoxin for the indicated times. Whole cell lysates (20 μg of protein) were analyzed by immunoblot for the following: ERK5; phosphorylated, active ERK1/2; phosphorylated, active JNK1 and JNK2; and phosphorylated, active p38. Each time point was run in triplicate. Band intensities were quantitated by densitometry for the graphical representation of the data. The units shown for pERK5 represent the ratio of the shifted ERK5 band to the total of the upper and lower bands as described by Kato et al. (1998). The bars represent the average of triplicates ± S.D. Asterisks denote values that were determined to be statistically significantly different from the zero time point ($p < 0.01$). The data shown are representative of at least three independent experiments.

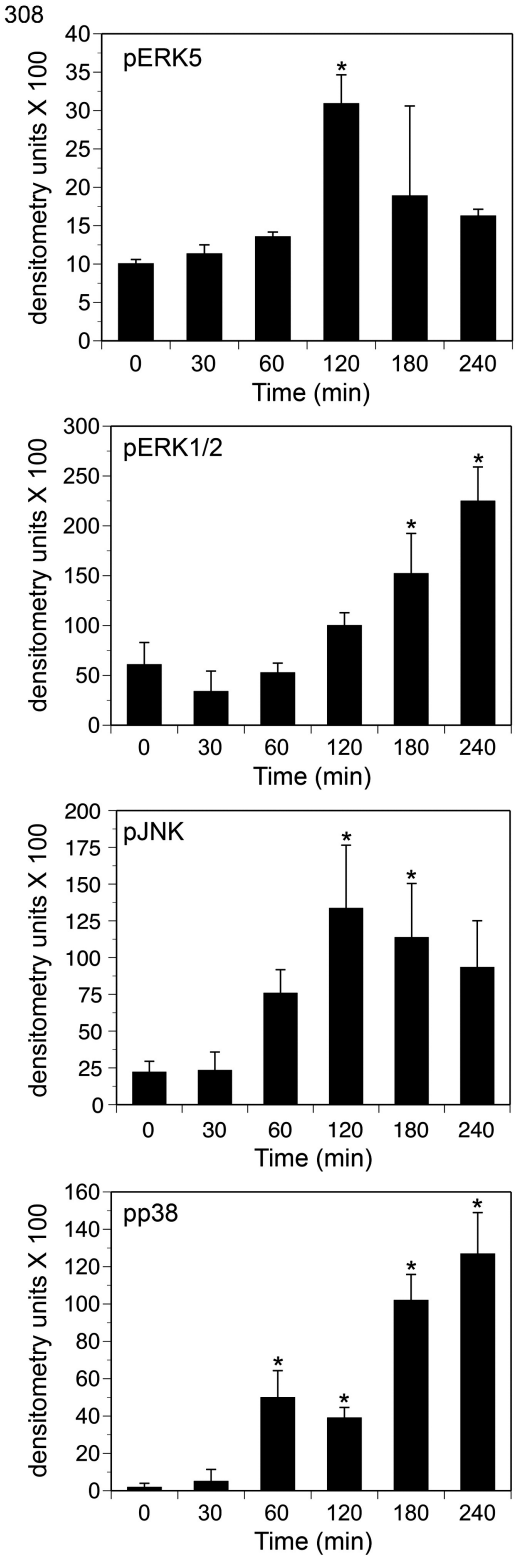

Fig. 4. Palytoxin stimulates ERK5 with a different time course than ERK1/2, JNK, and p38 in 308 cells.

308 cells were incubated with 100 pM palytoxin for the indicated times. Whole cell lysates (20 μg of protein) were analyzed by immunoblot for the following: ERK5; phosphorylated, active ERK1/2; phosphorylated, active JNK1 and JNK2; and phosphorylated, active p38 (pp38). Each time point was run in triplicate. For the graphical representation of the data, band intensities were quantitated by densitometry. The units shown for pERK5 represent the ratio of the shifted ERK5 band to the total of the upper and lower bands as described by Kato et al. (1998). The bars represent the average of triplicates ± S.D. Asterisks denote values that were determined to be statistically significantly different from the zero time point ($p < 0.01$). The data shown are representative of at least three independent experiments.

Next, we determined if the prototypical phorbol ester tumor promoter TPA modulates ERK5 in HeLa and 308 cells. We previously demonstrated that although palytoxin and TPA bind to different cellular receptors, the initially distinct signaling pathways stimulated by palytoxin and TPA can converge to regulate common downstream targets, including ERK1/2 (Warmka et al., 2002). In contrast to palytoxin, however, TPA did not stimulate a detectable increase in ERK5 phosphorylation in either cell line (Fig. 5, top panels) under conditions where it did activate ERK1/2 (Fig. 5, middle panels). This suggests that ERK5 represents a divergence in the signaling pathways activated by palytoxin and TPA in HeLa and 308.

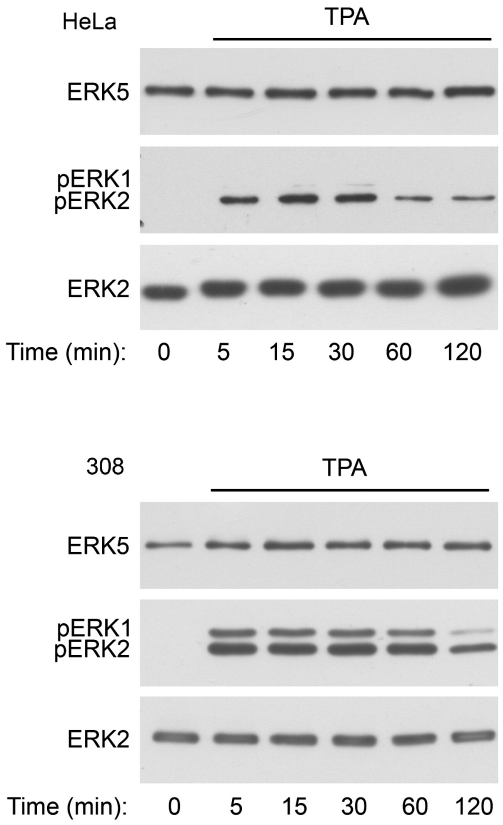

Fig. 5. TPA does not stimulate detectable ERK5 activation in HeLa or 308 cells. HeLa and 308 cells were incubated for the indicated times with 160 nM TPA. Whole cell lysates (20 μg of protein) were analyzed by immunoblot for the following: ERK5; phosphorylated, active ERK1/2 (pERK1 and pERK2); and total ERK2. The HeLa studies represent one experiment. The data shown for the 308 cells are representative of two independent experiments.

3.4.2 Palytoxin stimulates ERK5 through a Na+,K+-ATPase-dependent mechanism that is not mimicked by inhibition of protein synthesis or inhibition of serine/threonine or tyrosine phosphatases. The major membrane receptor for palytoxin is the Na+,K+-ATPase (Habermann, 1989). Accordingly, we found that incubation of HeLa cells with ouabain, which binds to the Na+,K+-ATPase, blocked the ability of palytoxin to stimulate the phosphorylation of ERK5 (Figs. 6A and C). These studies were not conducted in 308 cells because rodent cells are typically resistant to ouabain (Emanuel et al., 1988). Ouabain did not affect the ability of EGF to stimulate ERK5 phosphorylation (Fig. 6B), which indicates that ouabain does not cause a nonspecific

block in ERK5 phosphorylation. Finally ouabain alone did not stimulate a detectable increase in ERK5 phosphorylation under conditions where HeLa cells were incubated with concentrations of ouabain ranging from 100 nM to 1 mM over time courses that ranged from 2 to 240 min (Fig. 6B and data not shown). These results indicate that palytoxin activates ERK5 through a mechanism that requires its interaction with the Na+,K+-ATPase.

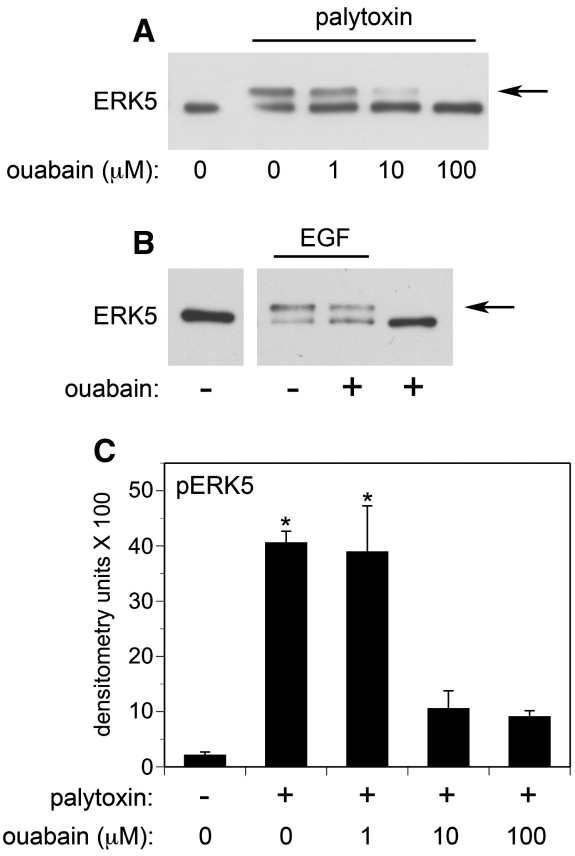

Fig. 6. Palytoxin stimulates ERK5 through a Na+,K+-ATPase-dependent pathway. (A) HeLa cells were incubated for 30 min with the indicated concentrations of ouabain. Palytoxin was added to a final concentration of 30 pM, where indicated by the underscore, and the cells were incubated for 120 min. Whole cell lysates (20 μg protein) were analyzed for ERK5 by immunoblot. The arrow marks the slower migrating form of ERK5. (B) HeLa cells were incubated for 30 min in the absence (−) or presence (+) of 100 μM ouabain. EGF was added to a final concentration of 3 nM, where indicated by the underscore, and the cells were incubated for 20 min. Whole cell lysates (20 μg protein) were analyzed for ERK5 by immunoblot. The arrow marks the slower migrating form of ERK5. (C) HeLa cells were incubated for 30

min with the indicated concentrations of ouabain. Palytoxin was not (−) or was (+) added to a final concentration of 30 pM and the cells were incubated for 120 min. Whole cell lysates were analyzed for ERK5 by immunoblot. Each point was run in triplicate. The band intensities were quantitated by densitometry. The units shown for pERK5 represent the ratio of the shifted ERK5 band to the total of the upper and lower bands. This method for quantitating the ERK5 band shift was conducted as described by Kato et al. (1998). The bars represent the average of triplicates ± S.D. Asterisks denote values that were determined to be statistically significantly different from control (absence of ouabain and palytoxin) ($p < 0.05$). The palytoxin data shown are representative of at least three independent experiments.

We were interested in determining whether the protein synthesis inhibitor cycloheximide could mimic the effect of palytoxin on ERK5 phosphorylation because we previously showed that palytoxin increases ERK1/2 phosphorylation in 308 cells by stimulating a loss of the phosphatase MKP-3, which is an unstable protein (Warmka et al., 2004). Incubation of HeLa and 308 cells with cycloheximide did not stimulate a detectable increase in ERK5 phosphorylation (Fig. 7, upper panels). Cycloheximide did stimulate the phosphorylation of ERK1/2 in both cell lines, which indicates that the compound is active under the conditions of these studies (Fig. 7, middle panels). Altogether, these results indicate that palytoxin does not stimulate the phosphorylation of ERK5 by blocking the production of an unstable protein.

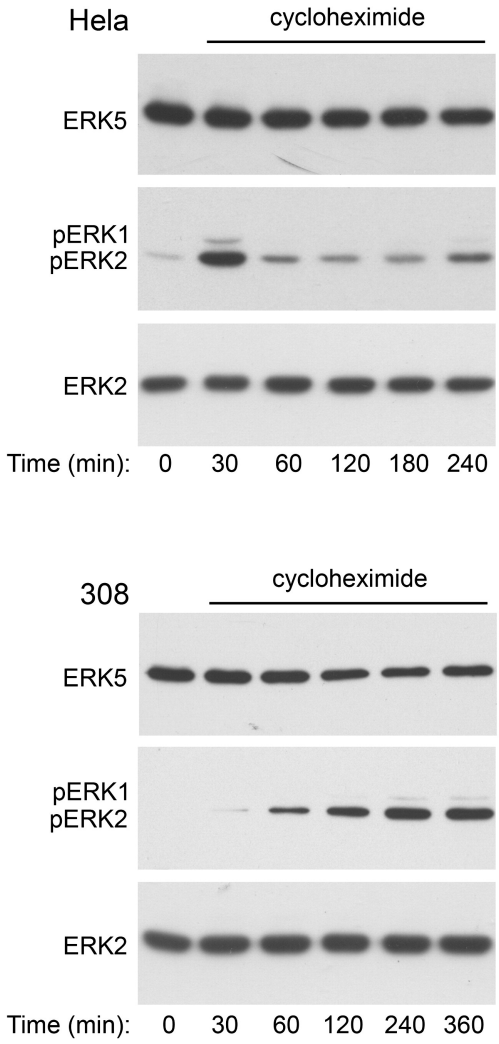

Fig. 7. The protein synthesis inhibitor cycloheximide does not mimic the effect of palytoxin on ERK5. HeLa and 308 cells were incubated for the indicated times with 36 μM cycloheximide. Protein from whole cell lysates (20 μg) was analyzed by immunoblot analysis for the following: ERK5; phosphorylated, active ERK1/2 (pERK1 and pERK2); and total ERK2. The HeLa studies represent one experiment. The data shown for the 308 cells are representative of two independent experiments.

Like other major members of the MAPK family, ERK5 is activated by phosphorylation of specific tyrosine and threonine residues (Mody et al., 2003). Because we previously demonstrated that palytoxin stimulates the phosphorylation of ERK1/2 in 308 cells by stimulating a loss of phosphatase action (Warmka et al., 2004), we wanted to determine if inhibiting major classes of phosphatases could mimic the effect of palytoxin on ERK5. Sodium orthovanadate, which inhibits tyrosine phosphatases, did not stimulate

a detectable increase in ERK5 phosphorylation in either HeLa or 308 cells (Fig. 8, upper panels). Sodium orthovanadate stimulated the rapid and sustained phosphorylation of ERK1/2 in both cell lines, however (Fig. 8, middle panels). These results highlight the difference between the regulation of ERK1/2 and ERK5 by protein tyrosine phosphatases, and indicate that palytoxin is unlikely to activate ERK5 by inhibiting this class of phosphatases.

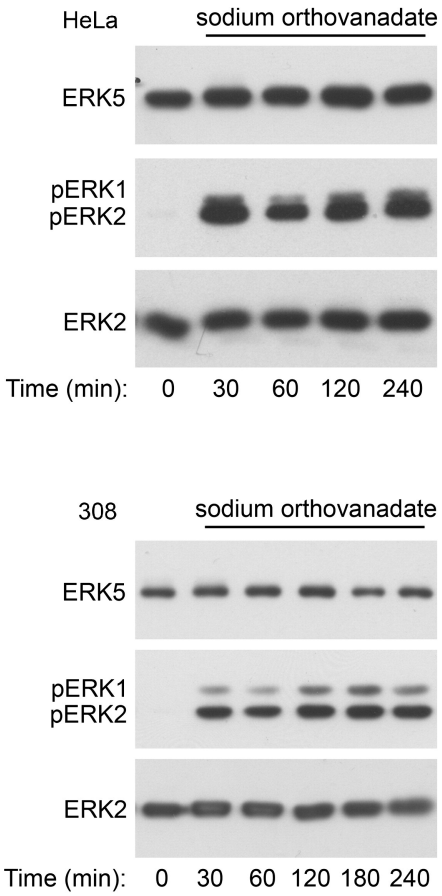

Fig. 8. The tyrosine phosphatase inhibitor sodium orthovanadate does not mimic the effect of palytoxin on ERK5. HeLa and 308 cells were incubated for the indicated times with 1 mM sodium orthovanadate. Protein (20 μg) from whole cell lysates was analyzed by immunoblot for the following: ERK5; phosphorylated, active ERK1/2 (pERK1 and pERK2); and total ERK2. The data shown are representative of at least two independent experiments.

Okadaic acid is a selective inhibitor of the serine threonine phosphatase protein

phosphatase 2A at the concentration used in these studies (Bialojan and Takai, 1988; Millward et al., 1999). Incubation of HeLa cells with okadaic acid for 240 min resulted in a slight increase in ERK5 phosphorylation (Fig. 9, top panel), but a dramatic increase in phospho-ERK1/2 (Fig. 9, middle panel). Incubation of 308 cells with okadaic acid stimulated a detectable increase in both ERK5 and ERK1/2 phosphorylation by 120 and 60 min, respectively (Fig. 9). The difference between the sensitivity of HeLa and 308 cells to okadaic acid may be due to cell type-dependent differences in the expression of specific phosphatases. Okadaic acid stimulates the gradual accumulation of both phospho-ERK1/2 and phospho-ERK5 (Fig. 9). Like okadaic acid, palytoxin stimulates the gradual accumulation of phospho-ERK1/2, but in contrast to okadaic acid, palytoxin stimulates transient ERK5 phosphorylation (Fig. 3 and Fig. 4). These results indicate that although ERK5 is a common target of these two non-TPA-type tumor promoters, palytoxin and okadaic acid modulate ERK5 through distinct mechanisms.

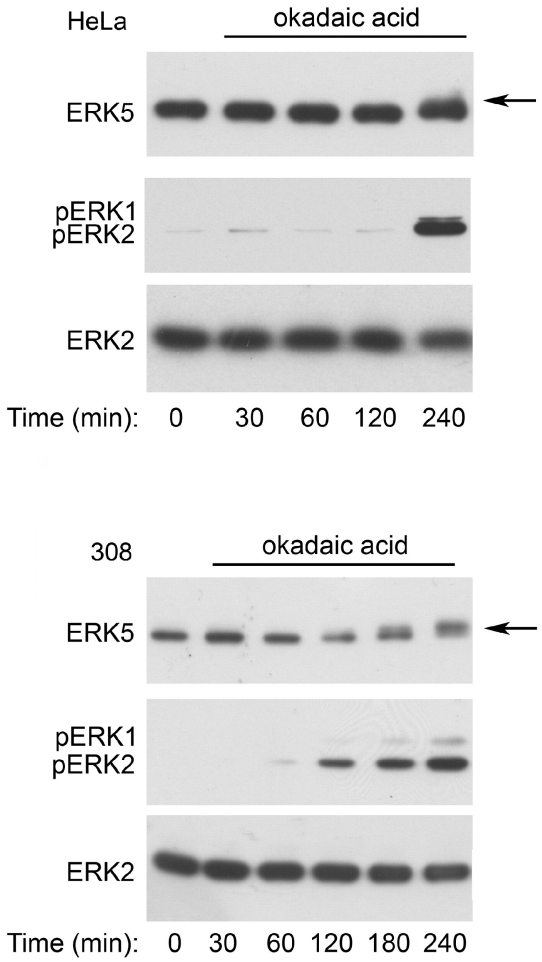

Fig. 9. Okadaic acid stimulates ERK5 phosphorylation with different kinetics than palytoxin in 308 cells. HeLa and 308 cells were incubated for the indicated times with 120 nM okadaic acid. Protein (20 μg) from whole cell lysates was analyzed by immunoblot for the following: ERK5; phosphorylated, active ERK1/2 (pERK1 and pERK2); and total ERK2. The arrow marks the slower migrating form of ERK5. The data shown are representative of at least two independent experiments.

3.4.3 ERK5 contributes to palytoxin-stimulated c-Fos gene expression. We previously reported that palytoxin modulates c-Fos in 308 mouse keratinocytes (Warmka et al., 2002). We concluded that palytoxin modulated c-Fos through an ERK1/2-dependent pathway based on the observation that the ability of palytoxin to increase c-Fos levels was blocked by PD98059, which inhibits MEK1/2, the kinases that phosphorylate and activate ERK1/2. Two lines of evidence led us to investigate the role of ERK5 in the ability of palytoxin to increase c-Fos RNA levels. First, several types of

MEK1/2 inhibitors can also inhibit MEK5, the kinase that phosphorylates and activates ERK5 (Kamakura et al., 1999; Mody et al., 2001). Consequently, in some cell types these pharmacological agents can inhibit the activation of ERK5, as well as ERK1/2. Second, studies indicate that both ERK1/2 and ERK5 play a role in serum-stimulated c-Fos gene expression (Sasaki et al., 2006).

To investigate the role of ERK5 in palytoxin-induced c-Fos gene expression, we first identified a concentration of the pharmacological agent U0126 (3 μM) that blocks the ability of palytoxin to activate ERK1/2, but not ERK5 in 308 and HeLa cells (Figs. 10A and B). Next, we used real-time PCR to determine how incubation of the cells with 3 μM U0126 affected palytoxin-induced c-Fos gene expression. In 308 cells, 3 μM U0126 partially blocked palytoxin-induced c-Fos gene expression; c-Fos gene expression was inhibited by approximately 80% at 120 min and 70% at 180 min (Fig. 10C). Incubation of 308 cells with 10 μM U0126, which blocked both palytoxin-stimulated ERK1/2 and ERK5 activation (Fig. 10A), resulted in almost complete inhibition of palytoxin-stimulated c-Fos gene expression (Fig. 10C). These results indicate that although ERK1/2 plays an important role in palytoxin-induced c-Fos gene expression, ERK5 also contributes to the modulation of c-Fos by palytoxin in 308 cells. Likewise, 3 μM U0126 inhibited palytoxin-stimulated c-Fos gene expression by approximately 70% in HeLa cells (Fig. 10D). We were not able to efficiently block palytoxin-stimulated ERK5 activation with U0126 in HeLa cells (Fig. 10B). We were able to achieve efficient knockdown of ERK5 in HeLa cells using shRNA, however (Fig. 11A). Knockdown of ERK5 caused a partial block in palytoxin-induced c-Fos gene expression in HeLa cells at 60 min (approximately 50%) (Fig. 11B). There was no detectable effect of ERK5 knockdown on palytoxin-induced c-Fos gene expression at 180 min (Fig. 11B). Knockdown of ERK5 did not affect the ability of TPA to induce c-Fos gene expression (Fig. 11C). This indicates that the effect of ERK5 knockdown on palytoxin-induced c-Fos gene expression is not nonspecific, and furthermore that TPA and palytoxin can modulate c-Fos through activation of different MAPK family members.

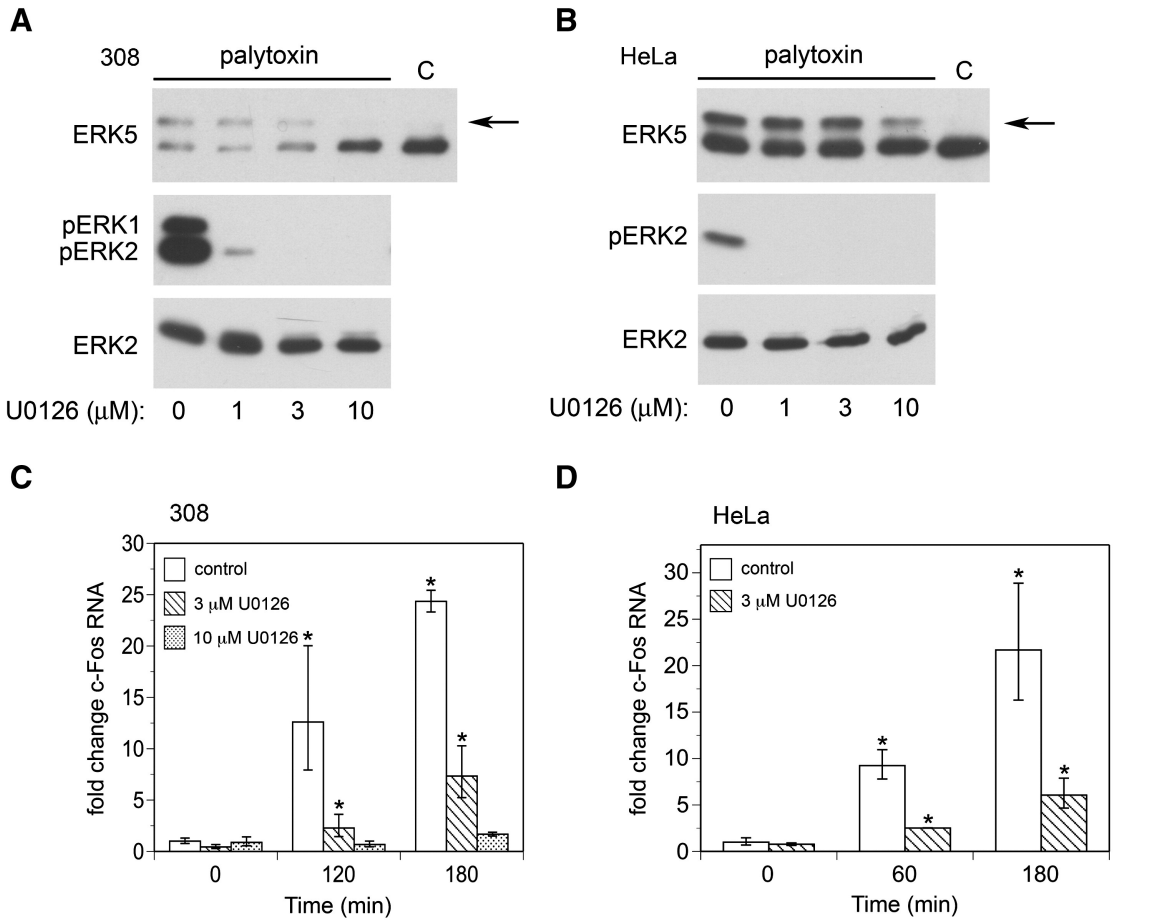

Fig. 10. U0126 inhibits palytoxin-stimulated increases in c-Fos RNA in HeLa and 308 cells. 308 (A) and HeLa (B) cells were incubated with the indicated concentrations of U0126 for 30 min. Palytoxin was added to a final concentration of 100 pM in 308 cells and 30 pM in HeLa cells. After 120 min, the cells were lysed. Protein (20 μg) from whole cell lysates was analyzed by immunoblot for the following: ERK5; phosphorylated, active ERK1/2 (pERK1 and pERK2); and total ERK2. The lane denoted "C" indicates lysates prepared from cells that were not treated with palytoxin or U0126, and therefore represents basal ERK5. The arrow marks the slower migrating form of ERK5. (C) 308 cells were incubated for 30 min in the absence (open bars) or presence of either 3 μM U0126 (hatched bars) or 10 μM U0126 (dotted bars) for 30 min. Palytoxin was added to a final concentration of 100 pM and the cells were incubated for the indicated times. (D) HeLa cells were incubated in the absence (open bars) or presence of 3 μM U0126 (hatched bars) for 30 min. Palytoxin was added to a final concentration of 30 pM and the cells were incubated for the indicated times. The cells were lysed and RNA levels were determined by quantitative real-time PCR analysis and the comparative C_t method. Data were normalized to GAPDH RNA levels and expressed relative to the zero time point for control. The bars represent the average of triplicates ± SEM. Asterisks denote values that were determined to be statistically significantly different from the zero time

point ($p < 0.05$). The data shown are representative of at least two independent experiments.

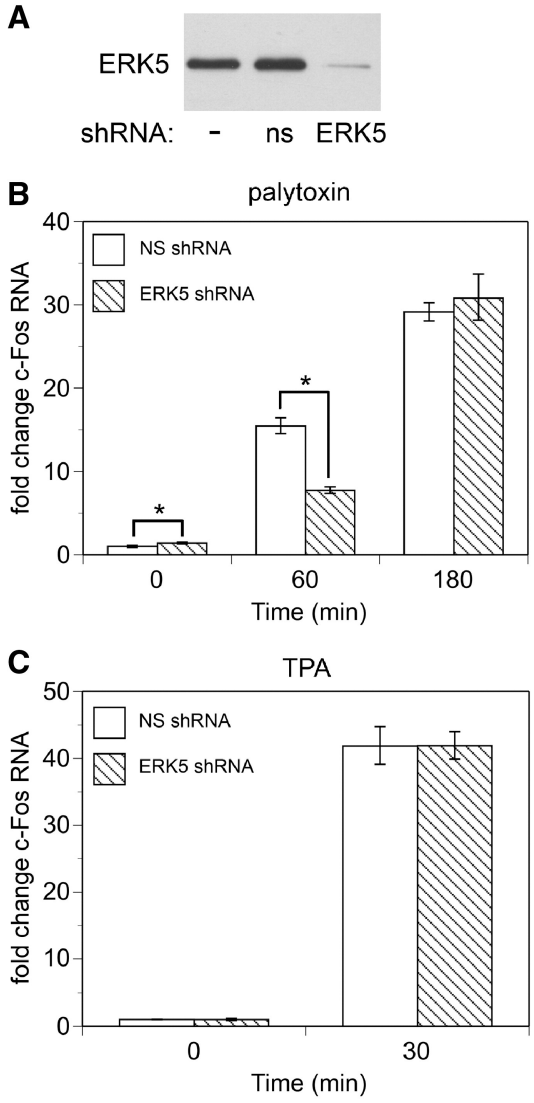

Fig. 11. ERK5 knockdown inhibits palytoxin-induced c-Fos expression. (A) Whole cell lysates were prepared from HeLa cells that were either not transduced (−), that stably express non-silencing shRNA (ns), or that stably express ERK5 shRNA (ERK5). Protein (20 μg) from the whole cell lysates was analyzed by immunoblot for ERK5. HeLa cells that stably express non-silencing shRNA (NS, open bars), or that stably express ERK5 shRNA (ERK5 shRNA, hatched bars), were (B) incubated for the indicated times with 30 pM palytoxin or (C) incubated for 30 min with 160 nM TPA. c-Fos RNA levels were determined by quantitative real-time PCR analysis and the comparative C_t method. Data were normalized to GAPDH RNA levels and expressed relative to nontreated HeLa cells that stably express non-silencing shRNA (NS). The bars represent the average of triplicates ± SEM. Asterisks indicate $p < 0.05$, ERK5 shRNA compared

to NS for each time point. The difference between basal c-Fos gene expression in ERK5 knockdown cells vs. NS cells was never greater than 1.4 fold. The TPA data represent one experiment. The palytoxin data shown are representative of three independent experiments.

3.5 Discussion

The studies reported here demonstrate, for the first time, that ERK5 plays a role in the signaling pathways stimulated by the non-TPA-type tumor promoter palytoxin. Moreover, to our knowledge, this is the first report that the interaction of a toxicological or pharmacological agent with the Na+,K+-ATPase results in the modulation of ERK5. We did not detect any effect of ouabain on ERK5, although we previously detected activation of ERK1/2, JNK, and p38 by ouabain in HeLa cells (Li and Wattenberg, 1998). Therefore, activation of ERK5 represents a difference in the signaling pathways stimulated by two agents that bind to the Na+,K+-ATPase. This is also the first report that the non-TPA-type tumor promoter okadaic acid stimulates ERK5 activation. By contrast to palytoxin and okadaic acid, the prototypical phorbol ester tumor promoter TPA did not stimulate detectable ERK5 activation in HeLa and 308 cells. Altogether, the results presented here indicate that ERK5 represents an alternative signaling molecule through which different types of tumor promoters can modulate nuclear targets.

ERK5, like the other three major MAPKs, is activated by phosphorylation of specific tyrosine and threonine residues (reviewed by Dhillon et al. (2007)). MAPK activity is determined by the balance between the phosphorylation and activation by upstream kinases, and the dephosphorylation and inactivation by phosphatases. We have found that palytoxin can modulate the activity of other MAPK family members both through activation of upstream kinases (MAPKKs) and by inhibiting phosphatase action (Kuroki et al., 1997; Li and Wattenberg, 1999; Warmka et al., 2004). For example, we previously showed that palytoxin stimulates the phosphorylation and activation of JNK and p38 through activation of the upstream kinases SEK1, MKK3, and MKK6 (Kuroki et al., 1997; Li and Wattenberg, 1999). We found that U0126, which can inhibit MEK5 (Mody et al., 2001), the kinase that phosphorylates and activates ERK5, inhibits palytoxin-stimulated ERK5 activation in 308 cells and partially inhibits ERK5 activation in HeLa

cells. These results indicate that MEK5 plays a role in the activation of ERK5 by palytoxin. The mechanisms by which palytoxin-stimulated ion flux stimulates MEK5 remain to be determined. We previously showed that in 308 cells palytoxin increases ERK1/2 activity not through the activation of MEK1/2, but instead by downregulating MKP-3, an ERK1/2-specific phosphatase that is elevated in this cell line (Warmka et al., 2004). The slow accumulation of phospho-ERK1/2 observed in palytoxin-treated 308 cells is characteristic of phosphatase inhibition. The transient nature of palytoxin-stimulated ERK5 phosphorylation suggests that palytoxin does not increase ERK5 activity by inactivating a phosphatase. Our finding that the phosphatase inhibitors sodium orthovanadate and okadaic acid do not mimic palytoxin action supports this conclusion.

Our studies indicate that ERK5 plays a role in the modulation of c-Fos by palytoxin. We found that a low concentration of U0126, which blocks the stimulation of ERK1/2, but not ERK5, by palytoxin, only partially inhibited c-Fos gene expression. This suggested that other signaling pathways are also be involved in the modulation of this proto-oncogene by palytoxin. Two lines of evidence support the conclusion that ERK5 is involved in the signaling pathways that mediate palytoxin-stimulated c-Fos gene expression. First, a concentration of U0126 that blocks both ERK1/2 and ERK5 further blocked the ability of palytoxin to increase c-Fos RNA in 308 cells. Second, knockdown of ERK5 by shRNA in HeLa cells inhibited palytoxin-stimulated c-Fos gene expression. Knockdown on ERK5 resulted in a significant decrease in c-Fos gene expression at 60 min, but did not appear to significantly affect palytoxin-stimulated c-Fos gene expression at 180 min. This may be because palytoxin-stimulated ERK1/2 activation can compensate for the loss of ERK5 at this time point. At 60 min, palytoxin-stimulated ERK5 activity may predominate over ERK1/2 activity (see Fig. 3). By 180 min, ERK5 activity is decreasing, while ERK1/2 activity is continuing to increase; the increase in palytoxin-stimulated ERK1/2 activity by 180 min may be sufficiently high that ERK5 is no longer required to maintain elevated c-Fos gene expression. The observation that 3 μM U0126, which blocks the stimulation of ERK1/2 but not ERK5 in HeLa cells, does not totally block palytoxin-induced c-Fos gene expression at 180 min (see Fig. 10D) suggests that pathways in addition to ERK1/2 and ERK5 also contribute to palytoxin-induced c-Fos

gene expression in HeLa cells. Interestingly, there appears to be considerable redundancy in the action of various MAPK families. For example, the transcription factor Sap1a, which has been implicated in the transcriptional regulation of c-Fos, can be modulated by both ERK1/2 and ERK5 (Janknecht et al., 1995; Strahl et al., 1996; Kamakura et al., 1999; Yordy and Muise-Helmericks, 2000). Elk-1, another transcription factor involved in the regulation of c-Fos gene expression, can be modulated by ERK1/2, JNK, and p38 (Cavigelli et al., 1995; Gille et al., 1995; Whitmarsh et al., 1995; Raingeaud et al., 1996). This helps explain why c-Fos is a common target of tumor promoters that trigger diverse signals. Whereas TPA modulates c-Fos through activation of ERK1/2 (Zeliadt et al., 2004), palytoxin can modulate c-Fos through the activation of ERK1/2, ERK5, and perhaps other pathways as well.

Different types of studies suggest that ERK5 is involved in carcinogenesis. For example, it has been reported that ERK5 protein is elevated in tissue from malignant human prostate cancer tissue relative to normal tissue (McCracken et al., 2008). Furthermore, whereas the MEK1 inhibitor PD184352 blocked proliferation of the PC3 prostate cancer cell line at high concentrations that inhibit ERK5, PD184352 did not block proliferation of PC3 cells at low concentrations that inhibit ERK1/2 but not ERK5 (McCracken et al., 2008). Active ERK5 has also been detected in human breast cancer tissue and in tumor tissue from an animal model of breast cancer (Montero et al., 2009). ERK5 also appears to be involved in the signaling pathways that regulate the adhesion and motility of metastatic breast and prostate cancer cell lines (Sawhney et al., 2009). A role for ERK5 in angiogenesis during tumorigenesis has also been suggested by studies conducted using ERK5 knockout mice (Hayashi et al., 2005). ERK5 has also been implicated in the regulation of the proto-oncogenes c-Fos, Fra-1, and c-Jun, which further supports the idea that aberrant regulation of ERK5 may be involved in carcinogenesis (Kato et al., 1997; Terasawa et al., 2003). The observation that ERK5 is involved in asbestos-stimulated proliferation of a murine alveolar type II epithelial cell line (C10) suggests that ERK5 may be a target of environmental carcinogens (Scapoli et al., 2004). Finally, our observation that two non-TPA-type tumor promoters, palytoxin and okadaic acid, activate ERK5 suggests that ERK5 may also be involved in early stages of

carcinogenesis.

Establishing the role of ERK5 in palytoxin-stimulated tumor promotion requires further study. The mechanisms by which palytoxin stimulates tumor promotion are not clear. Palytoxin is cytotoxic in cell culture and also caused toxicity when used in the multi-stage mouse skin model (Fujiki et al., 1986). Although palytoxin may stimulate cell proliferation *in vivo*, palytoxin may also stimulate tumor promotion by other mechanisms. For example, it is possible that initiated cells that express oncogenic Ras are resistant to palytoxin-induced cytotoxicity, thus giving a growth advantage to initiated cells. Alternatively, palytoxin may stimulate the release of agents from cells that stimulate the growth of neighboring cells or perhaps induce an inflammatory response that contributes to tumor promotion. For example, palytoxin stimulates arachidonic acid metabolism and the release of prostaglandins in other systems (Levine et al., 1986; Lazzaro et al., 1987; Miura et al., 2006). Our observation that palytoxin stimulates ERK5 activation in two different cell types suggests that the role of ERK5 should be examined in various types of systems in which palytoxin stimulates responses that are likely to be involved in carcinogenesis.

Humans are likely to be exposed to palytoxin through two main routes. Palytoxin is isolated from corals found in Hawaii and the Caribbean Islands (Moore and Scheuer, 1971; Ishida et al., 1983). Humans can be exposed to palytoxin through the food chain (Mebs, 1998); palytoxin has been linked to poisonings due to consumption of crabs, mackerel, and sardines (Alcala et al., 1988; Kodama et al., 1989; Onuma et al., 1999). Another route of exposure to palytoxin is through the maintenance of aquariums (Hoffmann et al., 2008). The corals that produce palytoxin are commonly found in aquariums used in exhibitions as well as aquariums maintained as a hobby. Exposure can occur from inhaling aerosolized water that contains palytoxin and through skin contact. Although palytoxin has been implicated in poisonings from consuming seafood and from cleaning an aquarium, to our knowledge, the amount of palytoxin that humans might be exposed to at nontoxic doses through consumption of seafood and exposure to water that contains palytoxin has not been estimated.

We have used the novel tumor promoter palytoxin to both identify common

biochemical targets of prototypical phorbol ester tumor promoters and non-TPA-type tumor promoters, such as c-Fos, and reveal alternate signaling pathways by which such potentially critical targets can be modulated. Altogether, these studies may help reveal mechanisms by which a broad range of agents can affect carcinogenesis.

Acknowledgments

We thank Kathleen F. Conklin (Department of Genetics, Cell Biology and Development, Institute of Human Genetics, Masonic Cancer Center, University of Minnesota) for her assistance with the studies that involved the use of lentiviral vectors, and Kathryn L. Schwertfeger (Department of Laboratory Medicine and Pathology, University of Minnesota) for her assistance with the studies that involved real-time PCR. This work was supported by National Institutes of Health grant RO1-CA104609 (to E.V.W.). The National Institutes of Health was not involved in study design, collection, analysis, or interpretation of data, writing the manuscript, or the decision to submit the manuscript for publication.

Chapter IV

Multifunctional Prenylated Peptides for Live Cell Analysis

Rationale. Ras and other small GTPases are posttranslationally modified by lipid moieties that are required for their biological functions. This process, known as prenylation, consists of the addition of a 15-carbon (farnesyl) or 20-carbon (geranylgeranyl) isoprenoid group to the cysteine residue of the consensus "CAAX box" (where C is cysteine, A is any aliphatic amino acid, and X is any amino acid) found in the *C*-terminus of prenylated proteins (Wright and Philips, 2006; Zhang and Casey, 1996). Prenylation is an important determinant of subcellular localization of proteins and may also mediate protein-protein interactions (Kato et al., 1992; Marshall, 1993).

Our understanding of the biological role and mechanism of prenylation is incomplete, and much remains to be learned regarding the biological effects of prenylation on protein localization. One approach to study prenylation-dependent localization of proteins utilizes cells that overexpress epitope-tagged recombinant proteins (Michaelson et al., 2001). Another complementary approach is based on the use of truncated peptides derived from full-length prenylated proteins. Much of our understanding of the localization of prenylated peptides is based on *in vitro* studies utilizing artificial membranes or purified microsomes (Ghomashchi et al., 1995; Silvius and l'Heureux, 1994; Thissen and Casey, 1993). The localization of prenylated peptides in living cells remains unexplored, however. Therefore, we developed these cell-penetrating peptides to examine the uptake and localization of prenylated peptides in living cells.

Given the frequent role of Ras and other small GTPases in human cancer, there has been an interest in developing drugs to specifically target and inhibit the enzymes involved in prenylation (Hill et al., 2000; Zhu et al., 2003). For example, small molecule inhibitors that disrupt prenylation can cause mislocalization of Ras and impair Ras function (Kloog and Cox, 2000; Wright and Philips, 2006). Therefore, targeting prenylation with drugs is a promising therapy for solid tumors, and such inhibitors have been tested in Phase III clinical trials (Rowinsky et al., 1999; Sebti and Hamilton, 2000; Sousa et al., 2008). Because cell-penetrating peptides are promising tools for the

transport of cargo into cells, our studies may be useful for the drug development process (Wagstaff and Jans, 2006).

Results. We synthesized a series of cell-penetrating peptides with a sequence based on the *C*-terminus of the small GTPase CDC42. These peptides were equipped with three features: 1) a fluorophore to enable cellular visualization, 2) a specific, cell-penetrating moiety known as penetratin to facilitate cellular uptake of these peptides, and 3) a prenyl group (farnesyl or geranylgeranyl). We found that all penetratin-labelled peptides are rapidly taken up by cells through an energy-dependent process. Presence of a farnesyl or geranylgeranyl group causes peptides to be localized to a perinuclear region, similar to the localization of the parent protein, CDC42 (Michaelson et al., 2001). While our studies were in progress, we discovered that prenylated peptides that lacked the penetratin moiety could still be taken up by cells. Interestingly, uptake of peptides lacking penetratin was energy-independent. Peptides that lacked both penetratin and a prenyl moieties did not internalize, demonstrating the importance of the prenyl group for cellular uptake.

Conclusions and Significance. These studies are significant because they pave the way for future analysis of the biological role of prenylation in living cells. The amino acid sequence of the peptides used in this study is based on the region of CDC42 that is involved in interacting with the regulatory protein RhoGDI (Hoffman et al., 2000; Nomanbhoy and Cerione, 1996). Therefore, this peptide could be useful for probing the biological effects of preventing protein-protein interactions between CDC42-RhoGDI. The peptide sequence of these molecules could be modified for application to the study of other proteins, as well as other post-translational modifications, such as glycosylation and phosphorylation. Furthermore, prenylated peptides could be useful for monitoring the enzymatic processing of prenylated peptides in living cells because peptides containing an intact “CAAX box” are internalized.

These peptides are also of interest because of their ability to readily diffuse across cell membranes without apparent toxicity. These properties make prenylated cell-penetrating

peptides promising tools for the delivery of cargo into cells (Foged and Nielsen, 2008). Our studies may be particularly useful for the drug development process because we demonstrate that prenylated peptides enter cells directly, avoiding the potential problem of the peptides becoming entrapped within the endosomal transport system.

Contributions. I contributed directly to the work in this paper by performing all cell-based experiments. In collaboration with James Wollack, I tested the uptake of peptides, visualized the uptake by confocal microscopy, and quantified uptake using flow cytometry. I also contributed to preliminary and non-published work by assessing the toxicity of cell penetrating peptides in HeLa cells. The remainder of this chapter is adapted from the published paper, reproduced with permission from: Multifunctional Prenylated Peptides for Live Cell Analysis. 2009. James W. Wollack, Nicholette A. Zeliadt, Daniel G. Mullen, Gregg Amundson, Suzanne Geier, Stacy Falkum, Elizabeth V. Wattenberg, George Barany, and Mark D. Distefano. Journal of the American Chemical Society 131:7293-7303. Copyright 2009 American Chemical Society.

4.1 Abstract

Protein prenylation is a common post-translational modification present in eukaryotic cells. Many key proteins involved in signal transduction pathways are prenylated, and inhibition of prenylation can be useful as a therapeutic intervention. While significant progress has been made in understanding protein prenylation *in vitro*, we have been interested in studying this process in living cells, including the question of where prenylated molecules localize. Here, we describe the synthesis and live cell analysis of a series of fluorescently labeled multifunctional peptides, based on the *C*-terminus of the naturally prenylated protein CDC42. A synthetic route was developed that features a key Acm to Scm protecting group conversion. This strategy was compatible with acid-sensitive isoprenoid moieties and allowed incorporation of an appropriate fluorophore as well as a cell-penetrating sequence (penetratin). These peptides are able to enter cells through different mechanisms, depending on the presence or absence of the penetratin vehicle and the nature of the prenyl group attached. Interestingly, prenylated peptides

lacking penetratin are able to enter cells freely through an energy-independent process and localize in a perinuclear fashion. This effect extends to a prenylated peptide that includes a full "CAAX box" sequence (specifically, CVLL). Hence, these peptides open the door for studies of protein prenylation in living cells, including enzymatic processing and intracellular peptide trafficking. Moreover, the synthetic strategy developed here should be useful for the assembly of other types of peptides that contain acid-sensitive functionalities.

4.2 Introduction

Protein prenylation is a post-translational modification that consists of the addition of 15 (farnesyl) or 20 (geranylgeranyl) carbon isoprenoid units to specific cysteine residues positioned near the *C*-terminus of a protein (Schafer and Rine, 1992; Zhang and Casey, 1996; Chow et al., 1992). Based on labeling experiments with tritiated mevalonic acid, the biosynthetic precursor to farnesyl diphosphate and other isoprenoids, it has been estimated that 2% of the mammalian proteome is prenylated (Epstein, 1991). Moreover, the types of proteins that contain this modification include all members of the Ras superfamily of proteins and the gamma subunits of heterotrimeric G-proteins. Thus, essentially all signal transduction pathways involve prenylated proteins. The frequent occurrence of this modification, coupled with its crucial role in regulating cellular processes, has generated intense interest in the enzymology and function of protein prenylation. The "CAAX box" (CVLL sequence in this paper) is the recognition sequence for prenylation. The mature isoprenylated protein arises from a three-step process that consists of prenylation, followed by proteolysis of the "AAX" sequence, and methyl esterification of the new *C*-terminal cysteine. Due to the participation of mutant forms of Ras and related proteins in cancer, there has been intense interest in developing inhibitors of the enzymes involved in the prenylation process. The most successful work to date has targeted farnesyltransferase, resulting in the development of several drug candidates that are in phase 3 clinical trials (Sebti and Hamilton, 2000; Sousa et al., 2008; Zhu et al., 2003). The proteolytic and methylating enzymes also show promise as possible drug targets. Progress has also been made in understanding the function of

protein prenylation. In some cases, isoprenylation serves to direct membrane association (Kato et al., 1992), while, in other situations, the prenyl group is involved in mediating protein−protein interactions (Marshall, 1993).

Despite the important developments in prenylation research noted above, much remains unclear, particularly concerning the biological function of this modification. For example, some proteins show different patterns of localization, depending on their prenylation state and their *C*-terminal amino acid sequences (Michaelson et al., 2001). Changes in prenylation state have also been shown to alter a protein's biological activity (Roberts et al., 2006). One approach that can be used to investigate such issues is to prepare and study synthetic peptides derived from larger proteins. Such peptides allow the functions of particular segments of the protein to be studied in isolation; they also permit the introduction of synthetic moieties including non-natural residues, isoprenoid analogues, and spectroscopic probes that can facilitate biochemical analysis. To date, several studies have examined the binding of prenylated peptides to artificial lipid bilayers (Ghomashchi et al., 1995; Silvius and l'Heureux, 1994) and to microsomal membranes (Thissen and Casey, 1993) obtained via subcellular fractionation, but localization of prenylated peptides in living cells has yet to be probed. The purpose of the present studies is to complement such earlier *in vitro* work by developing methodology to prepare prenylated peptides that can be introduced into living cells and to examine their distribution therein.

Due to the key role of the extensively characterized Rho protein CDC42 in regulating cytoskeletal assembly, we chose to study peptides based on its *C*-terminal sequence. To facilitate introduction of these peptides into living cells, we elected to conjugate them to the cell penetrating peptide (CPP) sequence known as penetratin, via a disulfide linkage that would subsequently be cleaved in the reducing environment of the targeted cells. However, because the resulting peptides contain two cysteine residues (one for penetratin attachment and the other as the site of prenylation), it was necessary to devise an orthogonal protecting group strategy that would enable the two thiols to be differentiated. Here we describe the synthesis of a series of peptides (Figure 1) based on the *C*-terminus of CDC42 that are functionalized with varying isoprenoids, along with a fluorophore and

a penetratin sequence (**1c**, **2c**, and **3c**). The peptides were synthesized as *C*-terminal amides to provide enhanced stability while retaining the neutral charge state of the *C*-terminal methyl ester present in naturally prenylated peptides. A second series of fluorescently labeled prenylated peptides lacking the penetratin group was also prepared (**1a**, **2a**, and **3a**), along with a peptide containing a complete CVLL "CAAX box" sequence (**4**). Furthermore, a fluorescently labeled version of penetratin (**5**) was synthesized as a control.

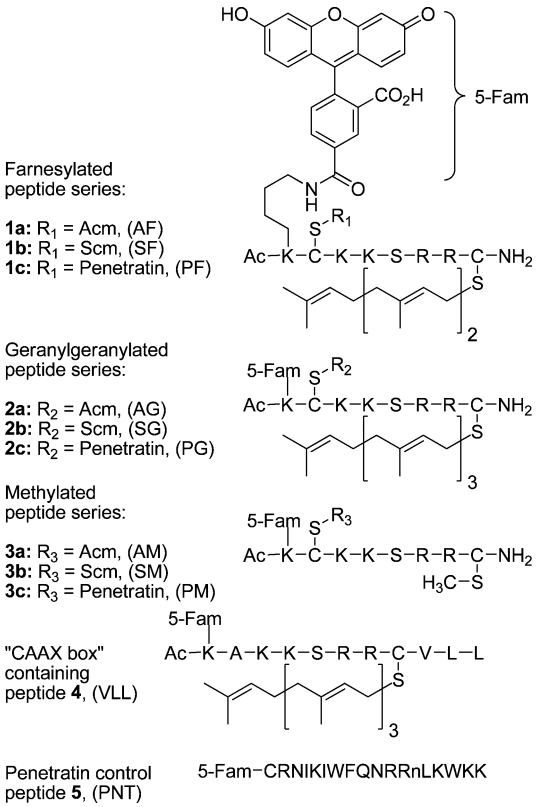

Figure 1. Multifunctional prenylated peptides for analysis in living cells.

Flow cytometry and confocal microscopy of living cells in conjunction with *in vitro* fluorescence measurement were then used to probe the entry and localization of these peptides. Interestingly, the presence of a farnesyl or geranylgeranyl group caused these peptides to target the perinuclear region within the cell, in a similar fashion to what has been observed with the parent protein CDC42 (Osmani et al., 2006; Nalbant et al., 2004).

In the course of these experiments, it was observed that the prenylated peptides lacking the penetratin group could also enter the cell and localize in a perinuclear fashion; this includes a peptide containing a complete "CAAX box". However, in those latter cases, the mechanism of entry appears to be different than that for those peptides functionalized with penetratin. In summary, the methodology reported here has allowed us to prepare peptides containing natural and non-natural modifications that can be introduced into living cells. Moreover, these peptides should provide a means for studying the enzymatic processing, including proteolysis and methylation, of prenylated species in living cells.

4.3 Experimental Procedures

4.3.1 Materials and Methods. HeLa cells were the generous gift of Dr. Audrey Minden (Department of Chemical Biology, Rutgers University). Petri dishes (35 mm) fitted with microwells (14 mm) and a No. 1.5 coverglass were from MatTek Corporation. Wheat germ agglutinin Alexa Fluor 594 conjugate, ProLong(R) Gold antifade reagent, Hoechst 34850, and DMEM (Dulbecco's Modified Eagle Medium) were from Invitrogen. Fetal bovine serum was from Intergen Company. C18 Sep-Pak cartridges were purchased from Waters. Twelve-well plates were from Corning Inc. Vydac 218TP54 and 218TP1010 columns were used for analytical and preparative RP-HPLC, respectively. All analytical and preparative RP-HPLC solvents, water and CH_3CN, contained 0.10% TFA, and retention times (t_R) are based on linear gradients (unless otherwise noted) starting from 100% H_2O to 40% H_2O/60% CH_3CN over 60 min. All solvents were of HPLC grade. DIEA and TFA were of Sequalog/peptide synthesis grade from Fisher. Fmoc-Cys(Me)-OH was from Bachem and Fmoc-Lys(Dde)-OH was from Nova Biochem. PAL-PEG-PS was from Applied Biostems. Preloaded CLEAR-Acid resins were from Peptides International. All other reagents were from Sigma Aldrich. In the following procedures, unless determined by UV spectroscopy, actual peptide content has not been taken into account. All procedures involving fluorescent derivatives were protected from light as much as possible to avoid bleaching the fluorophore.

4.3.2 Abbreviations. Ac, Acetyl; Acm, acetamidomethyl; BOC, *tert*-butyloxycarbonyl; BOP, (benzotriazol-1-yloxy)tris-(dimethylamino)phosphonium

hexafluorophosphate; *t*-Bu, *tert*-butyl; CLEAR, cross-linked ethoxylate acrylate resin; CPP, cell-penetrating peptide; DIC, *N,N'*-diisopropylcarbodiimide; Dde, 1-(4,4-dimethyl-2,6-dioxocyclohexylidene)ethyl; DIEA, diisopropylethylamine; DMEM, Dulbecco's Modified Eagle Medium; DMF, *N,N*-dimethylformamide; DTT, dithiothreitol; ESI-MS, electrospray ionization mass spectrometry; 5-Fam, 5-carboxyfluorescein; Far, farnesyl; FITC, fluorescein isothiocyanate; Fmoc, 9-fluorenylmethyloxycarbonyl; Gg, geranylgeranyl; HOBt, 1-hydroxybenzotriazole; Me, methyl; nL, norleucine; OAc, acetate; PAL, peptide amide linker; Pbf, 2,2,4,6,7-pentamethyldihydrobenzofuran-5-sulfonyl; PEG-PS, polyethylene glycol-polystyrene graft copolymer; PMSF, phenylmethanesulfonyl fluoride; Pnt, penetratin; RP-HPLC, reversed-phase high pressure liquid chromatography; Scm, S-carbomethoxysulfenyl; SPPS, solid-phase peptide synthesis; TFA, trifluoroacetic acid; Trt, trityl.

4.3.3 Peptide Synthesis. Linear peptides were synthesized by Fmoc-based SPPS on either Applied Biosystems 433A or Pioneer automated peptide synthesizers according to manufacturer protocols. Peptides were cleaved with freshly prepared Reagent K (King et al., 1990) (TFA−phenol−thioanisole−water−ethanedithiol 82.5:5:5:5:2.5) for 2 h, precipitated with Et_2O, and centrifuged to form a pellet which was washed with Et_2O. Crude peptides were purified by RP-HPLC.

4.3.3.1 General Procedure for Cysteine Alkylation: Prenylation of AcK(5-Fam)C(Acm)KKSRRC-NH_2 (11) To Produce 1a and 2a. Peptide **11** (1.0 equiv) and $Zn(OAc)_2 \cdot 2H_2O$ (5.0 equiv) were dissolved in DMF/1-butanol/0.10% aqueous TFA (2:1:1, v/v/v) (1.0 mL solvent per 2.0 mg peptide) (Xue et al., 1992). Either farnesyl bromide or geranylgeranyl bromide (4.0 equiv) was then added. The reaction was monitored by RP-HPLC and, once judged complete (typically 2 h), was diluted with 10 volumes of 0.10% aqueous TFA, filtered, and purified by RP-HPLC.

4.3.3.1.1 AcK(5-Fam)C(Acm)KKSRRC(Far)-NH_2 (1a). Reaction scale: 0.014 mmol, yield: 13 mg (54%), purity by RP-HPLC: 95%, t_R = 45 min, deconvoluted ESI-MS: calculated 1681.8, found 1681.8.

4.3.3.1.2 AcK(5-Fam)C(Acm)KKSRRC(Gg)-NH_2 (2a). Reaction scale: 0.010 mmol, yield: 10.5 mg (62%), purity by RP-HPLC: 94%, t_R = 58 min, deconvoluted

ESI-MS: calculated 1973.1, found 1973.0.

4.3.3.1.3 AcK(5-Fam)C(Acm)KKSRRC(Me)-NH_2 (3a). Peptide **3a** was synthesized by the above procedure, except Fmoc-Cys(Me)-OH was substituted for Fmoc-Cys(Trt)-OH during chain assembly on PAL-PEG-PS. Reaction scale: 0.025 mmol, yield: 19.9 mg (54%), purity by RP-HPLC: 99%, t_R = 25 min, deconvoluted ESI-MS: calculated 1491.7, found 1491.9.

4.3.3.1.4 AcK(5-Fam)AKKSRRC(Gg)VLL (4). The geranylgeranyl group was introduced onto the appropriate peptide precursor as it was for **2a**. Reaction scale: 0.012 mmol, yield: 12.7 mg (53%), purity by RP-HPLC: 98%, t_R = 50 min, deconvoluted ESI-MS: calculated 1749.9, found 1750.3.

4.3.3.2 General Procedure for Conversion of Peptides with Cys(Acm) Side-Chain Protection (1a, 2a, and 3a) to Peptides with Cys(Scm) (1b, 2b, and 3b). $CH_3O(CO)SCl$ (5.0 μL) was added to CH_3CN (0.20 mL) to give a 0.27 M stock solution. The Cys(Acm)-containing peptide was dissolved in DMF/CH_3CN (1:1, v/v) (1.0 mL solvent per 1.0 mg of peptide), and the peptide concentration was determined by UV spectroscopy of the 5-Fam chromophore (ε = 79 000, 492 nm, pH 9.0). The reaction and stock solution were cooled in an ice bath, and 1.0 equiv of $CH_3O(CO)SCl$ stock solution was added to the reaction. After 1 h, the reaction was analyzed by RP-HPLC. The percent conversion of Cys(Acm) to Cys(Scm) was calculated by comparing the peak areas of the product and starting peptide peaks (Figure 2). Sufficient additional stock $CH_3O(CO)SCl$ was then added to complete the reaction, based on the percent conversion observed after addition of the first equivalent of $CH_3O(CO)SCl$. The RP-HPLC monitoring and analysis were repeated after another 1 h of reaction time. If any precipitate of the product was observed, sufficient DMF was added to render the solution homogeneous, to ensure an accurate HPLC analysis of % conversion [Cys(Scm) is more hydrophobic than Cys(Acm) and, hence, less soluble]. When the reaction was judged complete, it was diluted with 10 volumes of 0.10% aqueous TFA, filtered, and purified by RP-HPLC. The pooled fractions of product from purification were used directly in the next step without concentration or lyophilization.

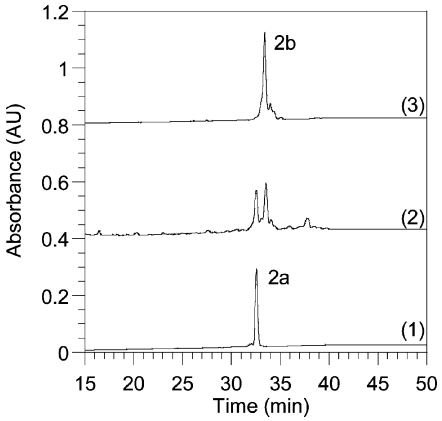

Figure 2. Reversed-phase HPLC analysis monitoring the progress of Acm to Scm conversion in a geranylgeranylated *C*-terminal CDC42 peptide. Gradient: 20−60% CH_3CN over 60 min. Chromatogram (1): Peptide **2a** (t_R = 32.5 min) before the addition of $CH_3O(CO)SCl$. Chromatogram (2): A mixture of Acm and Scm protected peptides **2a** and **2b** 1 h after $CH_3O(CO)SCl$ was added. Chromatogram (3): Complete conversion of Acm-protected peptide **2a** to Scm-modified peptide **2b** (t_R = 33.5 min).

4.3.3.2.1 AcK(5-Fam)C(Scm)KKSRRC(Far)-NH_2 (1b). Purity by RP-HPLC: 82%, t_R = 46 min, deconvoluted ESI-MS: calculated 1700.8, found 1701.0.

4.3.3.2.2 AcK(5-Fam)C(Scm)KKSRRC(Gg)-NH_2 (2b). Purity by RP-HPLC: 69%, t_R = 51 min, deconvoluted ESI-MS: calculated 1768.8, found 1768.6.

4.3.3.2.3 AcK(5-Fam)C(Scm)KKSRRC(Me)-NH_2 (3b). The crude product was isolated and used in the synthesis of **3c** without analytical characterization, t_R = 27 min.

4.3.3.2.4 AcK(5-Fam)C(Scm)KKSRRC(Scm)-NH_2. In early experiments to convert Cys(Acm) to Cys(Scm) in the Cys(Far)- and Cys(Gg)-containing peptides, excess $CH_3O(CO)SCl$ was used. A major early eluting contaminant peak (t_R = 30 min), observed on RP-HPLC, was isolated and identified as the bis(Scm) derivative, in which the Cys(prenyl) group had been cleaved by the excess $CH_3O(CO)SCl$ to yield Cys(Scm). This bis(Scm) derivative was completely stable in 0.10% aqueous TFA solutions for at least several weeks. Treatment of peptides containing prenylated cysteine residues with $CH_3O(CO)SCl$ to yield the corresponding Cys(Scm) derivative, followed by treatment with DTT or 2-mercaptoethanol, may prove useful as a mild method for removal of prenyl groups from cysteine. Deconvoluted ESI-MS: calculated 1586.6, found 1586.6.

4.3.3.3 General Procedure for Conjugation of AcK(5-Fam)C(Scm)KKSRRC(prenyl)-NH_2 with Penetratin To Provide Mixed Disulfide Peptides (1c, 2c, and 3c).

The concentrations of the Cys(Scm)-containing peptides were determined by UV spectroscopy of the 5-Fam chromophore (ε = 79 000, 492 nm, pH 9.0). $Zn(OAc)_2 \cdot 2H_2O$ (5.8 mg) was dissolved in 1.0 M sodium acetate (1.5 mL, pH 5.4) to give a 17 mM Zn^{2+} stock solution. Penetratin (**12**) was dissolved in 0.10% aqueous TFA (2.5 mg/mL, 0.70 mM), and the exact concentration was determined by assaying the free thiol content with Ellman's reagent. Penetratin (1.0 equiv) was added from the stock solution to the pooled Cys(Scm)-containing fractions, the reaction mixture was cooled in an ice bath, and $Zn(OAc)_2$ (5.0 equiv) from the stock solution was added. Next, sufficient sodium acetate (1.0 M, pH 5.4) was added to bring the overall acetate concentration to 0.067 M, and the pH of the reaction mixture was adjusted to pH 5.0−5.2 with 0.10 N NaOH. After 15 min, the reaction was analyzed by RP-HPLC, and additional penetratin from the stock was added as necessary to drive the reaction to completion. When the reaction was judged complete by RP-HPLC analysis (Figure 3), the pH was adjusted to the range 2−3 by addition of neat TFA and the mixture was filtered and purified by RP-HPLC. It is important to note that since this is a bimolecular reaction, the rate is highly dependent on concentration. For more dilute peptide solutions, one may have to wait longer than 15 min to analyze the extent of reaction. UV spectroscopic analysis underestimated the concentration of AcK(5-Fam)C(Scm)KKSRRC(prenyl)-NH_2 relative to penetratin. This is possibly due to the instability of the former peptide at pH 9.0.

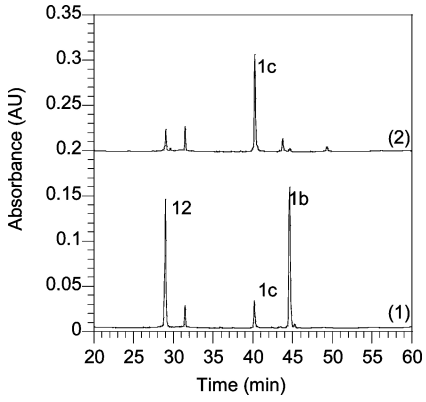

Figure 3. Reversed-phase HPLC analysis monitoring the progress of penetratin conjugation to a Scm-protected farnesylated *C*-terminal CDC42 peptide. Gradient: 0−60% CH_3CN over 60 min. Chromatogram (1): Penetratin (**12**) (t_R = 29.0 min) and peptide **1b** (t_R = 45 min) 24 h after the addition of $Zn(OAc)_2$, pH 2. Chromatogram (2): Formation of penetratin-modified peptide **1c** (t_R = 40 min) 24 h after adjusting to pH 5.2.

4.3.3.3.1 AcK(5-Fam)C(Pnt)KKSRRC(Far)-NH_2 (1c). Yield: 1.9 mg over 2 steps from 5.2 mg **1a** (16%), Purity by RP-HPLC: 95%, t_R = 40 min, deconvoluted ESI-MS: calculated 3925.1, found 3925.0.

4.3.3.3.2 AcK(5-Fam)C(Pnt)KKSRRC(Gg)-NH_2 (2c). Yield: 1.3 mg over 2 steps from 8.9 mg **1b** (6%), Purity by RP-HPLC: 99%, t_R = 48 min, deconvoluted ESI-MS: calculated 3993.2, found 3993.2.

4.3.3.3.3 AcK(5-Fam)C(Pnt)KKSRRC(Me)-NH_2 (3c). Yield: 4.5 mg over 2 steps from 5.0 mg **1c** (36%), Purity by RP-HPLC: 97%, t_R = 31 min, deconvoluted ESI-MS: calculated 3734.9, found 3734.4.

4.3.3.4 AcK(5-Fam)C(Acm)KKSRRC-NH_2 (11). The linear sequence was assembled on either PAL-PEG-PS or Rink-amide resin. DIC and HOBt were used for coupling to avoid racemization of cysteine (Han et al., 1997). The *N*-terminal lysine side chain was orthogonally protected with Dde. Acetic acid was coupled in the last instrument cycle to acetylate the *N*-terminus. The Dde protecting group was removed selectively by treating protected peptide resin (0.05 mmol) in a solid-phase reaction vessel with 5.0 mL of anhydrous NH_2NH_2/DMF (1:9, v/v), for 15 min, followed by washing with DMF (5 × 5.0 mL) (Bycroft et al., 1993). 5-Fam (38 mg, 0.10 mmol), DIC (16 mL, 0.10 mmol), and HOBt (13.5 mg, 0.10 mmol) were dissolved in DMF (2.0 mL) and then added to the peptide resin along with DMF washes (2 × 0.5 mL). The coupling reaction was allowed to tumble overnight, and then the peptide resin was washed with DMF (3 × 5.0 mL) and CH_2Cl_2 (3 × 5.0 mL) and dried *in vacuo*. The peptide was cleaved with Reagent K (King et al., 1990) (TFA−phenol−thioanisole−water−ethanedithiol 82.5:5:5:5:2.5) for 2 h, precipitated with Et_2O, and centrifuged to form a pellet, which was washed with Et_2O. The crude peptide was purified by RP-HPLC. Yield: 18−30 mg (24−40%), purity by RP-HPLC: >95%, t_R = 26 min, deconvoluted ESI-MS: calculated

1477.6, found 1477.4.

4.3.3.5 5-Fam-CRNIKIWFQNRRnLKWKK (5). The linear peptide was synthesized as for compound **11** except acetic acid was not coupled in the last instrument cycle to acetylate the *N*-terminus. 5-Fam was coupled to the N-terminus of side-chain protected peptide resin, using the same procedure described for fluorophore coupling used on compound 11. Purity by RP-HPLC: 97%, t_R = 37 min. Deconvoluted ESI-MS: calculated 2674.4, found 2674.4.

4.3.3.6 AcK(5-Fam)AKKSRRCVLL (Precursor to 4). The linear peptide sequence was synthesized using CLEAR-Acid resin (Kempe and Barany, 1996), and the 5-Fam fluorophore was coupled to the *N*-terminal lysine side chain of otherwise fully protected peptide resin as described for compound **11**. Purity by RP-HPLC: 99%, t_R = 34 min, deconvoluted ESI-MS: calculated 1700.9, found 1700.8.

4.3.3.7 CRNIKIWFQNRRnLKWKK (Penetratin) (12). Purity by RP-HPLC: 99%, t_R = 29 min, Deconvoluted ESI-MS: calculated 2316.3, found 2316.0.

4.3.3.8 Geranylgeranyl Bromide (Kale, 2001)**.** Geranylgeraniol (0.10 g, 0.69 mmol, 1.0 equiv) was dissolved in CH_2Cl_2 (4.2 mL). Next, polymer-supported PPh_3 (0.45 g, 1.438 mmol, 2.0 equiv) was added, and the solution was gently shaken. After the addition, the heterogeneous solution turned a light brown color. After 30 min, CBr_4 (0.27 g, 0.83 mmol, 1.2 equiv) was dissolved in 0.5 mL of CH_2Cl_2 and added to the mixture via syringe. This solution was stirred for 6 h, after which the polymer-supported reagent was removed by filtration and the resulting solution was concentrated to yield 0.11 g of geranylgeranyl bromide (89% yield). This crude product was stored at −20 °C. Just prior to use in the alkylation reaction, the calculated amount of geranylgeranyl bromide (4.0 equiv over peptide) was purified by solid phase extraction on a C18 Sep-Pak cartridge. The cartridge was first equilibrated with 5% CH_3CN in water that contained 0.10% TFA. The geranylgeranyl bromide was dissolved in 0.50 mL of DMF and applied to the column. The column was then washed with 10 mL of equilibration solvent and 10 mL of 50% CH_3CN in water that contained 0.10% TFA. The geranylgeranyl bromide was then eluted from the column directly into the reaction vessel with 5.0 mL of DMF. If this solid phase extraction procedure is not done, a large amount of disulfide impurity, rather than

the desired geranylgeranyl alkylation product, is formed in the reaction. ^{1}H NMR (300 MHz, CDC_{l3}) δ = 1.62 (s, 6H), 1.70 (s, 3H), 1.77 (s, 3H), 1.79 (s, 3H), 2.00−2.16 (m, 12H), 4.04 (d, 1H, *J* = 7.2 Hz), 5.11 (m, 3H) 5.54 (t, 1H, *J* = 7.2 Hz). ^{13}C NMR-DEPT (CDCl3) δ 16.0, 16.1, 16.2, 17.7, 25.8 (primary), 26.2, 26.7, 26.8, 29.8, 39.6, 39.7, 39.8, (secondary), 120.6, 123.5, 124.2, 124.4 (tertiary), 131.4, 135.1, 136.2, 143.7 (quaternary). HR-FAB-MS calculated for $C_{20}H_{33}Br$ $[M + NH_4]^+$ 370.21, found 370.21.

4.3.4 Determination of Peptide Concentrations for Cell Studies. Stock peptide solutions were diluted using 20 mM Tris buffer, pH 9.0, and DMSO so that the final concentration of DMSO was no greater than 0.10% by volume. UV spectroscopy of the 5-Fam chromophore was used to determine the concentrations of filtered peptide stock solutions (ε_{492} = 79 000, 492 nm, 20 mM Tris·HCl, pH 9.0) (Haugland, 2005).

4.3.5 Cell Culture. HeLa cells were grown in DMEM supplemented with 10% fetal bovine serum at 37 °C with 5.0% CO_2. For all experiments, 2.6×10^4 cells/cm^2 were seeded in culture dishes and grown for 24 h to 50% confluency.

4.3.6 Confocal Microscopy. HeLa cells were seeded in 35 mm glass bottom microwell dishes. Approximately 24 h after plating, cells were washed twice with serum-free DMEM and incubated for 1 h at 37 °C and 5.0% CO_2 in serum-free DMEM containing 1.0 μM peptide. Hoechst 34580 was added to 1 μg/mL during the final 20 min of incubation, and wheat germ agglutinin Alexa Fluor 594 conjugate was added to 5 μg/mL during the final 10 min of incubation. For ATP depletion, cells were washed twice with glucose-free, serum-free DMEM and then incubated for 2 h at 37 °C and 5.0% CO_2 in glucose-free, serum-free DMEM supplemented with 12 μM rotenone and 15 mM 2-deoxyglucose (Meriin, 1999). Then peptides, Hoechst 34850, and wheat germ agglutinin AlexaFluor 594 conjugate were added, and cells were incubated as described above. For peptide incubation at 4 °C, cells were washed twice with chilled serum-free DMEM supplemented with 25 mM HEPES (pH 7.3) and incubated with peptide, Hoechst 34850, and wheat germ agglutinin Alexa Fluor 594 conjugate as described above at 4 °C. After 1 h of total incubation, all cells were washed twice with PBS. Cells were then imaged either live in serum-free DMEM or fixed for 10 min at room temperature in 3.7% formaldehyde in PBS. Coverslips were mounted with ProLong Gold Antifade Reagent on

1 mm glass microscope slides. Cells were imaged using an Olympus FluoView 1000 confocal microscope with a 60× objective with an N.A. of 1.42. The 5-Fam fluorophore was imaged using fluorescein settings, Hoechst 34850 was imaged using DAPI settings, and wheat germ agglutinin Alexa Fluor 594 conjugate was imaged using Alexa Fluor 594 settings. All fluorescence and brightfield images were acquired simultaneously.

4.3.7 Quantitation of Cellular Uptake of Fluorescent Peptides Using Cell Lysates. Peptide stock solutions in Tris (20 mM, pH 9.0) were prepared so that when the peptide (237 μL) was diluted into serum-free DMEM (263 μL), the final concentrations of peptides would be 0.10, 0.30, 1.0, or 3.0 μM. The dilution kept the amount of Tris compared to DMEM constant, regardless of final peptide concentration. Dilution was required because of the differential solubility among peptides. HeLa cells (2.6×10^4 cells/cm^2) were seeded in 12 well plates and grown for 20 h to 50% confluency. Next, the media was removed and DMEM containing diluted peptide (500 μL) was added to each well. Cells were treated with each peptide in triplicate and were incubated for 1 h at 37 °C in 5.0% CO_2. At this time, the peptide-containing media was removed, and the wells were washed with PBS (1.0 mL, 137 mM NaCl, 2.7 mM KCl, 4.3 mM Na_2HPO_4, 1.4 mM KH_2PO_4, pH 7.3). Next, the cells were lysed with RIPA buffer (100 μL, 50 mM Tris·HCl, pH 7.4, 1.0% NP-40, 0.25% Na-deoxycholate, 150 mM NaCl, 1.0 mM EDTA) and scraped from the wells. The lysates were placed in 1.6 mL microcentrifuge tubes and centrifuged (1.0 min, 10 000 g). The fluorescence of the supernatant (490 nm excitation, 520 nm emission, 5 nm slit widths) was measured to quantitate the amount of internalized peptide. This measurement was then normalized against the amount of protein in the sample using the Bradford assay (BioRad) to measure the protein concentration. Each experiment was performed in triplicate, and the results are expressed as the mean relative fluorescence ± standard deviation.

4.3.8 Quantitation of Cellular Uptake of Fluorescent Peptides Using Flow Cytometry. HeLa cells were seeded in 6-well plates and treated with peptides as described for microscopy. After treatment for 1, 2, 3, or 4 h, cells were washed twice with PBS, trypsinized for 5 min, and resuspended to a total volume of 2 mL with DMEM/10% FBS. Cells were centrifuged for 5 min at 100 × g and resuspended in PBS

to a final volume of 2 mL. A total of 10 000 events for each sample were analyzed using a BD FACSCalibur (BD Biosciences). Each experiment was performed in triplicate, and the results are expressed as the geometric mean fluorescence ± standard deviation.

4.4 Results

4.4.1 Synthesis of Cysteine-Alkylated CDC42 *C*-Terminal Peptides. To prepare the desired multifunctional prenylated peptides for live cell analysis, our initial strategy was to synthesize farnesylated peptide **8** by alkylation of peptide **7** derived after manipulation and cleavage of the peptide resin **6**. Fluorescein isothiocyanate (FITC) was chosen as the fluorescence reporter because of its reasonable cost, high fluorescence, and ready reactivity with primary amines via the isothiocyanate group. Thus, after selective on-resin removal of the Dde protecting group from the N-terminal Ac-Lys with anhydrous hydrazine (Scheme 1), FITC (3 equiv), in the presence of DIEA (6 equiv), was coupled onto the lysine side chain (1 equiv) to install a thiourea-linked fluorophore. Final deprotection with Reagent K gave an orange peptide (**7**), in which one cysteine remains protected with the Acm group, while the free thiol of the second cysteine side chain is available for alkylation. Interestingly, alkylation of the deprotected thiol in this peptide with farnesyl bromide in the presence of $Zn(OAc)_2$ always resulted in mixtures of mono- (**8**) and dialkylated products (**9**) as determined by ESI-MS, even when only 1 equiv of farnesyl bromide was added slowly to the peptide. Since it has been reported previously that Zn^{2+}-catalyzed thiol alkylation under acidic conditions does not result in sulfonium ion formation (Xue et al., 1992) (dialkylation of a single Cys), it was concluded that a second site in the peptide was undergoing alkylation at a rate that was competitive with alkylation of the free thiol of the C-terminal cysteine. While the most likely second site is the thiourea moiety linking fluorescein and the peptide (as suggested by peptide **9**), we were unable to conclusively confirm the position of the second alkylation site by MS/MS sequence analysis due to complex fragmentation of the bis-alkylated peptide. To circumvent the dialkylation side reaction, FITC was replaced by 5-carboxyfluorescein (5-Fam) (Scheme 2) resulting in a fluorophore that was linked via an amide bond in lieu of a thiourea. As before, peptide-resin **6** was treated with anhydrous NH_2NH_2 to remove the

orthogonal Dde protecting group, and this was followed by acylation of the resulting amine with 5-Fam using DIC and HOBt to produce peptide-resin **10**. Cleavage from the resin and global deprotection afforded **11**, which was subsequently alkylated with a prenyl bromide to yield **1a** or **2a**. In contrast to what was observed with peptide **7** where the fluorescein was linked via a thiourea, peptide **11** yielded only the monoalkylated product **1a** or **2a**, with no trace of dialkylated side products. Thus, peptides **1a** and **2a** were efficiently prepared for use in cellular experiments, as well as for subsequent conversion to **1c** and **2c**. The methylated analogue (**3a**) was prepared by direct incorporation of *S*-methyl cysteine (via Fmoc-Cys(Me)-OH) during SPPS, since the *S*-methyl derivative lacks the acid lability characteristic of prenylated peptides. The geranylgeranylated peptide containing a full length "CAAX box" (**4**) was prepared in a similar fashion to that described for **2a**.

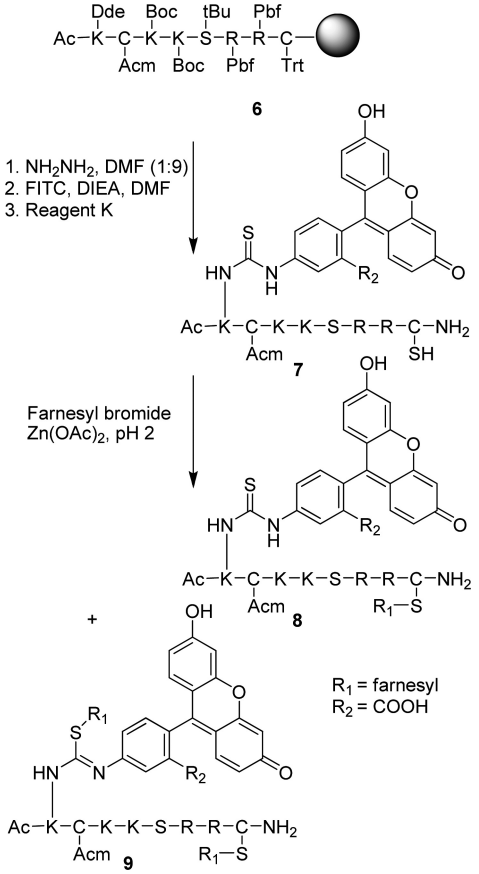

Scheme 1. Initial Strategy for Synthesis of Fluorescent Prenylated Peptides Labeled via FITC

Modification[a]

[a]Although **8** elutes as a single peak in HPLC analysis, it is likely that it is an isomeric mixture of the structure shown and is the isomer containing the farnesyl group on the thiourea sulfur atom.

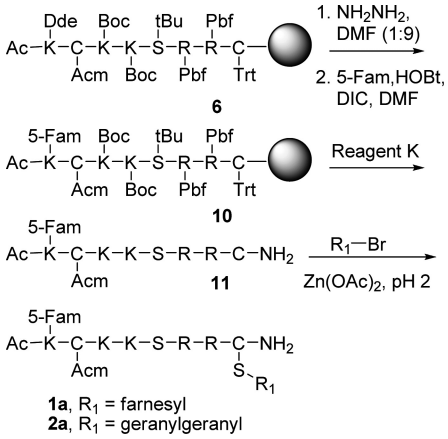

Scheme 2. Revised Strategy for the Synthesis of Fluorescent Prenylated Peptides Labeled via 5-Fam Incorporation

Next, for the preparation of **1c**–**3c**, it was necessary to unmask the Acm-protected cysteine present in **1a**–**3a** so that penetratin could be linked via a disulfide bond. Multiple attempts using mercuric acetate (Veber et al., 1972), the standard method for Acm removal, to accomplish this transformation were unsuccessful. These results are likely due to the presence of the alkene functional groups in the isoprenoid moiety that might readily undergo oxymercuration. A revised strategy was chosen in which the Acm protecting group was transformed into a more active Scm derivative (Scheme 3) (Hiskey et al., 1975). Conversion of Acm to Scm has the advantage of directly activating the thiol of cysteine to a species that can be used to form an unsymmetrical disulfide between the prenylated peptide and penetratin **12**. Initial reactions on prenylated derivative **1a** involved dissolving the peptide in MeOH/CH_3CN mixtures and treating with $CH_3O(CO)SCl$ from a stock solution in MeOH. Although conversion of Acm to Scm was observed, the reaction was not reliably reproducible. From model studies on Boc-Cys(Acm)-OH, it was determined that the MeOH stock solutions of $CH_3O(CO)SCl$ rapidly lost activity (data not shown). In contrast, stock solutions of $CH_3O(CO)SCl$ in CH_3CN are completely stable and active for at least 1 day. Thus, to reproducibly effect

the Cys(Acm) to Cys(Scm) conversion, alcohol-containing solvents must be avoided and the reaction should be performed in DMF/CH_3CN solvent mixtures. It was also found that the use of excess $CH_3O(CO)SCl$ resulted in cleavage of thioether-linked isoprenoids to Cys(Scm). However, this side reaction was avoided by careful titration of the $CH_3O(CO)SCl$ reagent into the reaction, with monitoring by RP-HPLC. An analysis of a typical example of this Cys(Acm) to Cys(Scm) conversion is presented in Figure 2. Chromatogram 1 shows a pure sample of starting peptide **2a**, chromatogram 2 shows a sample from the reaction at intermediate conversion, and chromatogram 3 shows the reaction upon completion where the only significant species present is the Scm-protected peptide **2b**. This approach was employed to prepare the Scm-protected peptides **1b**–**3b**.

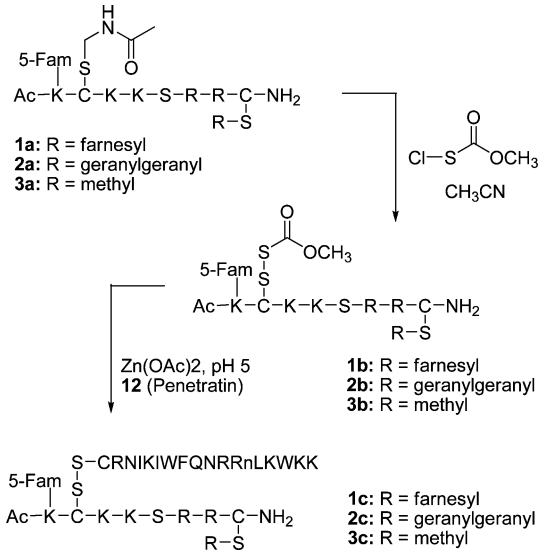

Scheme 3. Strategy for Linking Penetratin to Fluorescent Prenylated Peptides

Next, the preparation of the desired penetratin-linked prenylated peptides was undertaken, using the activated Scm-containing peptides described above. Initial attempts to form the desired unsymmetrical disulfides that link penetratin to the prenylated peptides involved dissolving a Cys(Scm)-containing peptide in phosphate buffer, pH 7.5, and then adding a solution of penetratin analogue **12** dissolved in 0.10% aqueous TFA. The solvents were carefully degassed, and the reaction was carried out under a N_2 atmosphere. The only peptides that were identified under those conditions were unreacted

12 and its related symmetrical disulfide dimer, while the Cys(Scm)-containing peptide appeared to have undergone decomposition. The instability of Cys(Scm)-containing peptides in phosphate buffer was confirmed by dissolving prenylated peptide 1b in buffer and monitoring by RP-HPLC. Complete decomposition was observed within 15 min (data not shown). The decomposition in phosphate near neutral pH was surprising, since Cys(Scm)-containing peptides are stable in 0.10% aqueous TFA for several days, and acidic reaction mixtures containing them can be evaporated to dryness without ill effect. Thus, it appeared reasonable to explore acidic conditions for forming the desired disulfide. When Cys(Scm)-containing peptide **1b** and penetratin analogue **12** were reacted in the presence of Zn^{2+} in 0.10% aqueous TFA, pH 2.0, a small amount of desired unsymmetrical disulfide **1c** was observed. Unfortunately, after the initial burst of product formation, the reaction stopped and no additional **1c** appeared, even after long reaction times. However, after the pH was raised into the range 5.0−5.3 by titration with 0.10 N NaOH, the reaction rapidly proceeded to completion. No disulfide scrambling or air oxidation of cysteine was observed under these mildly acidic reaction conditions. An analysis of such a reaction is presented in Figure 3. Chromatogram 1 shows the reaction after 24 h at pH 2.0; a small burst of product initially forms and then the reaction stops. After the adjusting to pH 5.2, the reaction is essentially complete in 24 h (Figure 3, Chromatogram 2). This procedure was employed for the synthesis of three penetratin-linked peptides (**1c**−**3c**) containing *S*-farnesyl, *S*-geranylgeranyl, and *S*-methyl modifications. With the synthesis of the desired prenylated peptide conjugates completed, we next proceeded to examine the distribution of these molecules in live cells.

4.4.2 Quantitative Uptake of Modified -KKSRRC-NH_2 Peptides. To evaluate the cellular uptake of the synthetic peptides prepared above, two methods were employed. Initially, this was accomplished by treating HeLa cells with each peptide over a range of concentrations, followed by washing, cell lysis, and quantitation of the internalized peptide via fluorescence spectroscopy. Using this method all peptides with the exception of **3a** were able to enter cells at concentrations ranging from 0.1 to 3.0 μM. While the entry of the penetratin conjugates was expected, the uptake of the geranylgeranylated CDC42 peptide (**2a**) lacking any penetratin moiety was surprising. To ensure the

observed uptake of prenylated peptides using this method was not merely due to peptide adsorption to plasma membranes, internalization was also measured using an alternative method where the cells were trypsinized prior to uptake analysis by flow cytometry. Trypsin digests and hence removes any peptide bound to the cell surface, thus allowing for the quantitation of only internalized peptide (Richard et al., 2003). Analysis of peptide concentrations in nontrypsinized cell samples (Figure 4) showed that incorporation of the geranylgeranylated CDC42 peptide without penetratin (**2a**) was comparable to that of the same peptide conjugated to penetratin (**2c**) at 0.3 and 1.0 μM; at 3.0 μM, the cellular uptake of **2a** was actually higher than that of **2c**. Such nonlinear changes in uptake at higher concentrations have been reported for other cationic cell-penetrating molecules (Duchardt et al., 2007). Analysis using trypsinized cell samples treated with 1.0 μM peptide showed 5-Fam labeled penetratin (**5**) entered cells 5-fold more than geranylgeranylated CDC42 peptide **2a** (Figure 5A). Interestingly peptide **2c**, which has both penetratin and geranylgeranyl moieties, entered cells 2-fold more than any of the other peptides examined suggesting that the effects of having an isoprenoid and a penetratin group may be additive. Thus, while these results indicate that some nonspecific surface adsorption occurs for the prenylated peptide **2a**, that peptide is clearly capable of gaining entry into cells even though it lacks the penetratin substructure.

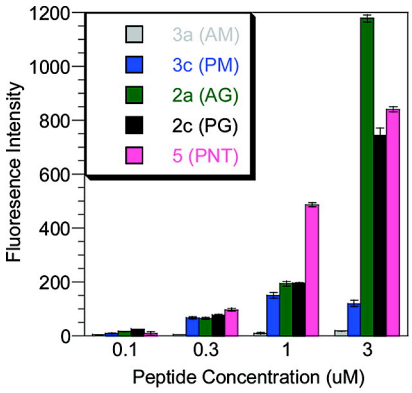

Figure 4. Uptake of 5-Fam labeled peptides in HeLa cells evaluated by fluorescence spectroscopy. Cells were treated with peptide at different concentrations (0, 0.1, 0.3, 1.0, 3.0 μM) for 1 h, washed, and lysed in RIPA buffer. The fluorescence of the lysates was then normalized against the amount of protein in the sample. Each experiment was performed in triplicate, and the results are expressed as the mean relative fluorescence ± standard deviation.

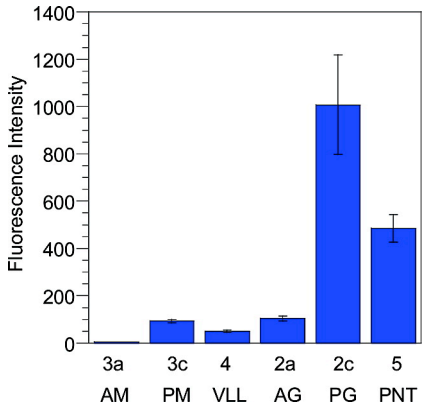

Figure 5. Uptake of CPPs in HeLa cells at 37 °C determined by flow cytometry. After incubation with peptide (1.0 μM) for 1 h, the cells were trypsinized and washed to remove any surface-bound peptide. Each bar represents the geometric mean fluorescence of 10 000 cells counted by FACS analysis, each experiment was performed in triplicate, and the results are expressed as the mean relative fluorescence ± standard deviation.

4.4.3 Cellular Internalization of Modified -KKSRRC-NH_2 Peptides. To gain a better understanding of the mechanism of entry of these peptides into cells and their distribution, confocal microscopy experiments were performed. As noted above, studies were performed in parallel with a fluorescently labeled penetratin peptide lacking the CDC42 sequence (**5**) to provide a benchmark for comparison. Figure 6 shows several confocal microscope images (of fixed cells) obtained after treating cells with different peptides. In each case, HeLa cells were treated with a given peptide for 1 h followed by washing to remove unincorporated probe. Cells were treated with two additional fluorescent markers to visualize the nucleus (blue) and cell membrane (red) and then examined by confocal microscopy to observe the localization of the peptide (green).

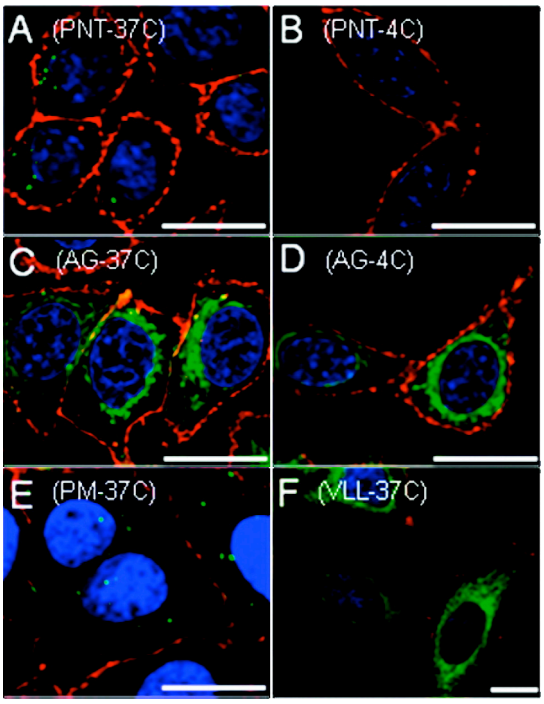

Figure 6. Confocal microscope images of fixed cells showing the uptake of CPPs in HeLa cells. After incubation with peptide (1.0 μM) for 1 h, the cells were washed, fixed, treated with ProLong Gold to limit fluorescence fading, and imaged. (A) 5-Fam labeled penetratin peptide **5** treated at 37 °C. (B) 5-Fam labeled penetratin peptide **5** treated at 4 °C. (C) Geranylgeranylated peptide **2a** treated at 37 °C. (D) Geranylgeranylated peptide **2a** treated at 4 °C. (E) Methylated penetratin linked peptide **3c** treated at 37 °C. (F) "CAAX box" containing peptide **4** treated at 37 °C. Hoechst 34850 blue DNA staining dye was used to stain the nucleus blue, wheat germ agglutinin Alexa Fluor 488 was used to stain the plasma membrane red, and peptides were visualized as green. Orange staining is due to colocalization of green peptide with red plasma membrane dye. Bars in the lower corners of the images represent a distance of 20 μm.

Panel A in Figure 6 shows the results observed with HeLa cells treated with the fluorescently labeled penetratin control peptide (**5**). That peptide manifested a punctate pattern of green fluorescence within the cell that is characteristic of endocytic entry. Interestingly, treatment of cells with the farnesylated CDC42 peptide conjugated to penetratin (**1c**) produced a diffuse distribution of green fluorescence within the cells, accompanied by some punctate fluorescence (See Supporting Information, S1). In contrast, treatment of cells with the methylated CDC42 peptide conjugated to penetratin (**3c**) produced a punctate pattern of fluorescence exclusively (Figure 6, panel E) similar to

that of the simple penetratin peptide (**5**). These two results indicated that the presence of the isoprenoid moiety was playing a central role in controlling the observed localization of the internalized peptides. Finally, treatment of cells with the geranylgeranylated CDC42 peptide (**2a**) that retained the Acm protecting group, and hence was not conjugated to penetratin (Figure 6, panel C), resulted in an intense diffuse distribution of green fluorescence within the cells localized to the perinuclear region. Similar, although less dramatic, results were observed with the Acm-protected farnesylated peptide (**1a**) but not with the corresponding methylated analogue (**3a**) (data not shown).

The observation that prenylated peptides lacking a cell penetrating peptide fusion could efficiently enter cells, coupled with their nonpunctate distribution, suggested that their mechanism of cellular uptake might differ from that of penetratin. To investigate that possibility, we repeated the experiments described above at lower temperature, since it has been well established that endocytic uptake is inhibited at 4 °C. Treatment of HeLa cells with the fluorescently labeled penetratin control peptide (**5**) at 4 °C showed no green fluorescence within the cells (Figure 6, panel B). Instead, the green peptide remained on the surface of the cells, colocalizing with the red plasma membrane marker producing an orange color at the plasma membrane (see also Supporting Information, S1). In contrast, treatment of HeLa cells at 4 °C with the geranylgeranylated CDC42 peptide (**2a**) lacking the penetratin moiety showed substantial uptake of the peptide (Figure 6, panel D); essentially, the behavior of this peptide was identical at the two different temperatures, suggesting that it does not enter through an endocytic pathway via depletion of intracellular ATP. To confirm that conclusion, cellular uptake was also examined in the presence of rotenone and 10 mM 2-deoxyglucose, which are known to inhibit processes that are energy dependent including endocytosis (Meriin et al., 1999). Treatment of HeLa cells with the fluorescently labeled penetratin control peptide (**5**) in the presence of rotenone and 10 mM 2-deoxyglucose resulted in no uptake, whereas significant uptake was observed with the geranylgeranylated peptides **2a** and **4** (see Supporting Information, S2).

Recent reports have surfaced which indicate that fixing cell samples can in some cases render the cells more permeable to penetrating molecules (Richard et al., 2003).

Since the microscopy experiments discussed above were completed on fixed cell samples, confocal microscopy imaging was also carried out on live HeLa cells treated with prenylated peptide **2a** and penetratin linked peptide **5**. Confocal images of live cells treated with penetratin peptide **5** at 37 °C showed perinuclear punctate fluorescence indicative of endocytotic uptake and looked identical to fixed samples treated under the same conditions (compare Figure 6, panel A to Figure 7, panel C). Images of ATP-depleted cells that were treated with peptide **5** lacked punctate fluorescence but showed a diffuse green staining throughout the cell that required an increase of laser power for visualization (Figure 7, panel D). The intensity of the green peptide signal was observed to be significantly less for ATP-depleted samples incubated with peptide **5**. The decrease of internalized peptide **5** in ATP-depleted samples was later confirmed by FACS analysis (Figure 8). Together these observations confirm previous experiments by Letoha et al. who concluded that penetratin-linked peptides internalize mainly by an endocytotic mechanism but can still gain entry to a lesser degree by direct transport (Letoha et al., 2003). In contrast, prenylated peptide **2a** did not show differential localization hinging on whether the treated cells were ATP-depleted (Figure 7, panels A and B). The images observed of live cells treated with peptide **2a** are very similar to those obtained of cells that were fixed after treatment with peptide (compare Figure 6, panel C to Figure 7, panel A). The only observed difference between live and fixed images of cells treated with prenylated peptides is an increase in green signal intensity for fixed samples. This corresponds to previous results by Richard et al. that showed fixing cells treated with CPPs can lead to an increase in cell permeability (Richard et al., 2003). Even though fixing may increase the amount of peptide that internalizes, it does not change the phenotypic localization of peptide. Thus, quantitation of CPP internalization is more accurately assessed from live cell samples using flow cytometry rather than using signal intensities from confocal images.

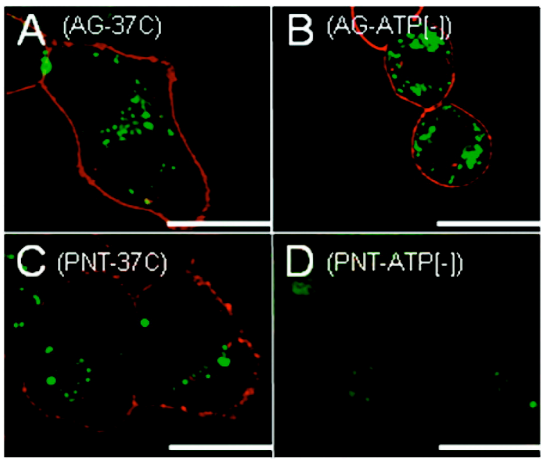

Figure 7. Live cell images showing the uptake of CPPs in HeLa cells. After incubation with peptide (1.0 μM) for 1 h, the cells were washed and imaged without fixation. (A) Geranylgeranylated peptide **2a** treated at 37 °C. (B) Geranylgeranylated peptide **2a** treated to ATP-depleted cells. (C) 5-Fam labeled penetratin peptide **5** treated at 37 °C. (D) 5-Fam labeled penetratin peptide **5** treated to ATP-depleted cells. Images in panels A−C were taken using the same laser parameters, while the image in panel D required higher laser power for visualization. The intensity of the red channel in panel D was also reduced to avoid obscuring the small amount of green fluorescence. Wheat germ agglutinin Alexa Fluor 488 was used to stain the plasma membrane red, and peptides were visualized as green. Orange staining is due to colocalization of green peptide with red plasma membrane dye. Bars in the lower corners of the images represent a distance of 20 μm.

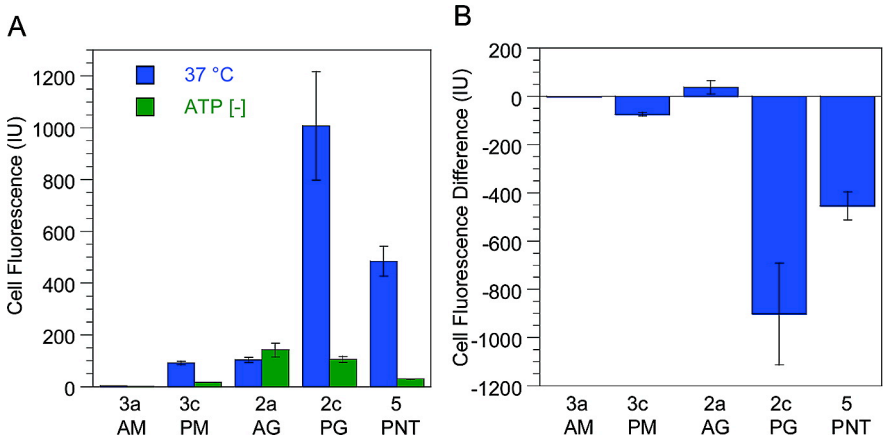

Figure 8. (A) Uptake of CPPs in HeLa cells treated at 37 °C (blue) and under ATP-depleting conditions (green) obtained by flow cytometry. (B) The difference between peptide uptake under ATP-depleted conditions and at 37 °C. This is calculated by subtracting the geometric mean fluorescence of cells treated at 37 °C from the geometric mean fluorescence of cells treated under ATP-depleted conditions. After

incubation with 1.0 μM peptide for 1 h, the cells were trypsinized and washed to remove any surface-bound peptide. Each bar represents the fluorescence of 10 000 cells counted by FACS analysis, each experiment was performed in triplicate, and the results are expressed as the mean relative fluorescence ± standard deviation.

The mechanistic conclusions from the above confocal experiments were corroborated by results acquired from peptide uptake data obtained via flow cytometry and fluorescence measurements. Penetratin-linked peptides **5** and **3c** showed significantly less cellular uptake in ATP-depleted cell samples compared to non-ATP-depleted controls, while geranylgeranylated peptide **2a** showed similar levels of internalization regardless of whether the treated cells were ATP-depleted (Figure 8A). The changes in the amount of peptide internalization are more clearly illustrated in Figure 8B which plots the difference between uptake under ATP-depleted conditions and uptake under normal (37 °C) conditions; negative values in that plot indicate that internalization requires ATP. As expected, large decreases were observed for peptides **5** and **3c** consistent with the established ATP-dependent mechanism for penetratin-mediated cell entry. In contrast peptide **2a** shows no similar decrease. Since ATP-depletion affects only endocytotic uptake, the above results suggest that prenylated peptides enter cells through a mechanism distinct from the endocytotic pathway that has been proposed for penetratin-linked peptides. The residual uptake observed for penetratin linked peptides **5** and **3c** can be attributed to a small amount of nonendosomal uptake that has been previously reported for penetratin linked molecules (Letoha et al., 2003). Peptide **2c** which has both a geranylgeranyl and a penetratin moiety showed ATP-depleted cell uptake similar to that of prenylated peptide **2a**. Thus under ATP-depleting conditions that prevent endocytic uptake, the presence of a prenyl group within peptides **2a** and **2c** is clearly the dominant structural feature responsible for the cell penetrating capability of these molecules.

4.4.4 Kinetics of Peptide Uptake. Since the results described above suggested that the prenylated peptides reported here internalize through a nonendosomal pathway, in contrast to penetratin, we decided to examine the rate of internalization for two representative peptides. Accordingly, we analyzed the kinetics of internalization for a

prenylated peptide, geranylgeranylated peptide **2a**, and for the Fam-labeled penetratin peptide **5** (Figure 9). In those experiments, HeLa cells were incubated with peptide (1.0 μM) for varying amounts of time, trypsinized, and the resulting cells were subjected to FACS analysis to quantify the amount of internalized peptide. 5-Fam-labeled penetratin (**5**) reached its maximum internalization level after 1 h of incubation and was observed to decrease with longer incubation periods. Internalization of geranylgeranylated peptide **2a** was at 70% of its maximum level after 1 h and leveled off after 2 h. After 4 h the internalized level of geranylgeranylated peptide **2a** exceeded that of 5-Fam-linked penetratin (**5**); this may reflect the greater stability of **2a** compared to **5**. Since peptide **2a** possesses both a blocked *N*-terminus (due to the 5-Fam) and a modified cysteine at its *C*-terminus, it is probably less susceptible to degradation by exoproteases; resistance to carboxypeptidase has previously been demonstrated for other prenylated peptides (Schafer and Rine, 1992; Edelstein et al., 1998). Since internalized levels of 5-Fam-linked penetratin begin to decrease and levels of geranylgeranylated peptide **2a** are near their maximum after 1 h, this length of incubation represents a good compromise for comparing the internalization of the various peptides reported here.

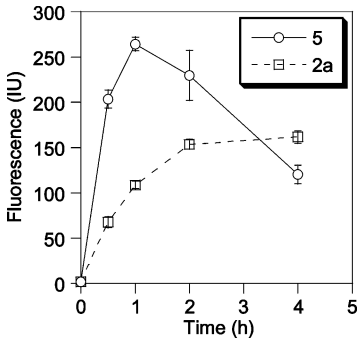

Figure 9. Time dependent uptake of CPPs. Cells were treated with 1 μM of geranylgeranylated peptide **2a** (□) or 5-Fam-linked penetratin peptide **5** (○). After incubation for different amounts of time the cells were trypsinized and washed to remove any surface-bound peptide. Each time point represents the fluorescence of 10 000 cells counted by FACS analysis, each experiment was performed in triplicate, and the results are expressed as the mean relative fluorescence ± standard deviation. Data points are connected to indicate the trend in each case.

4.4.5 Internalization of a Prenylated Peptide Including an Intact "CAAX Box". Given the interesting result that prenylated CDC42-derived peptides lacking a penetratin moiety could freely enter cells, we wanted to determine whether related peptides that contain an intact *C*-terminal "CAAX box" could also be introduced into living cells. To study this, a CDC42-derived peptide that included the natural *C*-terminal sequence CVLL was prepared and geranylgeranylated; this peptide lacked the second cysteine present in the other peptides and was hence considerably easier to synthesize. Standard SPPS assembly, followed by on-resin labeling with 5-Fam, cleavage, and alkylation of the resulting free thiol in the presence of $Zn(OAc)_2$ using geranylgeranyl bromide, gave peptide **4**. Treatment of HeLa cells with peptide **4** at 1.0 μM, followed by confocal microscopy, showed that the peptide was able to enter the cells and that it localized in a fashion similar to what was observed with the geranylgeranylated peptide lacking the intact "CAAX box" (**2a**) (Figure 6, compare panels F and C). Similar experiments performed at 4 °C and under ATP-depleted conditions showed that the peptide was still able to enter the cells, suggesting a nonendocytic mechanism for cellular uptake (see Supporting Information, S1 and S2). Interestingly the distribution of **4** appears more diffuse than that of **2a**. This probably reflects the more polar nature of **4** compared to **2a** since the *C*-terminus of **4** is anionic (carboxylate) whereas that of **2a** is neutral (amide). The greater polarity of **4** would then result in less dramatic partitioning between the cytosol and internal membranes compared with **2a**.

4.5 Discussion

Previous studies have shown how prenylated peptides localize in natural (Thissen and Casey, 1993) and artificial membranes (Ghomashchi et al., 1995; Silvius and l'Heureux, 1994). Such studies showed what types of membranes bind prenylated peptides but did not allow examination of the subcellular localization of prenylated peptides in live cells, or their processing therein. The goal of the work reported here was to develop synthetic methods for the preparation of multifunctional prenylated peptides and to demonstrate that they could be introduced into living cells and visualized by fluorescence techniques.

The peptide sequence used in this work, -KKSRRC-NH_2, is based on the *C*-terminal

hexapeptide from fully processed CDC42, a small GTP binding protein from the Ras superfamily that is involved in regulation of cytoskeletal assembly. This peptide, when prenylated, is known to bind to the effector protein RhoGDI (Hoffman et al., 2000). Thus, this peptide sequence was chosen to facilitate studies of prenylation and its role(s) in biological systems.

The syntheses of the desired multifunctional peptides **1a**−**3a** and **1c**−**3c** contained several design challenges. Once the linear peptide sequence was synthesized, it was necessary to achieve three subsequent modifications. First, the *C*-terminal cysteine needed to be prenylated, and second, a fluorophore needed to be attached so that the peptide could be visualized. Third, it was thought that a CPP sequence would be needed to traverse the cell membrane. To accommodate these modifications, two amino acids were added to the *N*-terminus, and a protection scheme that included three dimensions of orthogonality was chosen. Since the all-trans double bonds of the prenyl groups are not stable to the acidic final cleavage conditions used in Fmoc-based SPPS, these moieties were attached to the peptide in solution subsequent to cleavage from the resin (Naider and Becker, 1997). Also, to avoid scrambling the disulfide linkage among the two cysteines, penetratin was added last in the synthetic sequence. To differentiate between the two cysteines, orthogonal protection for the cysteine closest to the *N*-terminus was accomplished with an Acm group (Veber et al., 1972), and for the *C*-terminal cysteine a Trt group was employed.

The selective introduction of a fluorophore onto the *N*-terminal lysine side chain is best accomplished on-resin while the peptide is still fully protected, through the use of orthogonal Dde protection (Bycroft et al., 1993). Initially, an FITC fluorophore was coupled through a thiourea linkage; however this linkage was subject to alkylation during the subsequent prenylation reaction (Scheme 1). Thus, the fluorescent labeling reagent, FITC, was replaced by 5-Fam which resulted in a less problematic amide linkage to the Lys side chain. Following installation of the fluorophore and subsequent cleavage from the resin, the thiol group on the *C*-terminal cysteine was prenylated with Zn^{2+} catalysis using the elegant procedure developed by Naider and co-workers (Naider and Becker, 1997); these conditions have been shown to not disturb the all-trans alkene

stereochemistry present in prenyl groups, and they allow the Acm protected cysteine to remain masked.

With the peptide containing the prenyl group selectively installed on the desired cysteine, attention was next focused on linking the penetratin moiety to the second cysteine. Initially, it was envisioned that the Acm group would be deprotected to produce a free thiol that could then be reacted with an activated form of penetratin to produce the desired disulfide-linked peptides. However, efforts to remove the Acm group with Hg^{2+} were unsuccessful, probably due to additional reactions with the alkenes present in the isoprenoid moiety. To circumvent this problem, the Acm element was converted to the more reactive Scm group via treatment with $CH_3O(CO)SCl$, following the pioneering work of Kamber (Kamber, 1973). Investigations by Hiskey and co-workers (Hiskey et al., 1975) and Kemp et al. (Kemp and Carey, 1989) suggested that thioethers exhibit a range of reactivity with $CH_3O(CO)SCl$, and our own experiments showed that excess sulfenyl chloride reagent converts a prenylated cysteine moiety to Cys(Scm). The key finding here is that titration of peptides containing both Cys(Acm) and a prenylated Cys with $CH_3O(CO)SCl$ and careful monitoring by HPLC leads to clean conversion to the desired Scm-modified molecules. This methodology for selective Acm removal in the presence of allylic thioethers may be generalized to peptides that contain multiple cysteines that must be differentiated, including prenylated and palmitylated sequences. A further important advantage of this strategy is that it results in the production of an activated disulfide that can then be used for direct reaction with penetratin; no separate activation of the latter peptide is required. This feature enabled the preparation of molecules in which the cell-penetrating group (penetratin) is conjugated to the target peptide by a cleavable disulfide linker. Internally, cells house a reductive environment which is known to cleave disulfide bonds linking penetratin to its cargo (Saito et al., 2003). In contrast to simple fusion proteins (e.g., penetratin fused to the *N*-terminus of the CDC42 peptide) this approach allows for the study of the effects of the peptide independently from the effects of penetratin. Even though penetratin is internalized, it has been shown to be nontoxic at concentrations well above those employed here (Saar, 2007).

Once the peptides were synthesized, they were tested for uptake into cells. Initially it

was thought that a cell-penetrating peptide sequence would be needed for cellular uptake of these CDC42 *C*-terminal prenylated peptides. Interestingly, all prenylated peptides were able to gain entry into the cells, regardless of whether or not penetratin was attached. Imperiali et al. have shown that polybasic sequences followed by a large hydrophobic group exhibit cell-penetrating properties (Carrigan and Imperiali, 2005). The prenylated peptides used in the present study have the sequence (KKSRRC-NH_2) with multiple positively charged lysine and arginine residues and a hydrophobic prenyl chain. Wender et al. have thoroughly studied how changing the hydrophobicity and altering the number of Arg residues in a polyarginine-based CPP modulates its cell penetrating properties (Wender et al., 2000). In those studies, peptides with less than six Arg or Lys residues showed little cellular internalization. Interestingly the peptide studied in the work reported here has only four charged residues but still exhibits large levels of internalization due to the presence of a nonpolar isoprenoid; consistent with that requirement, it should be noted that peptide **3a** which lacked prenyl or penetratin modifications was unable to cross cellular membranes. These results demonstrate the importance of prenyl modification of CDC42 *C*-terminal peptides for transversing cellular membranes. Moreover, the molecules reported here manifest an additional feature that makes them particularly interesting; peptide isoprenylation appears to result in specific subcellular localization to membrane bound organelles around the nucleus. While earlier work by Imperiali and co-workers demonstrated that cationic peptides functionalized with hydrophobic groups can gain entry into cells, those peptides manifested a uniform distribution within the cells. In contrast, the prenylated peptides described here show specific localization to the perinuclear region of the cell. That localization may be due to the physical properties of the peptides, their association with specific proteins within the cell, or some combination of both; experiments to address this question are in progress.

It is also important to point out apparent differences in the internalization mechanisms for the peptides described here. Penetratin-linked peptides have been shown to enter cells mainly though an energy-dependent pathway (Abes et al., 2007). Other CPPs have been shown to enter cells through both energy-dependent and -independent pathways. The data

reported here show that while prenylated peptides conjugated to penetratin may enter cells through multiple pathways, the peptides lacking the penetratin moiety clearly enter via an energy-independent process. This is particularly significant since it allows prenylated peptides to be introduced directly into cells and avoids the potential problem of having them become trapped within the vesicular transport system. Beyond their intended use in studies of protein prenylation, the peptides described here may serve as cell penetrating peptides in their own right. Compared to polyarginine sequences, penetratin and Tat, the molecules reported here are significantly smaller; in fact, they are more similar in size to the cholesterol-based synthetic receptors created by Petersen and co-workers (Boonyarattanakalin et al., 2007; Boonyarattanakalin et al., 2004; Martin and Peterson, 2003).

In summary, we describe here the synthesis of a series of multifunctional peptides based on the *C*-terminus of CDC42. The molecules include a fluorophore for cellular visualization, a cell penetration moiety to facilitate cellular entry, and a prenyl group. These peptides readily enter cells and are nontoxic at physiologically relevant concentrations. The ability of these peptides to be readily internalized, coupled with their lack of toxicity, makes them ideal to probe the relationship between prenyl group structure and localization in living cells. Since a prenylated peptide incorporating an intact "CAAX box" is also internalized, this molecule makes it possible to follow the enzymatic processing of prenylated peptides in living cells. Given the fact that the enzymes involved in prenylation and subsequent processing events are important targets for the development of therapeutic agents for cancer treatment, the synthetic probes reported here should provide significant utility in the drug development process. Moreover, the methodology reported here is not limited to the specific peptides described herein. Given the large number of prenylated proteins and their crucial role in signal transduction pathways, the synthetic strategy described here should enable the preparation of peptides with a diverse range of non-natural isoprenoid structures and a variety of different sequences (Duckworth et al., 2007; Krzysiak et al., 2007; Dawe et al., 1997; Kale et al, 2001). Finally, it should be noted that prenylated peptides are not the only type of post-translational modification that can be prepared using the strategy

reported here. The synthesis of cell-penetrating forms of glycosylated and phosphorylated peptides also present similar challenges. Introduction of disulfide-linked penetratin and other cell-penetrating moieties via the mild methods reported here should prove to be useful for the preparation of those and many other types of modified peptides.

Acknowledgment

The authors thank Dr. Marion Navratil for helpful discussions and Mr. Jerry Sedgewick and Mr. John Oja of the University of Minnesota Biomedical Image Processing Lab for technical assistance regarding cell imaging. We would like to acknowledge the assistance of the Flow Cytometry Core Facility of the Masonic Cancer Center, a comprehensive cancer center designated by the National Cancer Institute, supported in part by P30 CA77598. This work was supported by the National Institutes of Health (Grant Nos. GM058842, CA104609, and T32GM008347).

4.6 Supporting Information

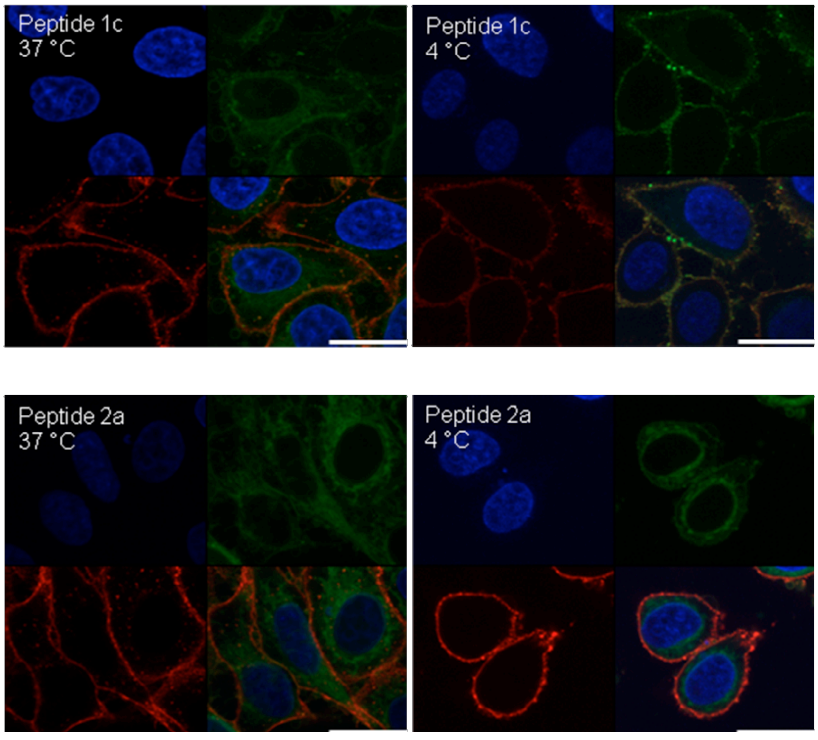

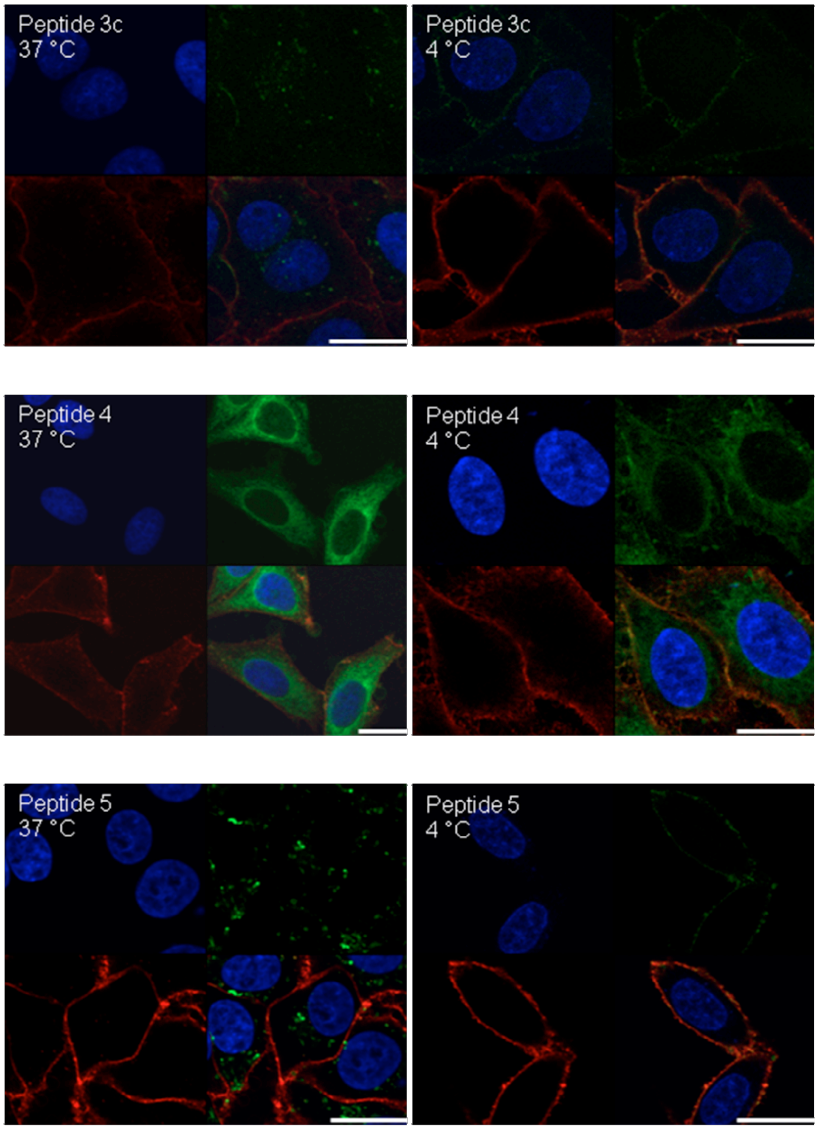

Figure S1. Uptake of cell penetrating peptides **1c**, **2a**, **3c**, **4**, **5** in fixed HeLa cells treated with 1 μm peptide at 37 and 4 °C. Upper left panels show only blue channel (nucleus). Upper right panels show only green channel (peptide). Lower left panels show only red channel (plasma membrane). Lower right panels show all channels combined (orange is colocalization of red and green). Bars in lower right corners represent 20 μm.

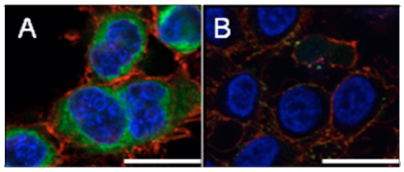

Figure S2. HeLa cells treated with energy poisons (12 μM rotenone and 15 mM 2-deoxyglucose) to deplete ATP production followed by treatment with 1 μM peptide **4** (panel A) or 1 μM of peptide **5** (panel B) for 1 h. These images are of fixed cells after treatment. This experiment indicates penetratin labeled peptides enter through an ATP dependent process while prenylated peptides can enter through ATP independent pathways. Other prenylated peptides (**1a, 2a**) localized in a similar fashion to **4** when ATP production was blocked while penetratin peptide **3c** localized in a similar fashion to **5** (data not shown) under the same conditions. Bars in lower right corner represent 20 μm.

Chapter V

Investigation of the sequence and length dependence for cell-penetrating prenylated peptides

Rationale. In Chapter IV, I discussed the development of novel cell-penetrating prenylated peptides. Previous studies of non-prenylated, cell-penetrating peptides indicate that a net positive charge and a hydrophobic domain are important for peptide internalization (Carrigan and Imperiali, 2005). We provided evidence that a prenyl group was necessary for cellular uptake of our new peptides via an energy-independent process (Wollack et al., 2009). We undertook these studies to examine how prenylation might affect the size and charge needed for efficient cellular uptake of peptides.

The ability of prenylated peptides to readily diffuse across cell membranes without apparent toxicity makes these molecules promising tools for the delivery of cargo into cells (Wagstaff and Jans, 2006). However, progress in the application of cell-penetrating peptides as delivery agents has been hindered by their relatively large size and net charge, and a general lack of information of the mechanisms by which peptides are internalized. As the next step towards understanding the mechanism of peptide internalization, we undertook the studies described in this chapter to examine how peptide length and amino acid identity determine the degree of cellular uptake of prenylated peptides.

Results. We synthesized a series of geranylgeranylated peptides with different charges and lengths. These peptides were also labeled with a fluorophore to enable cellular visualization. We found that the cell-penetrating property of these peptides was largely dependent on the presence of the prenyl moiety. Reducing the number of positively charged amino acids did not significantly impair peptide uptake. Also, peptides could be shortened to as little as two amino acids and still exhibit significant levels of cellular internalization. In agreement with our previous studies, all prenylated peptides in this series were rapidly internalized through an energy-independent process.

Conclusions and Significance. These studies are significant because we demonstrate

that prenylated peptides as short as two amino acids can be internalized. This is in contrast to previously studied cell-penetrating peptides, which are typically between 5 and 20 amino acids (Wagstaff and Jans, 2006). Furthermore, our studies suggest that the hydrophobicity of the geranylgeranyl moiety is an important feature enabling efficient cellular uptake of these peptides. This is in contrast to other cell-penetrating peptides, which rely heavily on the presence of multiple basic amino acids for efficient uptake (Carrigan and Imperiali, 2005). We also provide evidence that prenylated peptides are taken up through an ATP-independent process, which may allow peptides to avoid endosomal entrapment. This finding may be important for the development of cell-penetrating peptides as cargo-delivery tools, since endosomal transport may render the molecules inaccessible to the rest of cell, or target them for lysosomal degradation (Wagstaff and Jans, 2006).

Contributions. I contributed directly to the work in this paper by performing all cell-based experiments. In collaboration with James Wollack, I monitored the uptake of peptides using confocal microscopy and flow cytometry. The remainder of this chapter is the published paper, reprinted from *Bioorganic & Medicinal Chemistry Letters*, Vol 20, James W. Wollack, Nicholette A. Zeliadt, Joshua D. Ochocki, Daniel G. Mullen, George Barany, Elizabeth V. Wattenberg, and Mark D. Distefano, "Investigation of the sequence and length dependence for cell-penetrating prenylated peptides," pp 161-163, Copyright (2010), with permission from Elsevier.

5.1 Abstract

Cell penetrating peptides are useful delivery tools for introducing molecules of interest into cells. A new class of cell penetrating molecules has been recently reported—cell penetrating, prenylated peptides. In this study a series of such peptides was synthesized to examine the relationship between peptide sequence and level of peptide internalization and to probe their mechanism of internalization. This study revealed that prenylated peptides internalize via a non-endocytotic pathway regardless of sequence. Sequence length and identity was found to play a role in peptide uptake but prenylated

sequences as short as two amino acids were found to exhibit significant cell penetrating properties.

5.2 Results

Prenylation is a post-translational modification resulting in the addition of a 15 (farnesyl) or 20 (geranylgeranyl) carbon isoprenoid chain near a protein's *C*-terminus (Schafer and Rine, 1992; Zhang and Casey, 1996; Chow et al., 1992). The 1% of the proteome that is prenylated (Barbacid, 1987) consists of proteins that end in specific amino acid sequences which flag the protein for enzymatic modification. Prenyl modification is important for the localization of the protein inside of cells and is crucial to the protein's role in cellular signaling (Roberts et al., 2006; Michaelson et al., 2001). Recently we discovered that prenylated peptides have intrinsic cell penetrating properties (Wollack et al., 2009). These previous studies determined that the prenyl moiety on these peptides was crucial for their internalization but did not examine the relationship between the peptide length and sequence in modulating their levels of internalization.

Most cell penetrating peptides are from five to twenty amino acids long and have several positively charged amino acids (Hansen et al., 2008). Both a net positive charge and degree of hydrophobicity play crucial roles in CPP internalization (Carrigan and Imperiali, 2005). The size and charge of many of these molecules hinder their attractiveness as molecular transporters. This study examines the role that prenylation plays in reducing both the size and charge needed for cellular entry. A series of geranylgeranylated peptides differing in charge and length were synthesized to study the contribution prenylation plays on cell penetrating ability relative to sequence identity and charge.

Peptides were assembled by automated Fmoc SPPS, starting with Rink-amide (peptides **1–6, 9**) or Rink acid (peptides **7–8**) resin using an ABI 430 Synthesizer (Fig. 1). A 5-Fam fluorophore was coupled to either the *N*-terminus or to lysine side chains through the use of an orthogonal protection strategy employing a Dde group (1-(4,4-dimethyl-2,6-dioxocyclo-hexylidene)ethyl). Peptides were then cleaved from the resin and prenylated using geranylgeranyl bromide and $Zn(OAc)_2$ (Xue et al., 1992). For

peptide **8** the sequence Fam-KKSRRC(Acm)VLL was prepared and the Acm protecting group (acetamidomethyl) was converted to a Scm (*S*-carboxymethyl) group by treatment with $CH_3O(CO)SCl$ under acidic conditions (Hiskey at al., 1975). The more reactive Scm group then underwent disulfide exchange upon treatment with penetratin (Pnt) at pH 2.

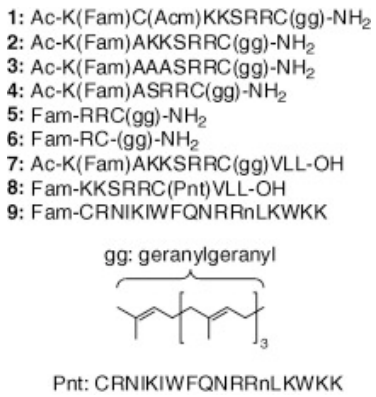

Figure 1. Cell penetrating peptides tested in this study. Compounds **1–7** have prenyl modifications on cysteine via thioether linkages. The linkage between Pnt and Cys in compound **8** is via a mixed disulfide. Lower case n in Pnt sequence encodes a norleucyl residue.

The internalization of fluorescein-linked peptides was investigated using a combination of confocal laser scanning microscopy (CLSM) and fluorescence activated cell sorting (FACS) analysis. For microscopy HeLa cells were treated for 1 h, washed, fixed in 3.7% formaldehyde and imaged. Live cell images were obtained from similarly prepared cells that were not subjected to the formaldehyde treatment. For microscopy, Hoechst 34850 and wheat germ agglutinin Alexa Fluor 594 conjugate were used to identify the nucleus and plasma membrane, respectively (Fig. 2). Live images of treated cells were comparable to fixed images. This observation, along with the observation of significant peptide uptake from flow cytometry analysis of live cell samples, suggests that fixing cell samples did not render them more permeable to uptake. Examples of fixed and live cell images are shown in panels A–D and E–H in Figure 2. To quantify the internalization levels of the various peptides, cells were treated with peptide (0.3–3.0 μM) for 1 h at 37 °C, trypsinized, and washed to remove any peptide adhered to the cell surface before FACS analysis.

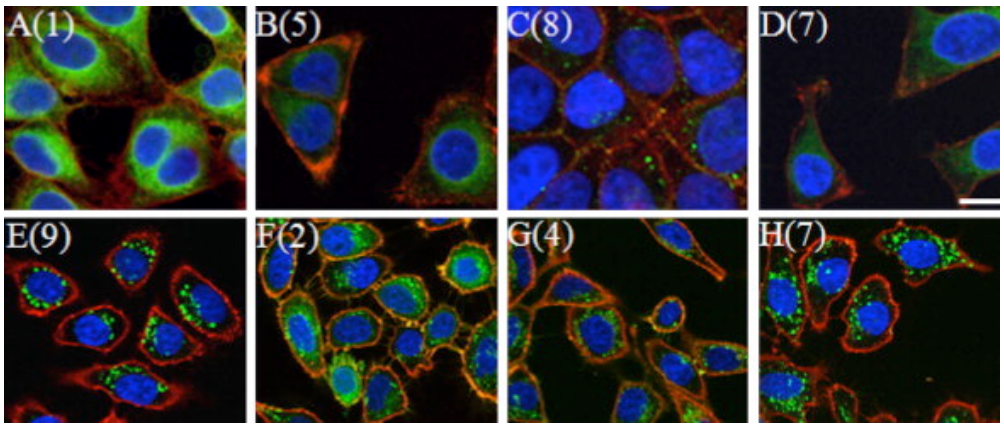

Figure 2. Confocal microscopy images of HeLa cells treated with cell-penetrating peptides. Cells in panels A–D were treated with 1 μM peptide for 1 h and fixed before imaging. Cells in panels E–H were treated with 3 μM peptide and imaged live. Panel A: cells treated with peptide **1**. Panel B: cells treated with peptide **5**. Panel C: cells treated with peptide **8**. Panel D: cells treated with peptide **7**. Panel E: cells treated with peptide **9**. Panel F: cells treated with peptide **2**. Panel G: cells treated with peptide **4**. Panel H: cells treated with peptide **7**. Hoechst 34850 blue DNA staining dye was used to stain the nucleus blue and wheat germ agglutinin Alexa Fluor 594 was used to stain the plasma membrane red. The size bar represents a distance of 20 μm.

Using the above techniques, the contribution from various amino acids to cellular uptake of prenylated peptide **1** was investigated using the series of peptides shown in Figure 1. Peptide **2** showed that removing the Cys(Acm) residue from **1** did not affect internalization at any treated concentration (Student's t-test, $p > 0.05$, Fig. 3). Lysine's contribution to peptide uptake was investigated using peptides **3** and **4**. Removing lysines (peptide **4**) or changing lysines to alanine (peptide **3**) caused a decrease in peptide internalization for 3.0 μM treatments ($p < 0.05$), but did not hinder uptake when treated at lower concentrations (compare peptides **3** and **4** to peptide **2** in Fig. 3). Prenylated tripeptide **5** showed that truncating the peptide even further causes no statistically significant decreases in uptake ($p > 0.05$ for all concentrations, compare peptide **4** to **5** in Fig. 3). However truncating the sequence further caused statistically significant drops in internalization for 1.0 μM and 3.0 μM treatments ($p < 0.05$, compare peptide **6** to peptide **4** in Fig. 3). This result may be attributed to small amounts of peptide precipitation

observed for this peptide after incubation with cells for 1 h.

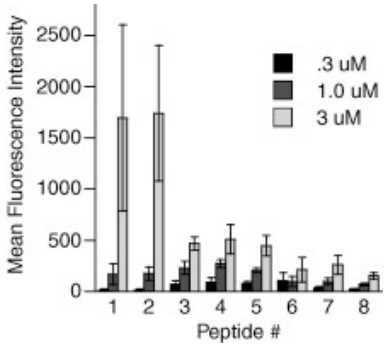

Figure 3. Uptake of peptides **1–8** in HeLa cells treated at 37 °C determined by FACS analysis. After incubation with 0.3 μM, 1.0 μM, or 3.0 μM peptide, the cells were trypsinized and washed to remove any surface-bound peptide and subsequently had their fluorescence measured by flow cytometry. Each bar represents the fluorescence of 10,000 cells counted by FACS analysis and each experiment was performed in triplicate. The results are expressed as the geometric mean relative fluorescence ± standard deviation (Macey, 2007).

The role of charge at the *C*-terminus was investigated by analyzing the uptake of peptide **7** which included the full 'CAAX box' of a naturally prenylated protein that ends in a terminal acid. Peptide **7** manifested lower overall levels of internalization for 3.0 μM treatments when compared to peptides **1–4** ($p < 0.05$) but had similar levels of uptake to these peptides for lower (0.3 μM) concentrations ($p > 0.05$). Unprenylated versions of **1–7** did not exhibit cellular uptake when analyzed by CLSM. This indicates that prenylation is necessary for this series of peptides to penetrate cells. Peptide **8**, a version of **7** in which the geranylgeranyl group was swapped with a penetratin moiety, had uptake levels similar to those of geranylgeranylated peptide **7** at all treated concentrations ($p > 0.05$). This indicates the geranylgeranyl group of peptide **7** contributes to cell penetrating ability as much as the penetratin peptide does for peptide **8**.

Using CLSM and FACS, the effects of temperature and reducing cellular ATP levels (Meriin et al., 1999) on the internalization of peptides **1–8** were also investigated to deduce information on the internalization mechanisms of these peptides (see CLSM images in S-1). Representative FACS data for HeLa cells treated with peptides **2** and **8**

with and without ATP depletion is shown in Figure 4; under ATP depleting conditions, a significant shift in the mean fluorescence (peptide internalization) was observed for peptide **8** but not for peptide **2**. A summary of the mean fluorescence obtained from FACS analysis is shown in Figure 5. All geranylgeranylated peptides (**1–7**) exhibited minimal changes in mean fluorescence upon ATP depletion. ($p > 0.05$). However, penetratin-linked peptide **8** showed substantially lower internalization levels when ATP was depleted ($p < 0.005$). In fact under those later conditions, the internalization of **8** was reduced to the levels comparable to those observed at 4 °C ($p > 0.05$). This suggests the prenylated peptides enter via an ATP-independent manner while penetratin linked peptide **8** enters via an ATP-dependent manner. All peptides showed reduced levels of internalization at 4 °C. Since cellular membranes have decreased fluidity at lower temperatures it is reasonable to expect lower internalization levels even for peptides that enter via energy-independent processes. This has been reported for other cell penetrating peptides (Letoha et al., 2003). CLSM experiments (see Fig. 2) also reveal morphological differences suggesting that the prenylated peptides enter cells via processes that are different than those for penetratin. Images of cells treated with penetratin-containing peptides (**8** and **9**) reveal a highly punctate pattern of fluorescence, characteristic of endocytotic uptake (for example, see Fig. 2E). In contrast, images of cells treated with prenylated peptides (**1–7**) are characterized by a more diffuse pattern of fluorescence (see Fig. 2F). Interestingly, variable amounts of punctate fluorescence are also observed with the prenylated peptides. The significance of those observations is not yet clear.

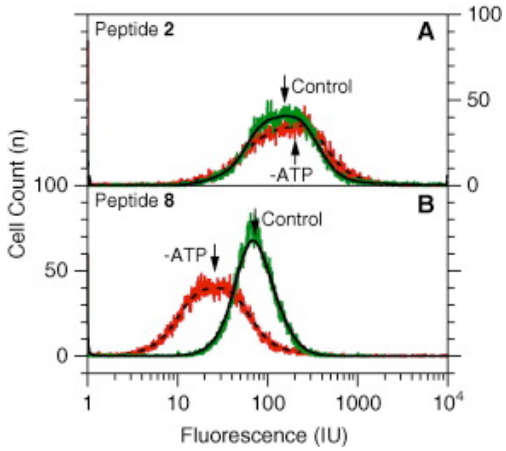

Figure 4. FACS analysis of HeLa cells treated with peptides **2** or **8** under control (37 °C) and ATP-depleted conditions. Panel A: analysis of cells treated with peptide **2**. Panel B: analysis of cells treated with peptide **8**. In each panel, raw data is shown in color (control, 37 °C: green; ATP-depleted: red) and smoothed data is shown as lines (37 °C: solid line; ATP-depleted: broken line).

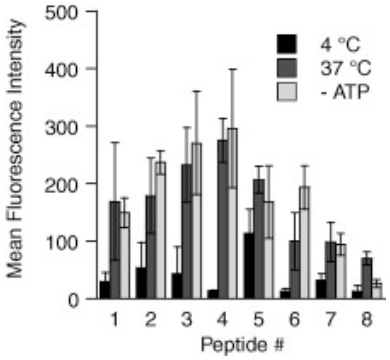

Figure 5. Uptake of peptides **1**–**8** in HeLa cells treated at 4 °C, 37 °C and under ATP-depleting conditions determined by FACS analysis. After incubation with 1.0 μM peptide, the cells were trypsinized and washed to remove any surface-bound peptide and subsequently had their fluorescence measured by flow cytometry. Each bar represents the fluorescence of 10,000 cells counted by FACS analysis and each experiment was performed in triplicate and the results are expressed as the geometric mean relative fluorescence ± standard deviation (Macey, 2007).

In conclusion the cell-penetrating ability of peptides presented here is determined primarily by their prenylation state. While **1** and **2** showed the highest levels of uptake at 3 μM, all prenylated peptides were internalized at 1 μM at levels comparable to or greater than penetratin-linked peptide **8** including tetrapeptide **5** and dipeptide **6**. This is

especially significant since most known cell penetrating peptides are at least four amino acids long. For instance oligoarginines are required to be at least five residues long in order to exhibit cell penetrating ability (Wender et al., 2000). Another appealing feature of these peptides is their ability to enter cells though ATP-independent processes. This allows them to avoid endosomal entrapment. Finally, we note that modification of peptides with other hydrophobic moieties such as decyl (Carrigan and Imperiali, 2005) or myristoyl groups (Ensenat-Waser et al., 2002) has been shown to increase a peptide's cell-penetrating ability; like geranylgeranylation, the hydrophobicity of these modifications may impart ATP-independent uptake. The size, uptake efficiency, and internalization mechanism make prenylated cell-penetrating molecules interesting candidates for further study as cellular transport vehicles.

Acknowledgements

The authors thank Mr. Gregg Amundson, Mr. Jerry Sedgewick and Mr. John Oja of the University of Minnesota Biomedical Image Processing Lab for technical assistance regarding cell imaging. We would like to acknowledge the assistance of the Flow Cytometry Core Facility of the Masonic Cancer Center, a comprehensive cancer center designated by the National Cancer Institute, supported in part by P30 CA77598. This work was supported by the National Institutes of Health (Grant Nos. GM058842, CA104609 and T32GM008347).

5.3 Supplementary data

5.3.1 Experimental Section

5.3.1.1 General. HeLa cells were the generous gift of Dr. Audrey Minden (Department of Chemical Biology, Rutgers University). Wheat germ agglutinin Alexa Fluor 594 conjugate, ProLong^{R} Gold antifade reagent, Hoechst 34850, and DMEM (Dulbecco's Modified Eagle Medium) were from Invitrogen. Fetal bovine serum was from Intergen Company. Vydac 12-Well plates were from Corning Inc. Vydac 218TP54 and 218TP1010 columns were used for analytical and preparative RP-HPLC, respectively. All analytical and preparative RP-HPLC solvents, water and CH_3CN,

contained 0.10% TFA; and retention times (t_R) are based on linear gradients (unless otherwise noted) starting from 100% H_2O to 40% H_2O:60% CH_3CN over 60 min. All solvents were of HPLC grade. DIEA and TFA were of Sequalog/peptide synthesis grade from Fisher. Fmoc-Lys(Dde)-OH was from Nova Biochem. PAL-PEG-PS was from Applied Biostems. Preloaded CLEAR-Acid resins were from Peptides International. All other reagents were from Sigma Aldrich. All procedures involving fluorescent derivatives were protected from light as much as possible in order to avoid bleaching the fluorophore.

5.3.1.2 Peptide Synthesis of 5-FAM labeled peptides. Linear peptides were synthesized by Fmoc-based SPPS on a Applied Biosystems 433A automated peptide synthesizer according to manufacturer protocols with the *N*-terminus set to be deprotected after the final coupling step. The peptide resin was then dried *in vacuo*. In a test tube, 2.0 mL of DMF enriched with 98 mM 5-FAM, 95 mM HOBt, and 95 mM DIPCDI was prepared for every 0.2 mmol of peptide on resin. The reagents were allowed to pre-incubate for 5 minutes before they were added to the resin contained within a solid phase reaction syringe. The test tube was then washed with an additional 2.0 mL of DMF and this was also added to the solid phase reaction syringe. The syringe was then tumbled overnight in the dark. The next morning the reaction was filtered and the beads were washed with DMF (4× 6.0 mL), and CH_2Cl_2 (4 × 6.0 mL). After washing with CH_2Cl_2 the resin was a brilliant orange color. The resin was then dried *in vacuo* for 2-4 h at which time the peptide was simultaneously deprotected and cleaved from the resin by tumbling in presence of 6.0 mL of freshly prepared Reagent K (TFA-phenol-thioanisole-water-ethanedithiol, 82.5:5:5:5:2.5) for 2 h. After cleavage, the peptide containing solution was filtered from the resin and diluted into ether. This resulted in an orange precipitate which was centrifuged and washed with Et_2O (2 × 50 mL). Crude peptides were purified by RP-HPLC. In all cases solvent A was 0.1% TFA in water and solvent B was 0.1% TFA in CH_3CN.

5.3.1.2.1 General Procedure for Cysteine Alkylation with a Geranylgeranyl Group. A 0.76 mM solution of peptide with a free cysteine was prepared in 1.5 mL of a 2:1 solution of DMF/ 0.1% TFA in water. To this, 500 μL of a

9.1 mM solution of geranylgeranyl bromide and 83 μL of 69 mM solution of $ZnOAc_2$ was added. The mixture was then stirred in the dark at rt. After stirring overnight, the reaction was deemed complete by RP-HPLC and it was diluted 5 fold into 0.1% TFA in water, purified by RP-HPLC, and lyophilized to a powder.

5.3.1.2.1.1 Ac-K(5-FAM)C(Acm)KKSRRC(gg)-NH_2 (1). RP-HPLC: t_R = 68 min (Gradient: 0% B for 10 min, 0-60% B over 60 min), deconvoluted ESI-MS: $[M+H]^+$ calculated 1973.1, found 1973.0.

5.3.1.2.1.2 Ac-K(5-FAM)AKKSRRC(gg)-NH_2 (2). RP-HPLC: t_R = 62 min (Gradient: 0% B for 10 min, 0-60% B over 60 min), deconvoluted ESI-MS: $[M+H]^+$ calculated 1646.9, found 1646.9.

5.3.1.2.1.3 Ac-K(5-FAM)AAASRRC(gg)-NH_2 (3). RP-HPLC: t_R = 66 min (Gradient: 0% B for 10 min, 0-60% B over 60 min), deconvoluted ESI-MS: $[M+H]^+$ calculated 1532.8, found 1532.7.

5.3.1.2.1.4 Ac-K(FAM)ASRRC(gg)-NH_2 (4). RP-HPLC: t_R = 66 min (Gradient: 0% B for 10 min, 0-60% B over 60 min), deconvoluted ESI-MS: $[M+H]^+$ calculated 1390.7, found 1390.7.

5.3.1.2.1.5 5-Fam-RRC(gerger)-NH_2 (5). RP-HPLC: t_R = 62 min (Gradient: 0% B for 20 min, 0-60% B over 60 min), deconvoluted ESI-MS: $[M+H]^+$ calculated 1062.5, found 1062.2.

5.3.1.2.1.6 5-Fam-RC(gerger)-NH_2 (6). RP-HPLC: t_R = 44 min (Gradient: 0% B for 20 min, 0-60% B over 60 min), deconvoluted ESI-MS: $[M+H]^+$ calculated 907.4, found 907.2.

5.3.1.2.1.7 Ac-K(5-FAM)AKKSRRC(gg)VLL (7). RP-HPLC: t_R = 70 min (Gradient: 0% B for 20 min, 0-60% B over 60 min), deconvoluted ESI-MS: $[M+H]^+$ calculated 1749.9, found 1750.3.

5.3.1.2.2 Synthesis of Disulfide-liked Penetratin Peptide 8. 5-FAM-KKSRRC(Acm)VLL was converted to 5-FAM-KKSRRC(Scm) using previously described procedures (Hiskey et al., 1975). The resulting Scm-containing peptide was dissolved in a minimal amount of DMSO and the concentration of the resulting solution was determined measuring the absorbance of the 5-FAM chromophore (ε_{492} = 79,000 cm^-

$^{1}M^{-1}$, pH 9.0). After the concentration of Cys(Scm)-containing peptide was determined, 40 µL of a 4.8 mM solution of peptide in DMF was prepared in a 1.5 mL centrifuge tube. Next, 105 µL of a 1.83 mM solution of penetratin in 0.1 M Na_2HPO_4, pH 8 was added to the peptide, followed by addition of 57 µL of 17 mM $ZnOAc_2$, in 1 M NaOAc, pH 5.4. Next an additional 161 µL of acetonitrile and 120 µL of DMF was added and the reaction was stirred for several hours. The reaction was then diluted 10 fold with 0.1 % TFA in water and was purified by RP-HPLC, t_R = 33 min (Gradient: 0% B for 26 min, 0-30% B over 1 min, 30-40 over 20 min). deconvoluted $[M+4H]^{+4}$ ESI-MS: calculated 3777.6, found 3778.

5.3.1.3 Cell Culture. HeLa cells were grown in DMEM supplemented with 10% (v/v) fetal bovine serum at 37 °C with 5% CO_2. For all experiments, 2.6 x 10^4 cells/cm^2 were seeded in culture dishes and grown for 24 h to approximately 50% confluency prior to incubation with the peptides.

5.3.1.4 Confocal Laser-Scanning Microscopy (CLSM). Confocal microscopy experiments were completed as previously described (Wollack et al., 2009).

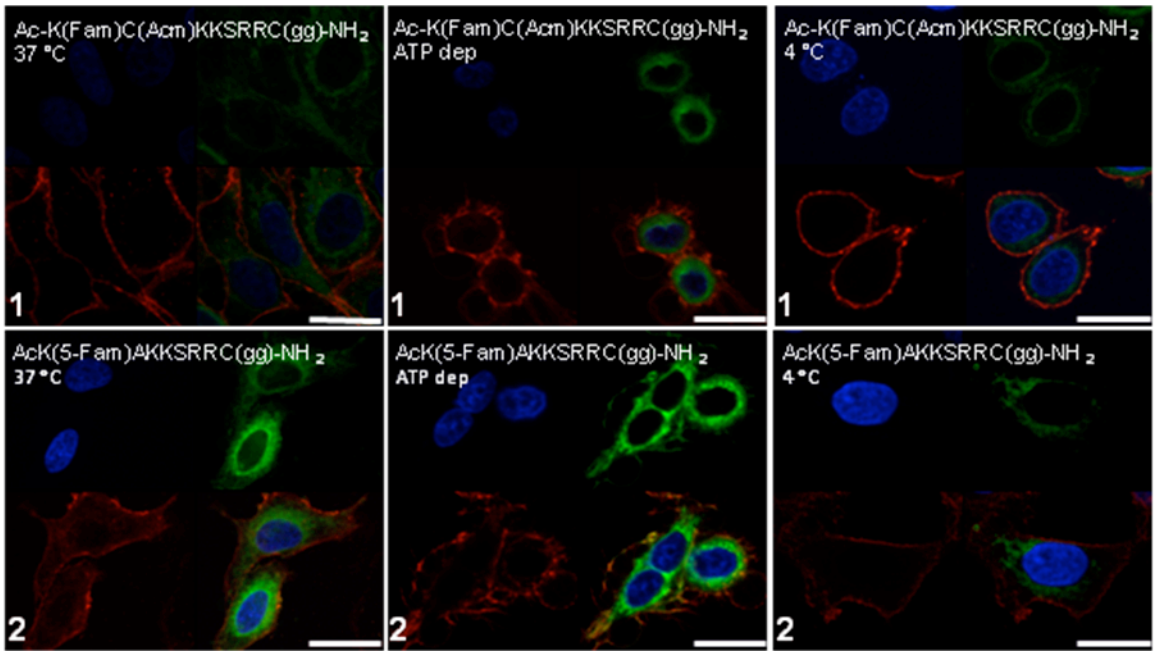

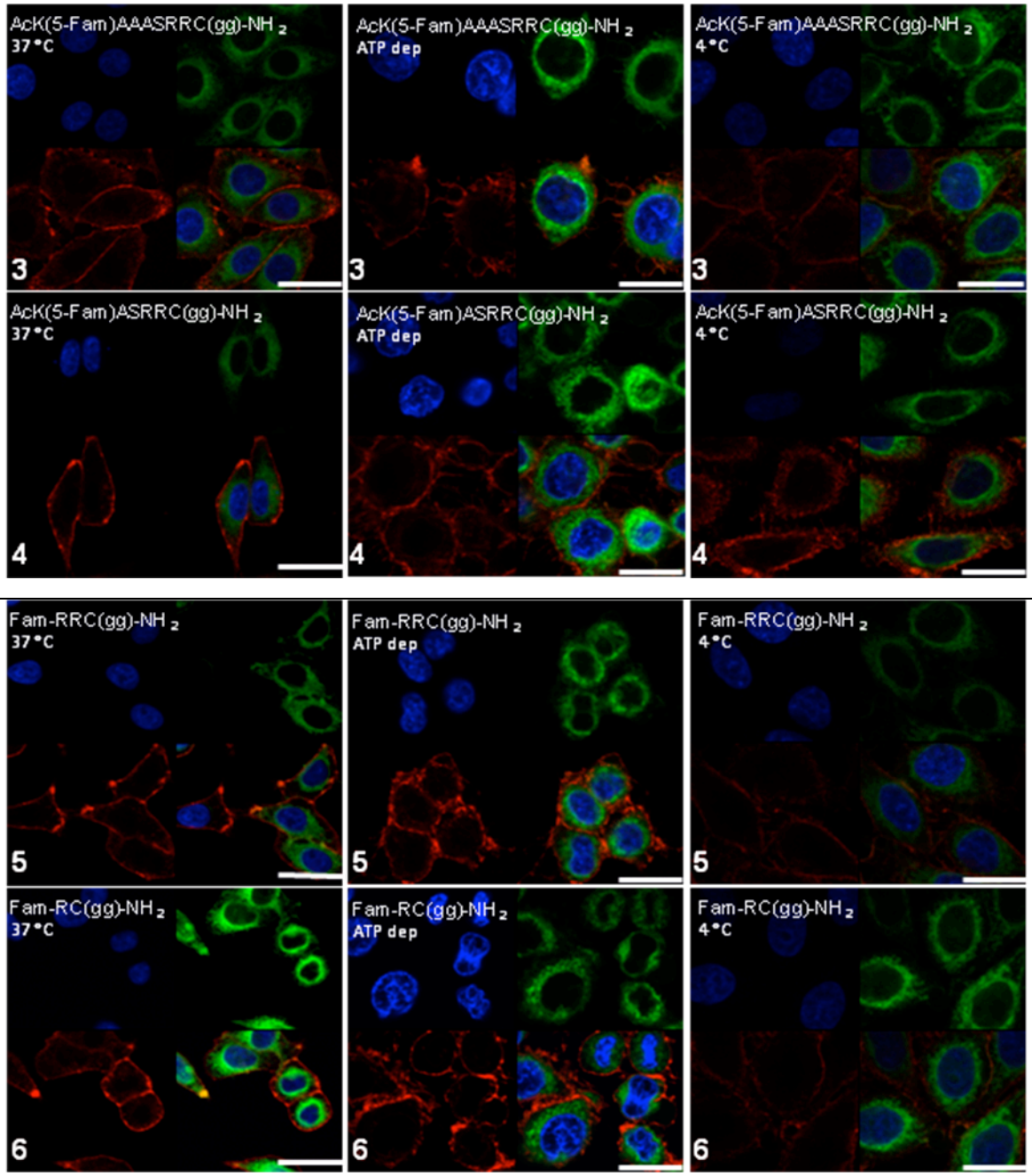
AcK(5-Fam)AAASRRC(gg)-NH 2
37 °C
3
AcK(5-Fam)AAASRRC(gg)-NH 2
ATP dep
3
AcK(5-Fam)AAASRRC(gg)-NH 2
4 °C
3
AcK(5-Fam)ASRRC(gg)-NH 2
37 °C
4
AcK(5-Fam)ASRRC(gg)-NH 2
ATP dep
4
AcK(5-Fam)ASRRC(gg)-NH 2
4 °C
4
Fam-RRC(gg)-NH 2
37 °C
5
Fam-RRC(gg)-NH 2
ATP dep
5
Fam-RRC(gg)-NH 2
4 °C
5
Fam-RC(gg)-NH 2
37 °C
6
Fam-RC(gg)-NH 2
ATP dep
6
Fam-RC(gg)-NH 2
4 °C
6

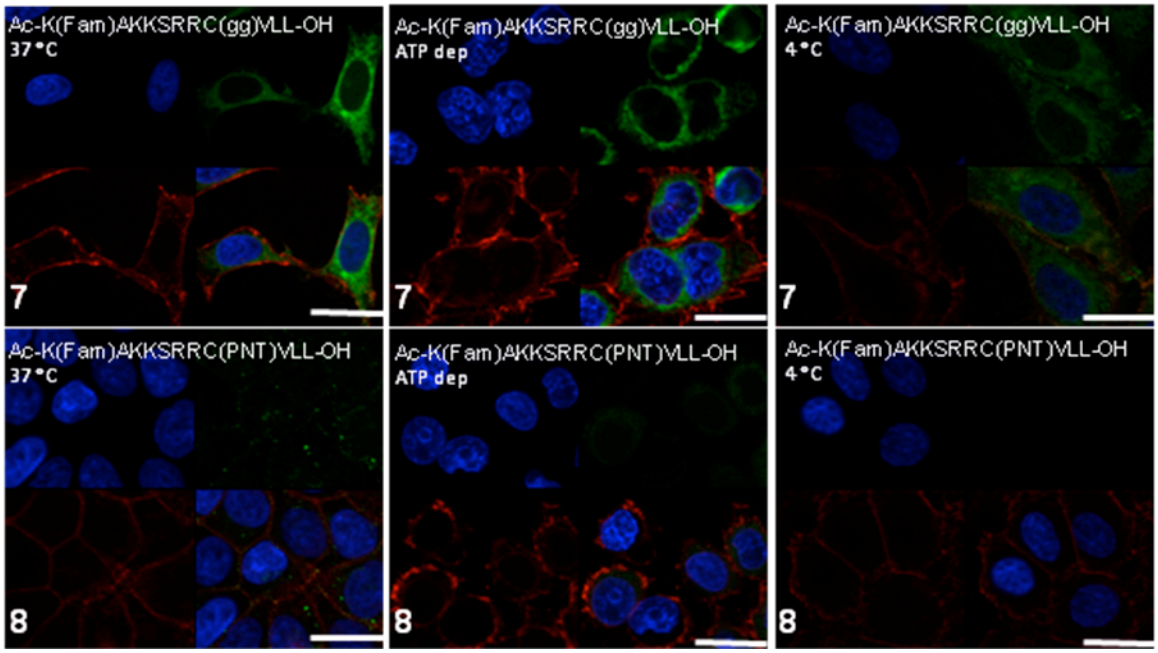

Figure S-1. Confocal microscopy images of HeLa cells treated with 1 μM concentrations of truncated CDC42 peptides **1-8** at 37 ºC (left), under ATP-depleted conditions (center), and at 4 ºC (right). Hoechst 34850 DNA staining dye was used to stain the nucleus (blue) and wheat germ agglutinin Alexa Fluor 488 was used to stain the plasma membrane (red). Bars in lower right corners represent 20 μm.

5.3.1.5 Fluorescence-Activated Cell Sorting (FACS). Flow cytometry experiments were completed as previously described (Wollack et al., 2009).

Chapter VI
Conclusions and Future Directions

The prevalence of dysregulated Ras/Raf/MEK1/2/ERK1/2 signaling in a significant number of human tumors highlights the urgent need to understand signaling through this pathway. This information will be important for the rational design of drug therapies and prevention strategies that target this pathway. Targeting the signaling molecules downstream of Ras or interfering with Ras prenylation represent two possible promising therapeutic strategies, although more mechanistic information is needed before success is likely. We undertook the studies described in this thesis to achieve two primary objectives: 1) to elucidate the signaling events that occur in cells with activated Ras upon exposure to tumor-promoting stimuli; and 2) to develop and characterize cell-penetrating peptides for the study of prenylation in living cells.

The studies described in Chapter II, as well as our previous studies with palytoxin (Warmka et al., 2004), demonstrate that MKP-3 is an unstable protein in cells. We and others established that ERK1/2 activation results in the destabilization of MKP-3 protein (Marchetti et al., 2005; Zeliadt et al., 2008). The studies by Marchetti, et al. used a tetracycline-inducible MKP-3 expression system, and demonstrated that MKP-3 is ubiquitinated and degraded by the proteasome (Marchetti et al., 2005). Another paper recently published by the same research group describes the serum-induced, mTOR-dependent destabilization of tet-induced MKP-3 (Bermudez et al., 2008). However, the degradation of endogenous MKP-3 may differ from exogenously expressed MKP-3, and needs to be investigated. There may also be a role for other proteases, such as cysteine and serine proteases, in the degradation of MKP-3. These possibilities could be investigated through the use of commercially available protease inhibitors, in a manner similar to that described for MKP-1 and MKP-2 (Brondello et al., 1999; Torres et al., 2003). Furthermore, the identity of the ubiquitin ligase that catalyzes ubiquitination of MKP-3 remains unknown. A recent study of the dual-specificity phosphatase MKP-1 demonstrated that the ubiquitin E3 ligase SCF^{Skp2} was involved in ERK1/2-dependent degradation of MKP-1 (Lin and Yang, 2006). Also, because some stimuli trigger the

ERK1/2-dependent stabilization of MKP-1 (Brondello et al., 1999) while others result in ERK1/2-dependent destabilization of MKP-1 (Lin et al., 2003; Lin and Yang, 2006), it may be worthwhile to examine additional ERK1/2 stimuli for their effects on MKP-3. In summary, mechanisms involved in MKP-3 degradation should be investigated more thoroughly because the loss of MKP-3 may contribute to carcinogenesis; preventing MKP-3 degradation may represent an important strategy for new anti-cancer therapies.

We found that knockdown of MKP-3 in cells with activated Ras led to an increase in basal pERK1/2 levels, consistent with the idea that MKP-3 serves to rein in oncogenic Ras signaling through the Raf/MEK1/2/ERK1/2 pathway. In DLD-1 cells, MKP-3 knockdown led to an increase in the phosphorylation of ERK1/2 substrates, such as p90RSK (unpublished data). However, our further investigations into the functional consequences of MKP-3 knockdown in cells were largely inconclusive. In contrast to other studies (Jurek et al., 2009; Okudela et al., 2009; Zhang et al., 2010), we did not observe any phenotypic changes or changes in cell proliferation in DLD-1 cells or H-Ras MCF10A cells incubated with MKP-3 siRNA. One possible explanation for our results is that other ERK1/2 phosphatases expressed in DLD-1 and H-Ras MCF10A cells compensate for the loss of MKP-3. For example, MKP-2 (DUSP4) has also been reported to be upregulated in cells with activated Ras (Warmka et al., 2004; Yip-Schneider et al., 2001). The role of MKP-2 in this context remains unexplored. Preliminary results from our lab suggest that MKP-5 (DUSP10) is also upregulated in H-Ras MCF10A cells relative to parental MCF10A cells. Therefore, combinatorial knockdown of multiple phosphatases may be needed to discern their roles in these cells. A similar approach was recently used to investigate the regulation of ERK1/2 by various DUSPs in HeLa cells (Caunt et al., 2008a; Caunt et al., 2008b). This approach could be used in cells with activated Ras to determine the specific role of DUSPs involved in carcinogenesis. Another possible explanation for why we did not observe changes in cellular growth rates when MKP-3 is knocked down is that perhaps siRNA knockdown does not last long enough to cause significant changes to more long-term cellular phenomenon, such as proliferation. However, we generated H-Ras MCF10A cells that stably express MKP-3 shRNA and thus maintain constitutive knockdown of MKP-3, and did not observe any

significant differences in morphology or growth rate. It is worth noting that our studies with H-Ras MCF10A cells were conducted with 2-dimensional cell cultures, but MCF10A cells can also be grown in three-dimensional culture, which is believed to better represent the cellular architecture found *in vivo* (Debnath and Brugge, 2005). Therefore, it would be interesting to determine whether an effect of MKP-3 knockdown is revealed when H-Ras MCF10A cells are grown in 3-D culture.

MKP-3 has been suggested to play a scaffolding role due to its cytoplasmic localization and ability to retain ERK1/2 in the cytoplasm (Karlsson et al., 2004). Future studies could address whether MKP-3 knockdown has an effect on the localization of ERK1/2. This possibility is significant, because spatiotemporal regulation of MAPK signaling has been shown to have profound effects on the biological response to diverse stimuli (Pouyssegur et al., 2002). Furthermore, MKP-3 has been shown to undergo nuclear-cytoplasmic shuttling, due in part to the presence of a nuclear export sequence (NES) that results in the active export of MKP-3 out of the nucleus (Karlsson et al., 2004). These studies demonstrated that MKP-3 accumulated in the nucleus of cells when an inhibitor of nuclear export was present; nuclear import no longer occurred when cells were incubated at 4 °C, suggesting an active nuclear import process. The mechanisms responsible for the nuclear import of MKP-3 remain unknown, however. The primary sequence of MKP-3 contains a potential NLS motif (^{120}KKLK^{123}, where K is lysine, L is leucine). Preliminary results from our lab do not support the hypothesis that this motif is involved in nuclear localization, however. Alternatively, nuclear import of MKP-3 could be achieved through its interaction with other nuclear-targeted proteins. Interestingly, MKP-3 contains an "LXXLL" motif (where L is leucine, and X is any amino acid), which typically mediates protein-protein interactions with the members of the nuclear hormone receptor family of transcription factors (Plevin et al., 2005). Indeed, MKP-3 has been purported to interact with the nuclear receptor ERα (Cui et al., 2005) Some nuclear receptors, including the estrogen receptors, undergo nuclear-cytoplasmic shuttling that can be regulated by ligand binding (Ylikomi et al., 1992). Further study is needed to determine the biological significance of the MKP-3-ERα interaction, and whether MKP-3 can interact with other nuclear receptors.

The primary sequence of MKP-3 also indicates the presence of a SUMO motif (^{122}LKDE^{125}, where L is leucine, K is lysine, D is aspartate, and E is glutamate). Sumoylation involves the covalent attachment of a ~101 amino acid SUMO protein to a lysine residue of the target protein. Sumoylation has been shown to alter protein function in several ways, including subcellular localization and protein stability (Dohmen, 2004). Our preliminary results using site-directed mutagenesis of the sumoylation motif in exogenously expressed MKP-3 did not reveal any apparent functional change in MKP-3 localization or function. Nevertheless, recent estimates suggest that only a very small fraction of a given protein is sumoylated at any given time (Hay, 2005); therefore, the functionality of this motif may need to be more thoroughly investigated. Given the important role of MKP-3 in regulating magnitude and duration of ERK1/2 activity, factors like sumoylation that may regulate MKP-3 stability and localization deserve further investigation.

Interestingly, two forms of the MKP-3 genes are expressed: the full-length version comprised of three exons, and a shorter, alternatively spliced version that lacks exon 2 (Furukawa et al., 1998). We and others have primarily focused on understanding the function of the full-length version of MKP-3. To date, very little is known about the regulation and function of the smaller form of MKP-3, including whether the truncated protein is even expressed in cells. Based on the RNA sequence of the splice variant, the catalytic domain and ERK1/2 kinase interaction motif (KIM) are predicted to be intact in the final protein product. By contrast, the truncated version would lack the NES that confers cytoplasmic localization (Karlsson et al., 2004), and the serine residues implicated in ERK1/2-dependent destabilization of MKP-3 (Marchetti et al., 2005). Therefore, this splice variant may have different subcellular localization and stability than the full-length protein, and it may have an important biological role that has been overlooked. For example, a recent report characterized the subcellular localization, substrate specificity, stability and phosphatase activity for a splice variant of MKP-2 (Cadalbert et al., 2010). This study revealed that, despite the absence of a KIM in the MKP-2 splice variant, the protein still displayed phosphatase activity, albeit with altered substrate specificity relative to the full-length protein. This is similar to other low

molecular weight DUSPs such as VHR, which lack an identifiable kinase interaction motif but can still inactivate MAPKs (Kondoh and Nishida, 2007).

The ERK1/2-mediated feedback regulation of MKP-3 expression that we describe in Chapter II may have important, clinically relevant implications for cancer treatment. Because MKP-3 expression often correlates with ERK1/2 activation in many cell types (Bloethner et al., 2005; Croonquist et al., 2003; Okudela et al., 2009; Sweet-Cordero et al., 2005), the presence of elevated MKP-3 expression may be a useful diagnostic or prognostic tool. In fact, MKP-3 was recently identified as part of a five-gene signature that was associated with greater lung cancer patient survival (Chen et al., 2007). Alternatively, MKP-3 might serve as a biomarker for tumors that exhibit elevated Ras/Raf/MEK1/2/ERK1/2 signaling, and may be useful in predicting patient outcome as well as tumor responsiveness to particular therapies (e.g. MEK1/2 inhibitors). Recently it was noted that elevated expression of MKP-3 is also associated with tamoxifen resistance in breast cancer (Cui et al., 2006). Therefore, knowledge of MKP-3 expression levels could be useful for choosing cancer among treatment regimens.

The information we provide on the regulation of MKP-3 expression may be useful for the study of disorders other than cancer. While defects in the Ras/Raf/MEK1/2/ERK1/2 pathway that lead to cancer in humans typically occur as somatic mutations in Ras or Raf, heritable germline mutations in Ras, Raf, or MEK1/2 can result in developmental disorders referred to as "Neuro-Cardio-Facial-Cutaneous" syndromes, all of which share phenotypic features including short stature, psychomotor delay, congenital heart defects, facial dysmorphism, skin abnormalities and a predisposition for the development of malignant tumors (Roberts and Der, 2007; Rodriguez-Viciana et al., 2006). Future studies could address the question of whether dysregulated expression of MKP-3 is involved in these developmental disorders. This is a likely possibility, given that MKP-3 plays a well-established role in development in many model organisms, including mouse, chick, zebrafish and Drosophila (Eblaghie et al., 2003; Kim et al., 2004; Li et al., 2007; Tsang et al., 2004). Furthermore, MKP-3 has been identified as an evolutionarily conserved marker of the pluripotent state in embryonic stem cells (Zhang et al., 2009). Therefore, it will be important to determine whether aberrant regulation of MKP-3 has an effect on

developmental programs.

Our results presented in Chapter III suggest that ERK5 may be involved in tumor promotion. Other studies indicate a role for ERK5 in cell proliferation, cell survival, and human cancers (Finegan et al., 2009; Kato et al., 1998; Mehta et al., 2003; Montero et al., 2009; Ostrander et al., 2007). Additional roles of ERK5 in other systems may have been overlooked, however, by the use of MEK1/2 inhibitors that have recently been found to also inhibit ERK5 activation (Mody et al., 2001). Therefore, the roles of ERK5 and ERK1/2 need to be re-evaluated. We have developed HeLa, MCF10A, and H-Ras MCF10A cell lines that stably express ERK5 shRNA. These cells, in combination with newly developed, highly specific MEK1/2 and MEK5 inhibitors (Bain et al., 2007; Tatake et al., 2008), could be used to investigate the redundant and unique roles of ERK1/2 and ERK5.

Our studies of cell-penetrating peptides, discussed in Chapters IV and V, pave the way for the analysis of prenylation in living cells. As discussed in the conclusions to those chapters, the peptides we developed could be used to specifically disrupt protein-protein interactions in cells, and would thus also be useful for the study of signaling mechanisms. Interestingly, the kinase interaction motif (KIM) of MKP-3 is comprised of several basic residues that may be amenable to its development as a cell-penetrating peptide. This sequence (^{61}IMLRRLQKGNLPVRALFTRC^{80}) is 20 amino acids long, and contains a *C*-terminal cysteine residue that could be prenylated for energy-independent cellular uptake. Such a peptide could be used to disrupt the interaction between MKP-3 and ERK1/2. This type of strategy may be particularly useful for targeting MKP-3 or other MKPs since specific inhibitors of individual phosphatases are not widely available (Lazo and Wipf, 2009). Other peptide-based inhibitors of ERK1/2-substrate interactions have been developed (Nichols et al., 2000; Volmat et al., 2001), but so far these do not have cell-penetrating ability. Their use is therefore restricted to *in vitro* experimentation, or they must be micro-injected, transfected, or exogenously expressed in cells. Unfortunately, such techniques do not ensure that all cells of the experimental population contain the peptide of interest. By contrast, our prenylated, cell-penetrating peptides exhibited uptake in nearly 100% of cells visualized. Therefore, using a cell-penetrating

peptide disrupt MKP-3-ERK1/2 interactions would be a simpler and more effective approach.

Altogether, the studies presented here provide new information regarding the biochemical mechanisms involved in the negative regulation of oncogenic signaling pathways. This thesis addresses one example of the exquisite ability cells have to adapt to the presence of oncogenic signaling by upregulating a negative regulator, which can turn components of the oncogenic pathway back off. Such adaptation provides one possible explanation for the long, multi-step nature of cancer. Inability to adapt, or loss of such an adaptation paves the way for tumorigenesis.

There have been many recent efforts to develop targeted therapies for cancers that have identifiable defects in specific signaling pathways. While this personalized approach seems promising, adaptation mechanisms will have to be further understood and should be taken into consideration during the drug development process. Given the complexity of signal transduction, this is not likely to be an easy task, but will undoubtedly be an exciting and fruitful area of research.

Bibliography

Abe, J., Kusuhara, M., Ulevitch, R.J., Berk, B.C., Lee, J.D., 1996. Big mitogen-activated protein kinase 1 (BMK1) is a redox-sensitive kinase. J. Biol. Chem. 271, 16586-16590.

Abes, S., Richard, J.-P., Thierry, A., Clair, P., Lebleu, B. In The handbook of cell-penetrating peptides; Langel, U., Ed.; CRC Press: Boca Raton, FL, 2007; pp 29-42.

Alcala, A.C., Alcala, L.C., Garth, J.S., Yasumura, D., Yasumoto, T., 1988. Human fatality due to ingestion of the crab Demania reynaudii that contained a palytoxin-like toxin, Toxicon 26, 105-107.

Almoguera, C., Shibata, D., Forrester, K., Martin, J., Arnheim, N., Perucho, M., 1988. Most human carcinomas of the exocrine pancreas contain mutant c-K-ras genes. Cell 53, 549-554.

Arkell, R.S., Dickinson, R.J., Squires, M., Hayat, S., Keyse, S.M., Cook, S.J., 2008. DUSP6/MKP-3 inactivates ERK1/2 but fails to bind and inactivate ERK5. Cell. Signal. 20, 836-843.

Bain, J., Plater, L., Elliott, M., Shpiro, N., Hastie, C.J., McLauchlan, H., Klevernic, I., Arthur, J.S., Alessi, D.R., Cohen, P., 2007. The selectivity of protein kinase inhibitors: a further update. Biochem. J. 408, 297-315.

Baird, W.M., Boutwell, R.K., 1971. Tumor-promoting activity of phorbol and four diesters of phorbol in mouse skin. Cancer Res. 31, 1074-1079.

Balmain, A., Pragnell, I.B., 1983. Mouse skin carcinomas induced in vivo by chemical carcinogens have a transforming Harvey-ras oncogene. Nature 303, 72–74.

Balmain, A., Ramsden, M., Bowden, G.T., Smith, J., 1984. Activation of the mouse cellular Harvey-ras gene in chemically induced benign skin papillomas. Nature 307, 658-660.

Barbacid, M., 1987. Ras Genes. Annu. Rev. Biochem. 56, 779-827.

Bermudez, O., Marchetti, S., Pages, G., Gimond, C., 2008. Post-translational regulation of the ERK phosphatase DUSP6/MKP3 by the mTOR pathway. Oncogene 27, 3685-3691.

Bhalla, U.S., Ram, P.T., Iyengar, R., 2002. MAP kinase phosphatase as a locus of flexibility in a mitogen-activated protein kinase signaling network. Science 297, 1018-1023.

Bialojan, A., Takai, A., 1988. Inhibitory effect of a marine-sponge toxin, okadaic acid, on protein phosphatases. Specificity and kinetics. Biochem. J. 256, 283-290.

Bloethner, S., Chen, B., Hemminki, K., Muller-Berghaus, J., Ugurel, S., Schadendorf, D., Kumar, R., 2005. Effect of common B-RAF and N-RAS mutations on global gene expression in melanoma cell lines. Carcinogenesis 26, 1224-1232.

Boonyarattanakalin, S., Hu, J., Dykstra-Rummel, S.A., August, A., Peterson, B.R., 2007. Endocytic delivery of vancomycin mediated by a synthetic cell surface receptor: rescue of bacterially infected mammalian cells and tissue targeting in vivo. J. Am. Chem. Soc. 129, 268-269.

Boonyrattanakalin, S., Martin, S.E., Dykstra, S.A., Peterson, B.R., 2004. Synthetic mimics of small mammalian cell surface receptors. J. Am. Chem. Soc. 126, 16379-16386.

Bos, J.L., 1989. ras oncogenes in human cancer: a review. Cancer Res. 49, 4682-4689.

Bos, J.L., Fearon, E.R., Hamilton, S.R., Verlaan-de Vries, M., van Boom, J.H., van der Eb, A.J., Vogelstein, B., 1987. Prevalence of ras gene mutations in human colorectal cancers. Nature 327, 293–297.

Breitschopf, K., Haendeler, J., Malchow, P., Zeiher, A.M., Dimmeler, S., 2000. Posttranslational modification of Bcl-2 facilitates its proteasome-dependent degradation: molecular characterization of the involved signaling pathway. Mol. Cell. Biol. 20, 1886-1896.

Britson, J.S., Barton, F., Balko, J.M., Black, E.P., 2009. Deregulation of DUSP activity in EGFR-mutant lung cancer cell lines contributes to sustained ERK1/2 signaling. Biochem. Biophys. Res. Commun. 390, 849-854.

Brondello, J.M., Brunet, A., Pouyssegur, J., McKenzie, F.R., 1997. The dual specificity mitogen-activated protein kinase phosphatase-1 and -2 are induced by the p42/p44MAPK cascade. J. Biol. Chem. 272, 1368-1376.

Brondello, J.M., Pouyssegur, J., McKenzie, F.R., 1999. Reduced MAP kinase phosphatase-1 degradation after p42/p44MAPK-dependent phosphorylation. Science 286, 2514-2517.

Brunet, A., Roux, D., Lenormand, P., Dowd, S., Keyse, S., Pouyssegur, J., 1999. Nuclear translocation of p42/p44 mitogen-activated protein kinase is required for growth factor-induced gene expression and cell cycle entry. EMBO J. 18, 664-674.

Bycroft, B.W., Chan, W.C., R., C.S., Hone, N.D.J., 1993. A novel lysine-protecting procedure for continuous flow solid phase synthesis of branched peptides. J. Chem. Soc., Chem. Commun., 778-779.

Cadalbert, L.C., Sloss, C.M., Cunningham, M.R., Al-Mutairi, M., McIntire, A., Shipley, J., Plevin, R., 2010. Differential regulation of MAP kinase activation by a novel splice variant of human MAP kinase phosphatase-2. Cell. Signal. 22, 357-365.

Campbell, S.L., Khosravi-Far, R., Rossman, K.L., Clark, G.J., Der, C.J., 1998. Increasing complexity of Ras signaling. Oncogene 17, 1395-1413.

Camps, M., Chabert, C., Muda, M., Boschert, U., Gillieron, C., Arkinstall, S., 1998a. Induction of the mitogen-activated protein kinase phosphatase MKP3 by nerve growth factor in differentiating PC12. FEBS Lett. 425, 271-276.

Camps, M., Nichols, A., Arkinstall, S., 2000. Dual specificity phosphatases: a gene family for control of MAP kinase function. FASEB. J. 14, 6–16.

Camps, M., Nichols, A., Gillieron, C., Antonsson, B., Muda, M., Chabert, C., Boschert, U., Arkinstall, S., 1998b. Catalytic activation of the phosphatase MKP-3 by ERK2 mitogen-activated protein kinase. Science 280, 1262-1265.

Carrigan, C.N., Imperiali, B., 2005. The engineering of membrane-permeable peptides. Anal. Biochem. 341, 290-298.

Castelli, M., Camps, M., Gillieron, C., Leroy, D., Arkinstall, S., Rommel, C., Nichols, A., 2004. MAP kinase phosphatase 3 (MKP3) interacts with and is phosphorylated by protein kinase CK2alpha. J. Biol. Chem. 279, 44731–44739.

Caunt, C.J., Armstrong, S.P., Rivers, C.A., Norman, M.R., McArdle, C.A., 2008a. Spatiotemporal regulation of ERK2 by dual specificity phosphatases. J. Biol. Chem. 283, 26612-26623.

Caunt, C.J., Rivers, C.A., Conway-Campbell, B.L., Norman, M.R., McArdle, C.A., 2008b. Epidermal growth factor receptor and protein kinase C signaling to ERK2: spatiotemporal regulation of ERK2 by dual specificity phosphatases. J. Biol. Chem. 283, 6241-6252.

Cavigelli, M., Dolfi, F., Claret, F.X., Karin, M., 1995. Induction of c-fos expression through JNK-mediated TCF/Elk-1 phosphorylation. EMBO J. 14, 5957-5964.

Chan, D.W., Liu, V.W., Tsao, G.S., Yao, K.M., Furukawa, T., Chan, K.K., Ngan, H.Y., 2008. Loss of MKP3 mediated by oxidative stress enhances tumorigenicity and chemoresistance of ovarian cancer cells. Carcinogenesis 29, 1742-1750.

Chang, F., Lee, J.T., Navolanic, P.M., Steelman, L.S., Shelton, J.G., Blalock, W.L., Franklin, R.A., McCubrey, J.A., 2003. Involvement of PI3K/Akt pathway in cell cycle progression, apoptosis, and neoplastic transformation: a target for cancer chemotherapy Leukemia 17, 590-603.

Chao, T.H., Hayashi, M., Tapping, R.I., Kato, Y., Lee, J.D., 1999. MEKK3 directly regulates MEK5 activity as part of the big mitogen-activated protein kinase 1 (BMK1) signaling pathway. J. Biol. Chem. 274, 36035-36038.

Chen, H.Y., Yu, S.L., Chen, C.H., Chang, G.C., Chen, C.Y., Yuan, A., Cheng, C.L., Wang, C.H., Terng, H.J., Kao, S.F., Chan, W.K., Li, H.N., Liu, C.C., Singh, S., Chen, W.J., Chen, J.J., Yang, P.C., 2007. A five-gene signature and clinical outcome in non-small-cell lung cancer. N. Engl. J. Med. 356, 11-20.

Chen, P., Hutter, D., Yang, X., Gorospe, M., Davis, R.J., Liu, Y., 2001. Discordance between the binding affinity of mitogen-activated protein kinase subfamily members

for MAP kinase phosphatase-2 and their ability to activate the phosphatase catalytically J. Biol. Chem. 276, 29440-29449.

Chen, R.H., Sarnecki, C., Blenis, J., 1992. Nuclear localization and regulation of erk- and rsk-encoded protein kinases. Mol. Cell. Biol. 12, 915-927.

Chen, Z., Gibson, T.B., Robinson, F., Silvestro, L., Pearson, G., Xu, B., Wright, A., Vanderbilt, C., Cobb, M.H., 2001. MAP kinases. Chem. Rev. 101, 2449-2476.

Chow, M., Der, C.J., Buss, J.E., 1992. Structure and biological effects of lipid modifications on proteins. Curr. Opin. Cell Biol. 4, 629-636.

Chu, Y., Solski, P.A., Khosravi-Far, R., Der, C.J., Kelly, K., 1996. The mitogen-activated protein kinase phosphatases PAC1, MKP-1, and MKP-2 have unique substrate specificities and reduced activity in vivo toward the ERK2 sevenmaker mutation. J. Biol. Chem. 271, 6497–6501.

Croonquist, P.A., Linden, M.A., Zhao, F., Van Ness, B.G., 2003. Gene profiling of a myeloma cell line reveals similarities and unique signatures among IL-6 response, N-ras-activating mutations, and coculture with bone marrow stromal cells. Blood 102, 2581-2592.

Cui, Y., Parra, I., Zhang, M., Hilsenbeck, S.G., Tsimelzon, A., Furukawa, T., Horii, A., Zhang, Z.Y., Nicholson, R.I., Fuqua, S.A., 2006. Elevated expression of mitogen-activated protein kinase phosphatase 3 in breast tumors: a mechanism of tamoxifen resistance. Cancer Res. 66, 5950-5959.

Cui, Y., Zhang, M., Parra, I., Osborne, C.K., Hilsenbeck, S.G., Tsimelzon, A., Fuqua, S.A.W., 2005. The MAPK inhibitor, MKP3, is an estrogen receptor {alpha} coactivator associated with tamoxifen resistance. AACR Meeting Abstracts 2005, 1031-c-1032.

Dawe, A.L., Becker, J.M., Jiang, Y., Naider, F., Eummer, J.T., Mu, Y.Q., Gibbs, R.A., 1997. Novel modifications to the farnesyl moiety of the a-factor lipopeptide pheromone from Saccharomyces cerevisiae: a role for isoprene modifications in ligand presentation. Biochemistry 36, 12036-12044.

Debnath, J., Brugge, J.S., 2005. Modelling glandular epithelial cancers in three-dimensional cultures. Nat. Rev. Cancer. 5, 675-688.

Dhillon, A.S., Hagan, S., Rath, O., Kolch, W., 2007. MAP kinase signalling pathways in cancer. Oncogene 26, 3279-3290.

DiGiovanni, J., 1992. Multistage carcinogenesis in mouse skin. Pharmacol. Ther. 54, 63-128.

Dohmen, R.J., 2004. SUMO protein modification. Biochim. Biophys. Acta 1695, 113-131.

Dowd, S., Sneddon, A.A., Keyse, S.M., 1998. Isolation of the human genes encoding the pyst1 and Pyst2 phosphatases: characterisation of Pyst2 as a cytosolic dual-specificity MAP kinase phosphatase and its catalytic activation by both MAP and SAP kinases. J. Cell. Sci. 111, 3389–3399.

Downward, J., 2003. Targeting RAS signalling pathways in cancer therapy. Nat. Rev. Cancer. 3, 11-22.

Duchardt, F., Fotin-Mleczek, M., Schwarz, H., Fischer, R., Brock, R., 2007. A comprehensive model for the cellular uptake of cationic cell-penetrating peptides. Traffic. 8, 848-866.

Duckworth, B.P., Chen, Y., Wollack, J.W., Sham, Y., Mueller, J.D., Taton, T.A., Distefano, M.D., 2007. A universal method for the preparation of covalent protein-DNA conjugates for use in creating protein nanostructures. Angew. Chemie (Int. Ed) 46, 8819-8822.

Dunn, K.L., Espino, P.S., Drobic, B., He, S., Davie, J.R., 2005. The Ras-MAPK signal transduction pathway, cancer and chromatin remodeling. Biochem. Cell Biol. 83, 1-14.

Ebisuya, M., Kondoh, K., Nishida, E., 2005. The duration, magnitude and compartmentalization of ERK MAP kinase activity: mechanisms for providing signaling specificity J. Cell. Sci. 118, 2997-3002.

Eblaghie, M.C., Lunn, J.S., Dickinson, R.J., Munsterberg, A.E., Sanz-Ezquerro, J.J., Farrell, E.R., Mathers, J., Keyse, S.M., Storey, K., Tickle, C., 2003. Negative feedback regulation of FGF signaling levels by Pyst1/MKP3 in chick embryos. Curr. Biol. 13, 1009-1018.

Edelstein, R.L., Weller, V.A., Distefano, M.D., Tung, J.S., 1998. Stereochemical analysis of the reaction catalyzed by yeast protein farnesyltransferase. J. Org. Chem. 63, 5298-5299.

Ekerot, M., Stavridis, M.P., Delavaine, L., Mitchell, M.P., Staples, C., Owens, D.M., Keenan, I.D., Dickinson, R.J., Storey, K.G., Keyse, S.M., 2008. Negative-feedback regulation of FGF signalling by DUSP6/MKP-3 is driven by ERK1/2 and mediated

by Ets factor binding to a conserved site within the DUSP6/MKP-3 gene promoter Biochem. J. 412, 287-298.

Emanuel, J.R., Schulz, J., Zhou, X.M., Kent, R.B., Housman, D., Cantley, L., Levenson, R., 1988. Expression of an ouabain-resistant Na,K-ATPase in CV-1 cells after transfection with a cDNA encoding the rat Na,K-ATPase alpha 1 subunit. J. Biol. Chem. 263, 7726-7733.

Ensenat-Waser, R., Martin, F., Barahona, F., Vazquez, J., Soria, B., Reig, J.A., 2002. Direct visualization by confocal fluorescent microscopy of the permeation of myristoylated peptides through the cell membrane. IUBMB Life 54, 33-36.

Epstein, W.W., Lever, D., Leining, L.M., Bruenger, E., Rilling, H.C., 1991. Quantitation of prenylcysteines by a selective cleavage reaction. Proc. Natl, Acad. Sci. U.S.A. 88, 9668-70.

Esparis-Ogando, A., Diaz-Rodriguez, E., Montero, J.C., Yuste, L., Crespo, P., Pandiella, A., 2002. Erk5 participates in neuregulin signal transduction and is constitutively active in breast cancer cells overexpressing ErbB2. Mol. Cell. Biol. 22, 270-285.

Fang, J.Y., Richardson, B.C., 2005. The MAPK signalling pathways and colorectal cancer. Lancet Oncol. 6, 322-327.

Farooq, A., Zhou, M.M., 2004. Structure and regulation of MAPK phosphatases. Cell. Signal. 16, 769-779.

Finegan, K.G., Wang, X., Lee, E.J., Robinson, A.C., Tournier, C., 2009. Regulation of neuronal survival by the extracellular signal-regulated protein kinase 5. Cell Death Differ. 16, 674-683.

Foged, C., Nielsen, H.M., 2008. Cell-penetrating peptides for drug delivery across membrane barriers. Expert Opin. Drug Deliv. 5, 105-117.

Franke, T.F., Yang, S.I., Chan, T.O., Datta, K., Kazlauskas, A., Morrison, D.K., Kaplan, D.R., Tsichlis, P.N., 1995. The protein kinase encoded by the Akt proto-oncogene is a target of the PDGF-activated phosphatidylinositol 3-kinase Cell 81, 727-736.

Franklin, C.C., Kraft, A.S., 1997. Conditional expression of the mitogen-activated protein kinase (MAPK) phosphatase MKP-1 preferentially inhibits p38 MAPK and stress-activated protein kinase in U937 cells. J. Biol. Chem. 272, 16917–16923.

Fresno Vara, J.A., Casado, E., de Castro, J., Cejas, P., Belda-Iniesta, C., Gonzalez-Baron, M., 2004. PI3K/Akt signalling pathway and cancer Cancer Treat. Rev. 30, 193-204.

Fujiki, H., Suganuma, M., Nakayasu, M., Hakii, H., Horiuchi, T., Takayama, S., Sugimura, T., 1986. Palytoxin is a non-12-O-tetradecanoylphorbol-13-acetate type tumor promoter in two-stage mouse skin carcinogenesis. Carcinogenesis 7, 707-710.

Furukawa, T., Fujisaki, R., Yoshida, Y., Kanai, N., Sunamura, M., Abe, T., Takeda, K., Matsuno, S., Horii, A., 2005. Distinct progression pathways involving the dysfunction of DUSP6/MKP-3 in pancreatic intraepithelial neoplasia and intraductal papillary-mucinous neoplasms of the pancreas. Mod. Pathol. 18, 1034-1042.

Furukawa, T., Sunamura, M., Motoi, F., Matsuno, S., Horii, A., 2003. Potential tumor suppressive pathway involving DUSP6/MKP-3 in pancreatic cancer. Am. J. Pathol. 162, 1807-1815.

Furukawa, T., Tanji, E., Xu, S., Horii, A., 2008. Feedback regulation of DUSP6 transcription responding to MAPK1 via ETS2 in human cells Biochem. Biophys. Res. Commun. 377, 317-320.

Furukawa, T., Yatsuoka, T., Youssef, E.M., Abe, T., Yokoyama, T., Fukushige, S., Soeda, E., Hoshi, M., Hayashi, Y., Sunamura, M., Kobari, M., Horii, A., 1998. Genomic analysis of DUSP6, a dual specificity MAP kinase phosphatase, in pancreatic cancer. Cytogenet. Cell Genet. 82, 156-159.

Ghomashchi, F., Zhang, X., Liu, L., Gelb, M.H., 1995. Binding of prenylated and polybasic peptides to membranes: affinities and intervesicle exchange. Biochemistry 34, 11910-11918.

Giehl, K., 2005. Oncogenic Ras in tumour progression and metastasis. Biol. Chem. 386, 193-205.

Gille, H., Strahl, T., Shaw, P.E., 1995. Activation of ternary complex factor Elk-1 by stress-activated protein kinases. Curr. Biol. 5, 1191-1200.

Gomez, A.R., Lopez-Varea, A., Molnar, C., de la Calle-Mustienes, E., Ruiz-Gomez, M., Gomez-Skarmeta, J.L., de Celis, J.F., 2005. Conserved cross-interactions in Drosophila and Xenopus between Ras/MAPK signaling and the dual-specificity phosphatase MKP3. Dev. Dyn. 232, 695–708.

Groom, L.A., Sneddon, A.A., Alessi, D.R., Dowd, S., Keyse, S.M., 1996. Differential regulation of the MAP, SAP and RK/p38 kinases by Pyst1, a novel cytosolic dual-specificity phosphatase. EMBO J. 15, 3621-3632.

Guan, K.L., Butch, E., 1995. Isolation and characterization of a novel dual specific phosphatase, HVH2, which selectively dephosphorylates the mitogen-activated protein kinase. J. Biol. Chem. 270, 7197–7203.

Habermann, E., 1989. Palytoxin acts through Na+,K+-ATPase. Toxicon 27, 1171-1187.

Halfar, K., Rommel, C., Stocker, H., Hafen, E., 2001. Ras controls growth, survival and differentiation in the Drosophila eye by different thresholds of MAP kinase activity. Development 128, 1687-1696.

Han, Y., Albericio, F., Barany, G.J., 1997. Occurrence and minimization of cysteine racemization during stepwise solid-phase peptide synthesis. J. Org. Chem. 62, 4307-4312.

Hanahan, D., Weinberg, R.A., 2000. The hallmarks of cancer Cell 100, 57-70.

Hancock, J.F., Cadwallader, K., Marshall, C.J., 1991a. Methylation and proteolysis are essential for efficient membrane binding of prenylated p21K-ras(B) EMBO J. 10, 641-646.

Hancock, J.F., Cadwallader, K., Paterson, H., Marshall, C.J., 1991b. A CAAX or a CAAL motif and a second signal are sufficient for plasma membrane targeting of ras proteins. EMBO J. 10, 4033-4039.

Hansen, M., Kilk, K., Langel, U., 2008. Predicting cell-penetrating peptides. Adv. Drug Deliv. Rev. 60, 572-579.

Haugland, R.P. The Handbook: A guide to fluorescent probes and labeling technologies, 10th ed.; Invitrogen: Carlsbad, CA, 2005; p 65.

Hay, R.T., 2005. SUMO: a history of modification. Mol. Cell 18, 1-12.

Hayashi, M., Lee, J.D., 2004. Role of the BMK1/ERK5 signaling pathway: lessons from knockout mice. J. Mol. Med. 82, 800-808.

Hayashi, M., Fearns, C., Eliceiri, B., Yang, Y., Lee, J.D., 2005. Big mitogen-activated protein kinase 1/extracellular signal-regulated kinase 5 signaling pathway is essential for tumor-associated angiogenesis. Cancer Res. 65, 7699-7706.

Hill, B.T., Perrin, D., Kruczynski, A., 2000. Inhibition of RAS-targeted prenylation: protein farnesyl transferase inhibitors revisited. Crit. Rev. Oncol. Hematol. 33, 7-23.

Hiskey, R.G., Muthukumaraswamy, N., Vunnam, R.R., 1975. Sulfur-containing polypeptides XVII. The S-carbomethoxysulfenyl derivatives as a protective group for cysteine. J. Org. Chem. 40, 950-953.

Hoffman, G.R., Nassar, N., Cerione, R.A., 2000. Structure of the Rho family GTP-binding protein Cdc42 in complex with the multifunctional regulator RhoGDI. Cell 100, 345-356.

Hoffmann, K., Hermanns-Clausen, M., Buhl, C., Buchler, M.W., Schemmer, P., Mebs, D., Kauferstein, S., 2008. A case of palytoxin poisoning due to contact with zoanthid corals through a skin injury. Toxicon 51, 1535-1537.

Hori, M., Inagawa, S., Shimazaki, J., Itabashi, M., Hori, M., 2000. Overexpression of mitogen-activated protein kinase superfamily proteins unrelated to Ras and AF-1 of estrogen receptor alpha mutation in advanced stage human breast cancer. Pathol. Res. Pract. 196, 817-826.

Howe, L.R., Leevers, S.J., Gomez, N., Nakielny, S., Cohen, P., Marshall, C.J., 1992. Activation of the MAP kinase pathway by the protein kinase raf. Cell 71, 335-342.

Hu, X., Moscinski, L.C., Valkov, N.I., Fisher, A.B., Hill, B.J., Zuckerman, K.S., 2000. Prolonged activation of the mitogen-activated protein kinase pathway is required for macrophage-like differentiation of a human myeloid leukemic cell line. Cell Growth Differ. 11, 191-200.

Hutter, D., Chen, P., Barnes, J., Liu, Y., 2000. Catalytic activation of mitogen-activated protein (MAP) kinase phosphatase-1 by binding to p38 MAP kinase: critical role of the p38 C-terminal domain in its negative regulation Biochem. J. 352 Pt 1, 155-163.

Ishida, Y., Takagi, K., Takahashi, M., Satake, N., Shibata, S., 1983. Palytoxin isolated from marine coelenterates. The inhibitory action on (Na,K)-ATPase. J. Biol. Chem. 258, 7900-7902.

Iyer, V.R., Eisen, M.B., Ross, D.T., Schuler, G., Moore, T., Lee, J.C., Trent, J.M., Staudt, L.M., Hudson, J.,Jr, Boguski, M.S., Lashkari, D., Shalon, D., Botstein, D., Brown, P.O., 1999. The transcriptional program in the response of human fibroblasts to serum. Science 283, 83-87.

Janknecht, R., Ernst, W.H., Nordheim, A., 1995. SAP1a is a nuclear target of signaling cascades involving ERKs. Oncogene 10, 1209-1216.

Jeffrey, K.L., Camps, M., Rommel, C., Mackay, C.R., 2007. Targeting dual-specificity phosphatases: manipulating MAP kinase signalling and immune responses. Nat. Rev. Drug Discov. 6, 391-403.

Jurek, A., Amagasaki, K., Gembarska, A., Heldin, C.H., Lennartsson, J., 2009. Negative and positive regulation of MAPK phosphatase 3 controls platelet-derived growth factor-induced Erk activation. J. Biol. Chem. 284, 4626-4634.

Kale, T.A. Photoactivatable prenylated cysteine analogs: synthesis and applications in studies of prenylated proteins. Ph.D., University of Minnesota, Minneapolis, 2001.

Kale, T.A., Raab, C, Yu, N., Dean, D.C., Distefano, M.D., 2001. A photoactivatable prenylated cysteine designed to study isoprenoid recognition. J. Am. Chem. Soc. 123, 4373-4381.

Kamakura, S., Moriguchi, T., Nishida, E., 1999. Activation of the protein kinase ERK5/BMK1 by receptor tyrosine kinases. Identification and characterization of a signaling pathway to the nucleus. J. Biol. Chem. 274, 26563-26571.

Kamata, H., Honda, S., Maeda, S., Chang, L., Hirata, H., Karin, M., 2005. Reactive oxygen species promote TNFalpha-induced death and sustained JNK activation by inhibiting MAP kinase phosphatases. Cell 120, 649-661.

Kamber, B., 1973. Die gezielte synthese offenkettiger asymmetrischer cystinpeptide mittels thiol-induzierter fragmentierung von sulfenylthiocarbonanten. Insulinfragmente mit intakter disulfidbrücke A^{20}-B^{19}. Helv. Chim. Acta 56, 1370-1381.

Karlsson, M., Mathers, J., Dickinson, R.J., Mandl, M., Keyse, S.M., 2004. Both nuclear-cytoplasmic shuttling of the dual specificity phosphatase MKP-3 and its ability to anchor MAP kinase in the cytoplasm are mediated by a conserved nuclear export signal. J. Biol. Chem. 279, 41882-41891.

Kato, K., Cox, A.D., Hisaka, M.M., Graham, S.M., Buss, J.E., Der, C.J., 1992. Isoprenoid addition to Ras protein is the critical modification for its membrane association and transforming activity. Proc. Natl. Acad. Sci. U. S. A. 89, 6403-6407.

Kato, Y., Kravchenko, V.V., Tapping, R.I., Han, J., Ulevitch, R.J., Lee, J.D., 1997. BMK1/ERK5 regulates serum-induced early gene expression through transcription factor MEF2C EMBO J. 16, 7054-7066.

Kato, Y., Tapping, R.I., Huang, S., Watson, M.H., Ulevitch, R.J., Lee, J.D., 1998. Bmk1/Erk5 is required for cell proliferation induced by epidermal growth factor Nature 395, 713-716.

Kawakami, Y., Rodriguez-Leon, J., Koth, C.M., Buscher, D., Itoh, T., Raya, A., Ng, J.K., Esteban, C.R., Takahashi, S., Henrique, D., Schwarz, M.F., Asahara, H., Izpisua Belmonte, J.C., 2003. MKP3 mediates the cellular response to FGF8 signalling in the vertebrate limb. Nat. Cell. Biol. 5, 513–519.

Kemp, D.S., Carey, R.I., 1989. Boc-L-Dmt-OH as a fully N,S-blocked cysteine derivative for peptide synthesis by prior thiol capture. Facile conversion of N-terminal Boc-L-Dmt-peptides to H-Cys(Scm)-peptides. J. Org. Chem. 54, 3640-3646.

Kempe, M., Barany, G.J., 1996. CLEAR: A novel family of highly cross-linked polymeric supports for solid-phase peptide synthesis. J. Am. Chem. Soc. 118, 7083-7093.

Keyse, S.M., 2000. Protein phosphatases and the regulation of mitogen-activated protein kinase signalling. Curr. Opin. Cell Biol. 12, 186-192.

Keyse, S.M., 1998. Protein phosphatases and the regulation of MAP kinase activity. Semin. Cell Dev. Biol. 9, 143-152.

Kim, M., Cha, G.H., Kim, S., Lee, J.H., Park, J., Koh, H., Choi, K.Y., Chung, J., 2004. MKP-3 has essential roles as a negative regulator of the Ras/mitogen-activated protein kinase pathway during Drosophila development. Mol. Cell. Biol. 24, 573-583.

King, D.S., Fields, C.G., Fields, G.B., 1990. A cleavage method which minimizes side reactions following Fmoc solid phase peptide synthesis. Int. J. Pept. Protein Res. 36, 255-266.

Kloog, Y., Cox, A.D., 2000. RAS inhibitors: potential for cancer therapeutics. Mol. Med. Today 6, 398-402.

Kodama, A.M., Hokama, Y., Yasumoto, T., Fukui, M., Manea, S.J., Sutherland, N., 1989. Clinical and laboratory findings implicating palytoxin as cause of ciguatera poisoning due to Decapterus macrosoma (mackerel). Toxicon 27, 1051-1053.

Kondoh, K., Nishida, E., 2007. Regulation of MAP kinases by MAP kinase phosphatases. Biochim. Biophys. Acta 1773, 1227-1237.

Krzysiak, A.J., Rawat, D.S., Scott, S.A., Pais, J.E., Handley, M., Harrison, M.L., Fierke, C.A., Gibbs, R.A., 2007. Combinatorial modulation of protein prenylation. ACS Chem. Biol. 2, 385-389.

Kuroki, D.W., Bignami, G.S., Wattenberg, E.V., 1996. Activation of stress-activator protein kinase/c-Jun N-terminal kinase by the non-TPA-type tumor promoter palytoxin. Cancer Res. 56, 637-644.

Kuroki, D.W., Minden, A., Sanchez, I., Wattenberg, E.V., 1997. Regulation of a c-Jun amino-terminal kinase/stress-activated protein kinase cascade by a sodium-dependent signal transduction pathway. J. Biol. Chem. 272, 23905-23911.

Lazo, J.S., Wipf, P., 2009. Phosphatases as targets for cancer treatment Curr. Opin. Investig Drugs 10, 1297-1304.

Lazzaro, M., Tashjian Jr., A.H., Fujiki, H., Levine, L., 1987. Palytoxin: an extraordinarily potent stimulator of prostaglandin production and bone resorption in cultured mouse calvariae. Endocrinology 120, 1338-1345.

Lee, J.D., Ulevitch, R.J., Han, J., 1995. Primary structure of BMK1: a new mammalian map kinase. Biochem. Biophys. Res. Commun. 213, 715-724.

Lefloch, R., Pouyssegur, J., Lenormand, P., 2008. Single and combined silencing of ERK1 and ERK2 reveals their positive contribution to growth signaling depending on their expression levels. Mol. Cell. Biol. 28, 511–527.

Legendre, F., Dudhia, J., Pujol, J.P., Bogdanowicz, P., 2003. JAK/STAT but not ERK1/ERK2 pathway mediates interleukin (IL)-6/soluble IL-6R down-regulation of Type II collagen, aggrecan core, and link protein transcription in articular chondrocytes. Association with a down-regulation of SOX9 expression. J. Biol. Chem. 278, 2903–2912.

Lerner, E.C., Zhang, T.T., Knowles, D.B., Qian, Y., Hamilton, A.D., Sebti, S.M., 1997. Inhibition of the prenylation of K-Ras, but not H- or N-Ras, is highly resistant to CAAX peptidomimetics and requires both a farnesyltransferase and a geranylgeranyltransferase I inhibitor in human tumor cell lines. Oncogene 15, 1283-1288.

Letoha, T., Gaal, S., Somlai, C., Czajlik, A., Perczel, A., Penke, B.J., 2003. Membrane translocation of penetratin and its derivatives in different cell lines. J. Mol. Recognit. 16, 272-279.

Levine, L., Xiao, D.M., Fujiki, H., 1986. Combinations of palytoxin or 12-O-tetradecanoylphorbol-13-acetate and recombinant human insulin growth factor-I or insulin synergistically stimulate prostaglandin production in cultured rat liver cells and squirrel monkey aorta smooth muscle cells. Prostaglandins 31, 669-681.

Levinthal, D.J., Defranco, D.B., 2005. Reversible oxidation of ERK-directed protein phosphatases drives oxidative toxicity in neurons. J. Biol. Chem. 280, 5875-5883.

Li, C., Scott, D.A., Hatch, E., Tian, X., Mansour, S.L., 2007. Dusp6 (Mkp3) is a negative feedback regulator of FGF-stimulated ERK signaling during mouse development Development 134, 167-176.

Li, S., Wattenberg, E.V., 1999. Cell-type-specific activation of p38 protein kinase cascades by the novel tumor promoter palytoxin. Toxicol. Appl. Pharmacol. 160, 109-119.

Li, S., Wattenberg, E.V., 1998. Differential activation of mitogen-activated protein kinases by palytoxin and ouabain, two ligands for the Na+,K+-ATPase. Toxicol. Appl. Pharmacol. 151, 377-384.

Lin, Y.W., Chuang, S.M., Yang, J.L., 2003. ERK1/2 achieves sustained activation by stimulating MAPK phosphatase-1 degradation via the ubiquitin-proteasome pathway. J. Biol. Chem. 278, 21534-21541.

Lin, Y.W., Yang, J.L., 2006. Cooperation of ERK and SCFSkp2 for MKP-1 destruction provides a positive feedback regulation of proliferating signaling J. Biol. Chem. 281, 915-926.

Liu, L., Cundiff, P., Abel, G., Wang, Y., Faigle, R., Sakagami, H., Xu, M., Xia, Z., 2006. Extracellular signal-regulated kinase (ERK) 5 is necessary and sufficient to specify cortical neuronal fate Proc. Natl. Acad. Sci. U. S. A. 103, 9697-9702.

Liu, T., Bohlken, A., Kuljaca, S., Lee, M., Nguyen, T., Smith, S., Cheung, B., Norris, M.D., Haber, M., Holloway, A.J., Bowtell, D.D., Marshall, G.M., 2005. The retinoid anticancer signal: mechanisms of target gene regulation. Br. J. Cancer 93, 310-318.

Macey, M.G. Flow cytometry: principles and applications, Macey, M.G., ed. Humana Press: Totowa, NJ, 2007.

Maillet, M., Purcell, N.H., Sargent, M.A., York, A.J., Bueno, O.F., Molkentin, J.D., 2008. DUSP6 (MKP3) null mice show enhanced ERK1/2 phosphorylation at baseline and increased myocyte proliferation in the heart affecting disease susceptibility J. Biol. Chem. 283, 31246-31255.

Marchetti, S., Gimond, C., Chambard, J.C., Touboul, T., Roux, D., Pouyssegur, J., Pages, G., 2005. Extracellular signal-regulated kinases phosphorylate mitogen-activated protein kinase phosphatase 3/DUSP6 at serines 159 and 197, two sites critical for its proteasomal degradation. Mol. Cell. Biol. 25, 854-864.

Marshall, C.J., 1995. Specificity of receptor tyrosine kinase signaling: transient versus sustained extracellular signal-regulated kinase activation. Cell 80, 179-185.

Marshall, C.J., 1993. Protein prenylation: a mediator of protein-protein interactions. Science 259, 1865-1866.

Martin, S.E., Peterson, B.R., 2003. Non-natural cell surface receptors: synthetic peptides

capped with cholesterylglycine efficiently deliver proteins into mammalian cells. Bioconjugate Chem. 14, 67-74.

McCawley, L.J., Li, S., Wattenberg, E.V., Hudson, L.G., 1999. Sustained activation of the mitogen-activated protein kinase pathway. A mechanism underlying receptor tyrosine kinase specificity for matrix metalloproteinase-9 induction and cell migration. J. Biol. Chem. 274, 4347–4353.

McCracken, S.R., Ramsay, A., Heer, R., Mathers, M.E., Jenkins, B.L., Edwards, J., Robson, C.N., Marquez, R., Cohen, P., Leung, H.Y., 2008. Aberrant expression of extracellular signal-regulated kinase 5 in human prostate cancer. Oncogene 27, 2978-2988.

Mebs, D., 1998. Occurrence and sequestration of toxins in food chains. Toxicon 36, 1519-1522.

Mehta, P.B., Jenkins, B.L., McCarthy, L., Thilak, L., Robson, C.N., Neal, D.E., Leung, H.Y., 2003. MEK5 overexpression is associated with metastatic prostate cancer, and stimulates proliferation, MMP-9 expression and invasion. Oncogene 22, 1381-1389.

Meriin, A.B., Yaglom, J.A., Gabai, V.L., Zon, L., Ganiatsas, S., Mosser, D.D., Zon, L., Sherman, M.Y., 1999. Protein-damaging stresses activate c-Jun N-terminal kinase via inhibition of its dephosphorylation: a novel pathway controlled by HSP72. Mol. Cell. Biol. 19, 2547-2555.

Michaelson, D., Silletti, J., Murphy, G., D'Eustachio, P., Rush, M., Philips, M.R., 2001. Differential localization of Rho GTPases in live cells: regulation by hypervariable regions and RhoGDI binding. J. Cell Biol. 152, 111-126.

Millward, T.A., Zolnierowicz, S., Hemmings, B.A., 1999. Regulation of protein kinase cascades by protein phosphatase 2A. Trends Biochem. Sci. 24, 186-191.

Miura, D., Kobayashi, M., Kakiuchi, S., Kasahara, Y., Kondo, S., 2006. Enhancement of transformed foci and induction of prostaglandins in Balb/c 3T3 cells by palytoxin: in vitro model reproduces carcinogenic responses in animal models regarding the inhibitory effect of indomethacin and reversal of indomethacin's effect by exogenous prostaglandins. Toxicol. Sci. 89, 154-163.

Mody, N., Campbell, D.G., Morrice, N., Peggie, M., Cohen, P., 2003. An analysis of the phosphorylation and activation of extracellular-signal-regulated protein kinase 5 (ERK5) by mitogen-activated protein kinase kinase 5 (MKK5) in vitro. Biochem. J. 372, 567-575.

Mody, N., Leitch, J., Armstrong, C., Dixon, J., Cohen, P., 2001. Effects of MAP kinase cascade inhibitors on the MKK5/ERK5 pathway FEBS Lett. 502, 21-24.

Montero, J.C., Ocana, A., Abad, M., Ortiz-Ruiz, M.J., Pandiella, A., Esparis-Ogando, A., 2009. Expression of Erk5 in early stage breast cancer and association with disease free survival identifies this kinase as a potential therapeutic target. PLoS One 4, e5565.

Moore, R.E., 1985. Structure of palytoxin. Fortschr. Chem. Org. Naturst. 48, 81-202.

Moore, R.E., Scheuer, P.J., 1971. Palytoxin: a new marine toxin from a coelenterate. Science 172, 495-498.

Moreno, T.A., Kintner, C., 2004. Regulation of segmental patterning by retinoic acid signaling during Xenopus somitogenesis. Dev. Cell. 6, 205-218.

Mourey, R.J., Vega, Q.C., Campbell, J.S., Wenderoth, M.P., Hauschka, S.D., Krebs, E.G., Dixon, J.E., 1996. A novel cytoplasmic dual specificity protein tyrosine phosphatase implicated in muscle and neuronal differentiation. J. Biol. Chem. 271, 3795-3802.

Muda, M., Boschert, U., Dickinson, R., Martinou, J.C., Martinou, I., Camps, M., Schlegel, W., Arkinstall, S., 1996. MKP-3, a novel cytosolic protein-tyrosine phosphatase that exemplifies a new class of mitogen-activated protein kinase phosphatase. J. Biol. Chem. 271, 4319-4326.

Muda, M., Theodosiou, A., Gillieron, C., Smith, A., Chabert, C., Camps, M., Boschert, U., Rodrigues, N., Davies, K., Ashworth, A., Arkinstall, S., 1998. The mitogen-activated protein kinase phosphatase-3 N-terminal noncatalytic region is responsible for tight substrate binding and enzymatic specificity. J. Biol. Chem. 273, 9323–9329.

Murphy, L.O., Blenis, J., 2006. MAPK signal specificity: the right place at the right time. Trends Biochem. Sci. 31, 268-275.

Murphy, L.O., Smith, S., Chen, R.H., Fingar, D.C., Blenis, J., 2002. Molecular interpretation of ERK signal duration by immediate early gene products. Nat. Cell. Biol. 4, 556–564.

Naider, F.R., Becker, J.M., 1997. Synthesis of prenylated peptides and peptide esters. Biopolymers 43, 3-14.

Nalbant, P., Hodgson, L., Kraynov, V., Toutchkine, A., Hahn, KM., 2004. Activation of endogenous Cdc42 visualized in living cells. Science 305, 1615-1619.

Newell, D.R., 2005. How to develop a successful cancer drug – molecules to medicines or targets to treatments? Eur. J. Cancer 41, 676-682.

Nichols, A., Camps, M., Gillieron, C., Chabert, C., Brunet, A., Wilsbacher, J., Cobb, M., Pouyssegur, J., Shaw, J.P., Arkinstall, S., 2000. Substrate recognition domains within extracellular signal-regulated kinase mediate binding and catalytic activation of mitogen-activated protein kinase phosphatase-3. J. Biol. Chem. 275, 24613-24621.

Nishimoto, S., Nishida, E., 2006. MAPK signalling: ERK5 versus ERK1/2 EMBO Rep. 7, 782-786.

Nishizuka, Y., 1984. The role of protein kinase C in cell surface signal transduction and tumour promotion. Nature 308, 693-698.

Nomanbhoy, T.K., Cerione, R., 1996. Characterization of the interaction between RhoGDI and Cdc42Hs using fluorescence spectroscopy. J. Biol. Chem. 271, 10004-10009.

Okudela, K., Yazawa, T., Woo, T., Sakaeda, M., Ishii, J., Mitsui, H., Shimoyamada, H., Sato, H., Tajiri, M., Ogawa, N., Masuda, M., Takahashi, T., Sugimura, H., Kitamura, H., 2009. Down-regulation of DUSP6 expression in lung cancer: its mechanism and potential role in carcinogenesis. Am. J. Pathol. 175, 867-881.

Onuma, Y., Satake, M., Ukena, T., Roux, J., Chanteau, S., Rasolofonirina, N., Ratsimaloto, M., Naoki, H., Yasumoto, T., 1999. Identification of putative palytoxin as the cause of clupeotoxism. Toxicon 37, 55-65.

Osmani, N., Vitale, N., Borg, J.-P., Etienne-Manneville, S., 2006. Scrib controls Cdc42 localization and activity to promote cell polarization during astrocyte migration. Curr. Biol. 16, 2395-2405.

Ostrander, J.H., Daniel, A.R., Lofgren, K., Kleer, C.G., Lange, C.A., 2007. Breast tumor kinase (protein tyrosine kinase 6) regulates heregulin-induced activation of ERK5 and p38 MAP kinases in breast cancer cells. Cancer Res. 67, 4199-4209.

Ouyang, B., Knauf, J.A., Smith, E.P., Zhang, L., Ramsey, T., Yusuff, N., Batt, D., Fagin, J.A., 2006. Inhibitors of Raf kinase activity block growth of thyroid cancer cells with RET/PTC or BRAF mutations in vitro and in vivo. Clin. Cancer Res. 12, 1785-1793.

Owens, D.M., Keyse, S.M., 2007. Differential regulation of MAP kinase signalling by dual-specificity protein phosphatases. Oncogene 26, 3203-3213.

Pages, G., Guerin, S., Grall, D., Bonino, F., Smith, A., Anjuere, F., Auberger, P., Pouyssegur, J., 1999. Defective thymocyte maturation in p44 MAP kinase (Erk 1)

knockout mice. Science 286, 1374–1377.

Pelech, S., 2006. Dimerization in protein kinase signaling. J. Biol. 5, 12.11–12.17.

Plevin, M.J., Mills, M.M., Ikura, M., 2005. The LxxLL motif: a multifunctional binding sequence in transcriptional regulation. Trends Biochem. Sci. 30, 66-69.

Pouyssegur, J., Volmat, V., Lenormand, P., 2002. Fidelity and spatio-temporal control in MAP kinase (ERKs) signalling. Biochem. Pharmacol. 64, 755-763.

Rajalingam, K., Schreck, R., Rapp, U.R., Albert, S., 2007. Ras oncogenes and their downstream targets Biochim. Biophys. Acta 1773, 1177-1195.

Raingeaud, J., Whitmarsh, A.J., Barrett, T., Derijard, B., Davis, R.J., 1996. MKK3- and MKK6-regulated gene expression is mediated by the p38 mitogen-activated protein kinase signal transduction pathway. Mol. Cell. Biol. 16, 1247-1255.

Raman, M., Chen, W., Cobb, M.H., 2007. Differential regulation and properties of MAPKs Oncogene 26, 3100-3112.

Ramnarain, D.B., Park, S., Lee, D.Y., Hatanpaa, K.J., Scoggin, S.O., Otu, H., Libermann, T.A., Raisanen, J.M., Ashfaq, R., Wong, E.T., Wu, J., Elliott, R., Habib, A.A., 2006. Differential gene expression analysis reveals generation of an autocrine loop by a mutant epidermal growth factor receptor in glioma cells. Cancer Res. 66, 867-874.

Ramos, J.W., 2008. The regulation of extracellular signal-regulated kinase (ERK) in mammalian cells Int. J. Biochem. Cell Biol. 40, 2707-2719.

Reffas, S., Schlegel, W., 2000. Compartment-specific regulation of extracellular signal-regulated kinase (ERK) and c-Jun N-terminal kinase (JNK) mitogen-activated protein kinases (MAPKs) by ERK-dependent and non-ERK-dependent inductions of MAPK phosphatase (MKP)-3 and MKP-1 in differentiating P19 cells. Biochem. J. 352 Pt 3, 701-708.

Reynolds, A., Leake, D., Boese, Q., Scaringe, S., Marshall, W.S., Khvorova, A., 2004. Rational siRNA design for RNA interference. Nat. Biotechnol. 22, 326–330.

Richard, J.P., Melikov, K., Vives, E., Ramos, C., Verbeure, B., Gait, M.J., Chernomordik, L.V., Lebleu, B.J., 2003. Cell-penetrating peptides. A reevaluation of the mechanism of cellular uptake. J. Biol. Chem. 278, 585-590.

Rita Sarközi, Bradley Miller, Verena Pollack, Elisabeth Feifel, Gert Mayer, Andrey Sorokin, Herbert Schramek, 2007. ERK1/2-driven and MKP-mediated inhibition of

EGF-induced ERK5 signaling in human proximal tubular cells. J. Cell. Physiol. 211, 88-100.

Roberts, M.J., Troutman, J.M., Chehade, K.A.H., Cha, H.C., Kao, J.P.Y., Huang, X., Zhan, C.-G., Peterson, Y.K., Subramanian, T., Kamalakkannan, S., Andres, D.A., Spielmann, H.P., 2006. Hydrophilic anilinogeranyl diphosphate prenyl analogues are Ras function inhibitors. Biochemistry 45, 15862-15872.

Roberts, P.J., Der, C.J., 2007. Targeting the Raf-MEK-ERK mitogen-activated protein kinase cascade for the treatment of cancer Oncogene 26, 3291-3310.

Rodriguez-Viciana, P., Tetsu, O., Tidyman, W.E., Estep, A.L., Conger, B.A., Cruz, M.S., McCormick, F., Rauen, K.A., 2006. Germline mutations in genes within the MAPK pathway cause cardio-facio-cutaneous syndrome. Science 311, 1287-1290.

Rowinsky, E.K., Windle, J.J., Von Hoff, D.D., 1999. Ras protein farnesyltransferase: A strategic target for anticancer therapeutic development J. Clin. Oncol. 17, 3631-3652.

Saar, K. In The handbook of cell-penetrating peptides, 2nd ed.; Langel, U., Ed.; CRC Press: Boca Raton, FL, 2007; pp 553-565.

Saito, G., Swanson, J.A., Lee, K.-D., 2003. Drug delivery strategy utilizing conjugation via reversible disulfide linkages: role and site of cellular reducing activities. Adv. Drug Deliv. Rev. 55, 199-215.

Santen, R.J., Song, R.X., McPherson, R., Kumar, R., Adam, L., Jeng, M.H., Yue, W., 2002. The role of mitogen-activated protein (MAP) kinase in breast cancer. J. Steroid Biochem. Mol. Biol. 80, 239–256.

Santos, S.D., Verveer, P.J., Bastiaens, P.I., 2007. Growth factor-induced MAPK network topology shapes Erk response determining PC-12 cell fate. Nat. Cell Biol. 9, 324-330.

Sasaki, T., Kojima, H., Kishimoto, R., Ikeda, A., Kunimoto, H., Nakajima, K., 2006. Spatiotemporal regulation of c-Fos by ERK5 and the E3 ubiquitin ligase UBR1, and its biological role. Mol. Cell 24, 63-75.

Sato, M., Vaughan, M.B., Girard, L., Peyton, M., Lee, W., Shames, D.S., Ramirez, R.D., Sunaga, N., Gazdar, A.F., Shay, J.W., Minna, J.D., 2006. Multiple oncogenic changes (K-RAS(V12), p53 knockdown, mutant EGFRs, p16 bypass, telomerase) are not sufficient to confer a full malignant phenotype on human bronchial epithelial cells. Cancer Res. 66, 2116-2128.

Sawhney, R.S., Liu, W., Brattain, M.G., 2009. A novel role of ERK5 in integrin-mediated cell adhesion and motility in cancer cells via Fak signaling. J. Cell. Physiol.

219, 152-161.

Scapoli, L., Ramos-Nino, M.E., Martinelli, M., Mossman, B.T., 2004. Src-dependent ERK5 and Src/EGFR-dependent ERK1/2 activation is required for cell proliferation by asbestos. Oncogene 23, 805-813.

Schafer, W.R., Rine, J., 1992. Protein prenylation: genes, enzymes, targets, and functions. Annu. Rev. Genet. 26, 209-37.

Schmittgen, T.D., Livak, K.J., 2008. Analyzing real-time PCR data by the comparative C(T) method. Nat. Protoc. 3, 1101-1108.

Schreck, R., Rapp, U.R., 2006. Raf kinases: oncogenesis and drug discovery. Int. J. Cancer 119, 2261-2271.

Sebolt-Leopold, J.S., Herrera, R., 2004. Targeting the mitogen-activated protein kinase cascade to treat cancer. Nat. Rev. Cancer. 4, 937-947.

Sebti, S.M., Hamilton, A.D., 2000. Farnesyltransferase and geranylgeranyltransferase I inhibitors and cancer therapy: lessons from mechanism and bench-to-bedside translational studies. Oncogene 19, 6584-6593.

Seth, D., Rudolph, J., 2006. Redox Regulation of MAP Kinase Phosphatase 3. Biochemistry 45, 8476-8487.

Shen, Y.H., Godlewski, J., Zhu, J., Sathyanarayana, P., Leaner, V., Birrer, M.J., Rana, A., Tzivion, G., 2003. Cross-talk between JNK/SAPK and ERK/MAPK pathways: sustained activation of JNK blocks ERK activation by mitogenic factors. J. Biol. Chem. 278, 26715-26721.

Shirasawa, S., Furuse, M., Yokoyama, N., Sasazuki, T., 1993. Altered growth of human colon cancer cell lines disrupted at activated Ki-ras. Science 260, 85–88.

Silvius, J.R., l'Heureux, F., 1994. Fluorimetric evaluation of the affinities of isoprenylated peptides for lipid bilayers. Biochemistry 33, 3014-3022.

Slack, D.N., Seternes, O.M., Gabrielsen, M., Keyse, S.M., 2001. Distinct binding determinants for ERK2/p38alpha and JNK map kinases mediate catalytic activation and substrate selectivity of map kinase phosphatase-1. J. Biol. Chem. 276, 16491-16500.

Slaga, T.J., 1983. Overview of tumor promotion in animals Environ. Health Perspect. 50, 3-14.

Slaga, T.J., Fischer, S.M., Nelson, K., Gleason, G.L., 1980. Studies on the mechanism of skin tumor promotion: evidence for several stages in promotion Proc. Natl. Acad. Sci. U. S. A. 77, 3659-3663.

Smith, T.G., Sweetman, D., Patterson, M., Keyse, S.M., Munsterberg, A., 2005. Feedback interactions between MKP3 and ERK MAP kinase control scleraxis expression and the specification of rib progenitors in the developing chick somite. Development 132, 1305-1314.

Sousa, S.F., Fernandes, P.A., Ramos, M.J., 2008. Farnesyltransferase inhibitors: a detailed chemical view on an elusive biological problem. Curr. Med. Chem. 15, 1478-1492.

Strahl, T., Gille, H., Shaw, P.E., 1996. Selective response of ternary complex factor Sap1a to different mitogen-activated protein kinase subgroups. Proc. Natl. Acad. Sci. U.S.A. 93, 11563-11568.

Strickland, J.E., Greenhalgh, D.A., Koceva-Chyla, A., Hennings, H., Restrepo, C., Balaschak, M., Yuspa, S.H., 1988. Development of murine epidermal cell lines which contain an activated rasHa oncogene and form papillomas in skin grafts on athymic nude mouse hosts. Cancer Res. 48, 165-169.

Sun, W., Kesavan, K., Schaefer, B.C., Garrington, T.P., Ware, M., Johnson, N.L., Gelfand, E.W., Johnson, G.L., 2001. MEKK2 associates with the adapter protein Lad/RIBP and regulates the MEK5-BMK1/ERK5 pathway. J. Biol. Chem. 276, 5093-5100.

Sweet-Cordero, A., Mukherjee, S., Subramanian, A., You, H., Roix, J.J., Ladd-Acosta, C., Mesirov, J., Golub, T.R., Jacks, T., 2005. An oncogenic KRAS2 expression signature identified by cross-species gene-expression analysis. Nat. Genet. 37, 48-55.

Tatake, R.J., O'Neill, M.M., Kennedy, C.A., Wayne, A.L., Jakes, S., Wu, D., Kugler, S.Z.,Jr, Kashem, M.A., Kaplita, P., Snow, R.J., 2008. Identification of pharmacological inhibitors of the MEK5/ERK5 pathway. Biochem. Biophys. Res. Commun. 377, 120-125.

Terasawa, K., Okazaki, K., Nishida, E., 2003. Regulation of c-Fos and Fra-1 by the MEK5-ERK5 pathway Genes Cells 8, 263-273.

Thissen, J.A., Casey, P.J., 1993. Microsomal membranes contain a high affinity binding site for prenylated peptides. J. Biol. Chem. 268, 13780-13783.

Torii, S., Nakayama, K., Yamamoto, T., Nishida, E., 2004. Regulatory mechanisms and function of ERK MAP kinases J. Biochem. 136, 557-561.

Torres, C., Francis, M.K., Lorenzini, A., Tresini, M., Cristofalo, V.J., 2003. Metabolic stabilization of MAP kinase phosphatase-2 in senescence of human fibroblasts. Exp. Cell Res. 290, 195-206.

Traverse, S., Gomez, N., Paterson, H., Marshall, C., Cohen, P., 1992. Sustained activation of the mitogen-activated protein (MAP) kinase cascade may be required for differentiation of PC12 cells. Comparison of the effects of nerve growth factor and epidermal growth factor. Biochem. J. 288 (Pt 2), 351-355.

Tsang, M., Maegawa, S., Kiang, A., Habas, R., Weinberg, E., Dawid, I.B., 2004. A role for MKP3 in axial patterning of the zebrafish embryo. Development 131, 2769-2779.

Turjanski, A.G., Vaque, J.P., Gutkind, J.S., 2007. MAP kinases and the control of nuclear events. Oncogene 26, 3240-3253.

Vantaggiato, C., Formentini, I., Bondanza, A., Bonini, C., Naldini, L., Brambilla, R., 2006. ERK1 and ERK2 mitogen-activated protein kinases affect Ras-dependent cell signaling differentially. J. Biol. 5, 14.1–14.15.

Veber, D.F., Milkowski, J.D., Varga, S.L., Denkewalter, R.G., Hirschmann, R., 1972. A novel thiol protecting group for cysteine. J. Am. Chem. Soc. 94, 5456-5461.

Vial, E., Marshall, C.J., 2003. Elevated ERK-MAP kinase activity protects the FOS family member FRA-1 against proteasomal degradation in colon carcinoma cells. J. Cell. Sci. 116, 4957-4963.

Vician, L., Basconcillo, R., Herschman, H.R., 1997. Identification of genes preferentially induced by nerve growth factor versus epidermal growth factor in PC12 pheochromocytoma cells by means of representational difference analysis. J. Neurosci. Res. 50, 32-43.

Vogelstein, B., Kinzler, K.W., 1993. The multistep nature of cancer. Trends Genet. 9, 138-141.

Volmat, V., Camps, M., Arkinstall, S., Pouyssegur, J., Lenormand, P., 2001. The nucleus, a site for signal termination by sequestration and inactivation of p42/p44 MAP kinases. J. Cell. Sci. 114, 3433-3443.

von Kriegsheim, A., Baiocchi, D., Birtwistle, M., Sumpton, D., Bienvenut, W., Morrice, N., Yamada, K., Lamond, A., Kalna, G., Orton, R., Gilbert, D., Kolch, W., 2009. Cell fate decisions are specified by the dynamic ERK interactome Nat. Cell Biol. 11, 1458-1464.

Wagstaff, K.M., Jans, D.A., 2006. Protein transduction: cell penetrating peptides and their therapeutic applications. Curr. Med. Chem. 13, 1371-1387.

Wang, X., Tournier, C., 2006. Regulation of cellular functions by the ERK5 signalling pathway. Cell. Signal. 18, 753-760.

Warmka, J.K., Mauro, L.J., Wattenberg, E.V., 2004. Mitogen-activated protein kinase phosphatase-3 is a tumor promoter target in initiated cells that express oncogenic Ras. J. Biol. Chem. 279, 33085-33092.

Warmka, J.K., Winston, S.E., Zeliadt, N.A., Wattenberg, E.V., 2002. Extracellular signal-regulated kinase transmits palytoxin-stimulated signals leading to altered gene expression in mouse keratinocytes. Toxicol. Appl. Pharmacol. 185, 8-17.

Wattenberg, E.V., 2007. Palytoxin: exploiting a novel skin tumor promoter to explore signal transduction and carcinogenesis. Am. J. Physiol. Cell. Physiol. 292, C24-32.

Wattenberg, E.V., Fujiki, H., Rosner, M.R., 1987. Heterologous regulation of the epidermal growth factor receptor by palytoxin, a non-12-O-tetradecanoylphorbol-13-acetate-type tumor promoter. Cancer Res. 47, 4618-4622.

Wellbrock, C., Karasarides, M., Marais, R., 2004. The RAF proteins take centre stage. Nat. Rev. Mol. Cell Biol. 5, 875-885.

Wender, P.A., Mitchell, D.J., Pattabiraman, K., Pelkey, E.T., Steinman, L., Rothbard, J.B., 2000. The design, synthesis, and evaluation of molecules that enable or enhance cellular uptake: peptoid molecular transporters. Proc. Natl. Acad. Sci. U.S.A. 97, 13003-13008.

Whitehurst, A., Cobb, M.H., White, M.A., 2004. Stimulus-coupled spatial restriction of extracellular signal-regulated kinase 1/2 activity contributes to the specificity of signal-response pathways. Mol. Cell. Biol. 24, 10145-10150.

Whitmarsh, A.J., Shore, P., Sharrocks, A.D., Davis, R.J., 1995. Integration of MAP kinase signal transduction pathways at the serum response element. Science 269, 403-407.

Woo, C.H., Shishido, T., McClain, C., Lim, J.H., Li, J.D., Yang, J., Yan, C., Abe, J., 2008. Extracellular signal-regulated kinase 5 SUMOylation antagonizes shear stress-induced antiinflammatory response and endothelial nitric oxide synthase expression in endothelial cells. Circ. Res. 102, 538-545.

Woods, D.C., Johnson, A.L., 2006. Phosphatase activation by EGF family ligands regulates Erk signaling in undifferentiated hen granulosa cells. Endocrinology 336,

4931–4940.

Wollack, J.W., Zeliadt, N.A., Mullen, D.G., Amundson, G., Geier, S., Falkum, S., Wattenberg, E.V., Barany, G., Distefano, M.D., 2009. Multifunctional prenylated peptides for live cell analysis J. Am. Chem. Soc. 131, 7293-7303.

Wright, L.P., Philips, M.R., 2006. Thematic review series: lipid posttranslational modifications. CAAX modification and membrane targeting of Ras. J. Lipid Res. 47, 883-891.

Xiao, Y.Q., Malcolm, K., Worthen, G.S., Gardai, S., Schiemann, W.P., Fadok, V.A., Bratton, D.L., Henson, P.M., 2002. Cross-talk between ERK and p38 MAPK mediates selective suppression of pro-inflammatory cytokines by transforming growth factor-beta. J. Biol. Chem. 277, 14884-14893.

Xue, C.B., Becker, J.M., Naider, F., 1992. Efficient regioselective isoprenylation of peptides in acidic aqueous solution using zinc acetate as catalyst. Tetrahedron Lett. 33, 1435-1438.

Yao, Y., Li, W., Wu, J., Germann, U.A., Su, M.S., Kuida, K., Boucher, D.M., 2003. Extracellular signal-regulated kinase 2 is necessary for mesoderm differentiation. Proc. Natl. Acad. Sci. U. S. A. 100, 12759–12764.

Yip-Schneider, M.T., Lin, A., Marshall, M.S., 2001. Pancreatic tumor cells with mutant K-ras suppress ERK activity by MEK-dependent induction of MAP kinase phosphatase-2. Biochem. Biophys. Res. Commun. 280, 992-997.

Ylikomi, T., Bocquel, M.T., Berry, M., Gronemeyer, H., Chambon, P., 1992. Cooperation of proto-signals for nuclear accumulation of estrogen and progesterone receptors. EMBO J. 11, 3681-3694.

Yordy, J.S., Muise-Helmericks, R.C., 2000. Signal transduction and the Ets family of transcription factors. Oncogene 19, 6503-6513.

Yuspa, S.H., 1986. Cutaneous chemical carcinogenesis J. Am. Acad. Dermatol. 15, 1031-1044.

Yuspa, S.H., 1998. The pathogenesis of squamous cell cancer: lessons learned from studies of skin carcinogenesis. J. Dermatol. Sci. 17, 1–7.

Yuspa, S.H., Morgan, D.L., 1981. Mouse skin cells resistant to terminal differentiation associated with initiation of carcinogenesis. Nature 293, 72-74.

Yuspa, S.H., Poirier, M.C., 1988. Chemical carcinogenesis: from animal models to molecular models in one decade Adv. Cancer Res. 50, 25-70.

Zarbl, H., Sukumar, S., Arthur, A.V., Martin-Zanca, D., Barbacid, M., 1985. Direct mutagenesis of Ha-ras-1 oncogenes by N-nitroso-N-methylurea during initiation of mammary carcinogenesis in rats. Nature 315, 382-385.

Zeliadt, N.A., Mauro, L.J., Wattenberg, E.V., 2008. Reciprocal regulation of extracellular signal regulated kinase 1/2 and mitogen activated protein kinase phosphatase-3 Toxicol. Appl. Pharmacol. 232, 408-417.

Zeliadt, N.A., Warmka, J.K., Wattenberg, E.V., 2003. Mitogen activated protein kinases selectively regulate palytoxin-stimulated gene expression in mouse keratinocytes. Toxicol. Appl. Pharmacol. 192, 212-221.

Zeliadt, N.A., Warmka, J.K., Winston, S.E., Kahler, R., Westendorf, J.J., Mauro, L.J., Wattenberg, E.V., 2004. Tumor promoter-induced MMP-13 gene expression in a model of initiated epidermis. Biochem. Biophys. Res. Commun. 317, 570-577.

Zhang, F.L., Casey, P.J., 1996. Protein prenylation: molecular mechanisms and functional consequences. Annu. Rev. Biochem. 65, 241-269.

Zhang, J., Nomura, J., Maruyama, M., Nishimoto, M., Muramatsu, M., Okuda, A., 2009. Identification of an ES cell pluripotent state-specific DUSP6 enhancer. Biochem. Biophys. Res. Commun. 378, 319-323.

Zhang, Z., Kobayashi, S., Borczuk, A.C., Leidner, R.S., LaFramboise, T., Levine, A.D., Halmos, B., 2010. Dual specificity phosphatase 6 (DUSP6) is an ETS-regulated negative feedback mediator of oncogenic ERK-signaling in lung cancer cells Carcinogenesis 31, 577-86.

Zhou, G., Bao, Z.Q., Dixon, J.E., 1995. Components of a new human protein kinase signal transduction pathway. J. Biol. Chem. 270, 12665-12669.

Zhu, K., Hamilton, A.D., Sebti, S.M., 2003. Farnesyltransferase inhibitors as anticancer agents: current status Curr. Opin. Investig. Drugs 4, 1428-1435.

Zimmermann, S., Rommel, C., Ziogas, A., Lovric, J., Moelling, K., Radziwill, G., 1997. MEK1 mediates a positive feedback on Raf-1 activity independently of Ras and Src. Oncogene 15, 1503-1511.

Zou, G.M., Chen, J.J., Ni, J., 2006. LIGHT induces differentiation of mouse embryonic stem cells associated with activation of ERK5 Oncogene 25, 463-469.